THE ANTI-INFLAMMATORY AND PRO-ANGIOGENIC CAPACITY OF HIGH-DENSITY LIPOPROTEINS IN DIABETIC WOUND HEALING

Zahra Lotfollahi

A Thesis submitted for the degree of Doctor of Philosophy in

The Discipline of Health and Medical Sciences, School of Medicine

Faculty of Health and Medical Sciences

July 2022

Table of Contents

THESIS ABSTRACT

Diabetes is the one of the most common metabolic disorders and is associated with a range of complications including diabetic foot ulcers (DFU) [1]. It is estimated that 25% of patients with diabetes develop DFU and of these a quarter do not heal resulting in amputation. This places them at risk of lower limb amputation [1]. There are currently no therapies that actively promote wound healing. It is increasingly being recognised that to improve biologically complex wound healing, an effective therapy requires pleiotropic actions that targets multiple facets of impaired wound healing such as prolonged inflammation and poor revascularisation. High-density lipoproteins (HDL) possess significant wound healing properties and regulate multiple important wound healing mechanisms including anti-inflammatory and pro-angiogenic effects. HDL has traditionally been viewed as an atheroprotective protein, with a well-established inverse relationship between plasma HDL-cholesterol levels and the risk of myocardial infarction (MI). Efforts to pharmacologically raise HDL in large-scale clinical trials have failed to show benefit on MI risk. This redirected the focus from HDL-cholesterol levels to HDL functionality as a better predictor of disease. The relationship between HDL functionality and diabetic wound healing is yet to be explored.

In this thesis we aimed to 1) determine the anti-inflammatory properties of topically applied reconstituted HDL (rHDL) in a murine model of wound healing and to track its fate, 2) compare changes in the functionality of HDL in patients with and without diabetes post-toe/s amputation over time, and 3) determine the relationship between HDL functionality and wound closure in patients with and without diabetes and an acute toe amputation/s.

Firstly, we utilised a murine model of diabetic wound healing to assess the effect of topical rHDL on wound inflammation. Diabetic mice had delayed wound healing and higher levels of

wound macrophages, when compared to non-diabetic mice. Topical application of rHDL completely rescued diabetes-impaired wound healing but had no effect on wound macrophage content. There were, however, significant reductions in the mRNA levels of inflammatory mediators *Rela* and *Ccl2*, and CCL2 protein in diabetic wounds following topical rHDL, 72hrs post-wounding. Overall, this study showed topical rHDL exhibits anti-inflammatory effects in diabetic wounds.

We next conducted a clinical study that determined changes in HDL functionality of patients with and without diabetes at the time of amputation (baseline), 1- and 6-months post amputation/s and tracked wound closure. We found that HDL isolated from patients with diabetes had impaired cholesterol efflux, anti-inflammatory and pro-angiogenic functionality, when compared to non-diabetic HDL at 1- and 6-months post-toe amputation/s. We identified a significant positive correlation between HDL-cholesterol levels and the rate of wound closure. Furthermore, there were significant negative correlations between the anti-inflammatory effects of HDL for *Ccl2* and *Icam1*, and the rate of wound healing in patients with diabetes 1-month post-amputation.

In conclusion, this thesis has demonstrated that topical rHDL has anti-inflammatory effects in diabetic wounds. This adds to its already well-characterised pro-angiogenic effects, making rHDL a potential wound healing therapy with important pleiotropic properties. Our clinical study revealed that HDL from patients with diabetes and toe amputations had impaired functionality. Furthermore, we identified for the first time that the anti-inflammatory functionality of HDL inversely correlated with wound closure rate, highlighting its potential as new predictive marker of healing. In conclusion, rHDL presents as an exciting new topical agent for improving wound healing in people with diabetes, and the anti-inflammatory capacity of endogenous HDL shows potential as a predictive biomarker for diabetic wound healing outcomes.

DECLARATION

I, Zahra Lotfollahi, certify that this work contains no material which has been accepted for the award of any other degree or diploma in my name in any university or other tertiary institution and, to the best of my knowledge and belief, contains no material previously published or written by another person, except where due reference has been made in the text. In addition, I certify that no part of this work will, in the future, be used in a submission in my name for any other degree or diploma in any university or other tertiary institution without the prior approval of the University of Adelaide and, where applicable, any partner institution responsible for the joint award of this degree. I give permission for the digital version of my thesis to be made available on the web, via the University's digital research repository, the Library Search and through web search engines, unless permission has been granted by the University to restrict access for a period of time. I acknowledge the support I have received for my research through the provision of an Australian Government Research Training Program Scholarship and the grant funded by the Hospital Research Foundation.

Zahra Lotfollahi

ACKNOWLEDGEMENTS

I never thought attending a meeting one week before moving to Melbourne for a new job would change my life forever. I'm so grateful that I attended that meeting, and I was introduced to one of the biggest idols in my life, Associate Professor Christina Bursill. The passionate presentation provided by Chris about the project excited me so much that I decided to cancel my move to Melbourne and pursue a PhD with Chris. Her positive attitude, continuous support, and trust, (even when I failed in my experiments!) compounded with a sense of humour helped fuel me to successfully complete my PhD. Thank you, Chris, I will forever be grateful for the opportunities and possibilities you provided me, which has led me to this point, and will carry me forward in future. You inspire me every day as a female scientist who overcomes the obstacles of being a leader, a great scientist, and above all, a loving mum. I can't wait to continue this project with you after my PhD, and I look forward to further opportunities to work alongside you.

In addition to my primary supervisor, I would like to thank my co-supervisors Professor Robert Fitridge and Dr Joe Dawson for their insightful comments and encouragements, and for supporting me to conduct this clinical trial. Their immense knowledge and plentiful experience guided me throughout my PhD candidature. My sincere thanks also go to Dr Joanne Tan, who patiently taught me laboratory skills and never refused to provide a helping hand. Words cannot describe how grateful I am for the constant mentoring and support I received from her. I am also sincerely grateful for Sophie's advice towards the construction of this thesis.

I would like to express my sincere gratitude to the other members of our clinical trial project; Neil, Lauren, Judith, Prue, Mohsen, and Zygmunt, for their support and contribution towards our project. I would like to thank my fellow lab mates; Anna, Emma, Khalia, Victoria, Ben, and Sanuja, for the stimulating discussions, assistance in using laboratory equipment, and most enjoyable times working together.

Lastly, I wish to express my deepest gratitude to my family. Thank you to my parents, Shamsolmolok and Mohammad, for their everlasting love, support, and motivation throughout my educational journey. I would not have been able to complete this PhD without your mental, emotional, and financial contribution. And finally, but most importantly, I would like to thank my husband, Andrew. Meeting you at SAHMRI was undoubtedly the best part of my PhD. Thank you for pushing me when I was very close to giving up, and never losing your faith in me. You continue to inspire me every day and my love for you grows more every day in my heart.

CONFRENCES

Oral: Zahra Lotfollahi, Anna Williamson, Joe Dawson, Peter Psaltis, Joanne Tan, Robert Fitridge, Christina Bursill. Anti-inflammatory and cholesterol efflux properties of high-density lipoproteins in diabetic wound healing. *The Australian Wound & Tissue Repair Society wound healing virtual symposium 2021*. Virtual presentation.

Oral: Zahra Lotfollahi, Anna E Williamson, Joanne TM Tan, Joe A Dawson, Robert A Fitridge, Christina A Bursill. Anti-inflammatory properties of High-Density Lipoproteins in diabetic wound healing. *The Wounds Australia National Conference 2021*. Virtual presentation.

Oral: Zahra Lotfollahi, Anna E Williamson, Joanne TM Tan, Joe A Dawson, Robert A Fitridge, Christina A Bursill. Anti-inflammatory properties of High-Density Lipoproteins in diabetic wound healing. *Australian Society for Medical Research 2020*. Virtual presentation.

Poster: Zahra Lotfollahi, Anna E Williamson, Joanne TM Tan, Joe A Dawson, Robert A Fitridge, Christina A Bursill. The anti-inflammatory properties of reconstituted High-Density Lipoproteins in diabetic wound healing. *Florey Postgraduate Research Conference 2020.* Virtual presentation.

Poster: Zahra Lotfollahi, Anna E Williamson, Joanne TM Tan, Joe A Dawson, Robert A Fitridge, Christina A Bursill. The anti-inflammatory properties of reconstituted High-Density Lipoproteins in diabetic wound healing. *The Australian Wound & Tissue Repair Society Symposium 2019*.

PUBLICATIONS FROM THIS THESIS

Lotfollahi, Z., Dawson J., Fitridge R., Bursill C. (2021). The anti-inflammatory and proangiogenic properties of High-Density Lipoproteins: an emerging role in diabetic wound healing". *Advances in Wound Care*. 10 (7): 370-80.

AWARDS

Award: Best PhD quickfire presenter. *The Australian Wound & Tissue Repair Society Wound Healing Virtual Symposium 2021.*

Award: Poster prize. *Florey Postgraduate Research Conference 2020.*

Award: Runner up poster prize. *The Australian Wound & Tissue Repair Society Symposium 2019.*

Scholarship: Research Training Program Stipend, *The University of Adelaide 2019-2022*.

ABBREVIATIONS

ABCA1	ATP-binding cassette transporter
ANOVA	Analysis of variance
apoA-I /II	Apolipoprotein A-I/II
BSA	Bovine serum albumin
CCL2	C-C motif chemokine ligand 2
CCL5	C-C motif chemokine ligand 5
cDNA	Complementary deoxyribonucleic acid
CEC	Cholesterol efflux capacity
CX3CL1	Fractalkine
DAPI	4′,6-diamidino-2-phenylindole
DFU	Diabetic foot ulcers
DNA	Deoxyribonucleic acid
ECM	Extracellular matrix
EDTA	Ethylenediaminetetraacetic acid
EGF	Epidermal growth factor
ELISA	Enzyme-linked immunosorbent assay
EPC	Endothelial progenitor cell
FBS	Foetal bovine serum
FGF	Fibroblast growth factor
HbA1c	Haemoglobin A1c
HCAEC	Human coronary artery endothelial cell
HDL	High-density lipoproteins
HIF	Hypoxia-inducible factor
ICAM-1	Intercellular cell adhesion molecule 1
IL	Interleukin
LDL	Low-density lipoprotein

MI	Myocardial infarction
MMP	Matrix metalloprotease
mRNA	Messenger ribonucleic acid
NF-κB	Nuclear factor of kappa B
PAD	Peripheral arterial disease
PBS	Phosphate-buffered saline
PCR	Polymerase chain reaction
PDGF	Platelet-derived growth factor
PI3K	Phosphoinositide 3-kinase
PIC	Protein inhibitor cocktail
PLPC	1-palmitoyl-2-linoleoyl phosphatidycholine
qPCR	Quantitative real-time polymerase chain reaction
rHDL	Reconstituted high-density lipoprotein
RIPA	Radioimmunoprecipitation assay
RNA	Ribonucleic acid
ROS	Reactive oxygen species
SEM	Standard error of the mean
S1P	Sphingosine-1-phosphate
SR-BI	Scavenger receptor class B type I
TBS	Tris-buffered saline
TGF	Transforming growth factor
Tris	Tris(hydroxymethyl)aminomethane
TNFα	Tumour necrosis factor alpha
TLR	Toll-like receptor(s)
VCAM-1	Vascular cell adhesion molecule 1

VEGF	Vascular endothelial growth factor
VEGFR	Vascular endothelial growth factor receptor

CHAPTER 1- INTRODUCTION

1.1 Wound healing

Wound healing is one of the most complex physiological processes in the human body. This process is critical for our survival as it stops excessive loss of blood through the wound (i.e. haemorrhage), prevents the development of systemic infection within the body and restores the normal anatomy of the skin to serve its physiological function [2]. This process is highly dynamic and consists of four continuous yet overlapping phases characterised by haemostasis, inflammation, proliferation, and tissue maturation and vascular remodelling (Figure 1.1). Successful wound healing requires all four phases to occur in a coordinated sequence and time frame. The timely transition from one phase of wound healing to the next is strictly regulated by multiple growth factors and cytokines at the wound site.

1.1.1 Haemostasis

Haemostasis is the initial stage and foundation step for the wound healing process and occurs in three steps: vasocontraction, primary haemostasis, and secondary haemostasis [3]. Immediately after an injury, the vessels in the affected area constrict to reduce bleeding and prevent blood loss [4]. Endothelin is an important vasoconstrictor which is released by damaged endothelial cells [3]. Additionally, a range of other vasoconstrictive compounds including catecholamines, serotonin, bradykinin, and histamine are released almost immediately after the injury to cause vasoconstriction [5]. After this short-lived vasocontraction (5 to 10 minutes) the affected blood vessels vasodilate to compensate for the hypoxia caused by the vasoconstriction, providing an opportunity for intravascular cells, platelets and fluid to pass through the vessel walls into the extravascular space which leads to the next phase, primary haemostasis [5].

Primary haemostasis is characterised by the formation of the platelet plug (or clot) [3]. Platelets or thrombocytes in normal circulation are in their non-adherent or “resting” state because of the endothelium’s anti-thrombin properties such as the production of nitric oxide, prostacyclin, and negatively charged heparin-like glycosaminoglycans which prevent platelet activation, attachment, and aggregation [6]. However, following wounding and rupture of blood

vessels, the thrombogenic subendothelial matrix is exposed and platelets are activated through G-protein coupled receptors and form a platelet plug [3, 5]. Secondary haemostasis involves coagulation and reinforcement of the platelet plug. The platelet plug forms dimers with fibronectin in the presence of activated factor XIII to form a provisional extracellular matrix (ECM) which serves as a scaffold for the efflux of cells such as neutrophils, monocytes, fibroblasts, and endothelial cells [4, 5]. This provisional ECM also secretes growth factors and cytokines such as platelet-derived growth factor (PDGF) and transforming growth factor (TGF) β1 to recruit inflammatory cells such as neutrophils, monocytes, and macrophages that initiate the inflammation stage of wound healing [7].

1.1.2 Inflammation

Inflammation starts with the migration of immune cells, especially polymorphonuclear leukocytes, to the wound site. This migration is mediated by cytokines, chemokines, and growth factors. The inflammation stages start within the first 6 h of the injury [5]. Neutrophils are the first immune cells to enter the wound site and are the predominant active immune cell type in the first 24 h post-wounding [8]. This invasion is mediated by a potent chemoattractant known as fibrinopeptide, which is the product of fibrinogen to fibrin conversion. The main role of neutrophils is to non-selectively destroy foreign bodies by releasing toxic granules containing toxic oxygen species and to phagocytose bacteria and extracellular debris from the wound area [5, 9]. Activated neutrophils release cytokines which, along with the degradation of proteins from the provisional ECM, attract circulating monocytes to the wound area within 24 h post-wounding [5].

Approximately 48 h after injury the migration of monocytes to the wound area is intensified and these monocytes differentiate into macrophages. Macrophages are the key regulators of the wound healing process as they take on distinct roles to ensure proper healing as their phenotype evolves during the different healing stages [10]. Whilst macrophages can acquire a range of phenotypes, the simplest classification is ‘M1-like’ pro-inflammatory and ‘M2-like’ anti-

inflammatory macrophages [11]. These phenotypes (or 'polarity') are based on their cell marker expression, cytokine secretion, and function.

During the early phases of inflammation, transcriptional changes in macrophages result in the formation of pro-inflammatory M1-like macrophages, which produce inflammatory cytokines such as interleukin (IL)-1, IL-6, and tumour necrosis factor (TNF)-α [10]. These macrophages also secrete matrix metalloproteinases (MMP)-2 and MMP-9 which break down the ECM and provide a path for infiltrating inflammatory cells and the clearance of pathogens, debris, and dead cells [12, 13]. During the later stages of the inflammatory wound healing phase, the macrophage population transitions into the anti-inflammatory M2-like macrophage phenotype [10].

1.1.3 Proliferation

The proliferation step of wound healing consists of re-epithelisation, angiogenesis, and fibroplasia. Invasion of fibroblasts and increased accumulation of collagen in the wound mediate the transition from the inflammatory to the proliferative stage of wound healing. During this stage, granulation tissue composed of new capillaries, fibroblast, and fibrous connective tissue is formed to fill the wound area beneath the scab. The purpose of this granulation tissue is to protect the wound from infection and provide a surface for re-epithelisation [5].

Shortly after an injury, epidermal cells (predominantly keratinocytes) at the margin of the wound undergo phenotypic changes such as retraction of intracellular monofilaments [14], dissolution of the physical connection between the cells, and formation of new peripheral actin filaments which allow cell movement [15, 16]. Mobilisation and migration of epithelial cells such as keratinocytes at the margin of the wound is the first predominant activity at the epithelisation stage of wound healing [17]. Subsequently, epithelial cells behind these leading

cells proliferate to fill the gap. Migration and proliferation of keratinocytes is mediated by multiple growth factors such as epidermal growth factor (EGF), TGF-α, and keratinocyte growth factor which are produced by epithelial cells, wound fibroblasts, and wound macrophages [5].

Simultaneously, in response to an injury, new blood vessels are formed through the process of angiogenesis which is initially led by endothelial cells. Angiogenesis is the process of new capillary growth from pre-existing vessels at the wound edges into an area previously unoccupied by vascular structures [5]. Tissue hypoxia within the wound area triggers the expression of the transcription factor hypoxia-inducible factor-1α (HIF-1α), a heterodimeric nuclear transcription factor responsible for mediating adaptive cellular responses to hypoxia. HIF-1α then induces the transcription of pro-angiogenic growth factors such as vascular endothelial factor (VEGF), EGF, fibroblast growth factor (FGF), and platelet derived growth factor (PDGF) [18]. These growth factors initiate the proliferation and migration of endothelial cells for the formation of new blood vessels [19]. In addition, endothelial progenitor cells from the bone marrow are recruited to the wound in response to CXCL12 (C-X-C motif chemokine 12), VEGF-A and MMP-9 and form a border along the injury site [20].

Another important process in the proliferation phase of wound healing is fibroplasia which is characterised by the migration and proliferation of mesenchymal cells (predominantly fibroblasts) [5]. These wound fibroblasts are stimulated by growth factors such as PDGF, TGF-β and FGF, as well as the ECM and have different characteristic features to normal fibroblasts such as myofibroblast appearance, abundant contractile features, intercellular tight junctions, and a distorted nuclear envelope [21].

1.1.4 Tissue maturation and vascular remodelling

The remodelling phase consists of regression of the vasculature, changes in ECM deposition, and the subsequent transition of granular tissue to scar tissue [3]. Wound closure is achieved by wound contraction as a result of α-smooth muscle cell actin expression by myofibroblasts [22]. As the wound progressively closes, the composition of the ECM changes from predominantly type III collagen to predominately type I collagen which is stronger [3]. After re-epithelisation, myofibroblasts within the granulation tissue continue to secrete MMPs and tissue inhibitor of metalloproteinases (TIMPs) to regulate the degradation of old collagen and the synthesis of new collagen [23]. Following ECM modification, TIMPs begin to block MMPs to halt further ECM degradation [3]. The blood vessels that infiltrate the healing wound are leaky as they lack tight cell-to-cell contact as well as scant pericyte coverage to allow increased immune cell infiltration into the wound [24]. During vascular remodelling, new vessels undergo pruning to generate stable and well-perfused blood vessels; this pruning occurs through endothelial cell apoptosis [25]. Once the epithelium is closed, the healed wound bed is no longer in a state of hypoxia which causes changes in hypoxia-responsive elements (HREs) through a negative-feedback mechanism. For example, endothelial cells express CXCR3 (C-X-C motif chemokine 3) which, after binding to its ligand CXCL10, inhibits endothelial tube formation, contributing to endothelial cell quiescence [3].

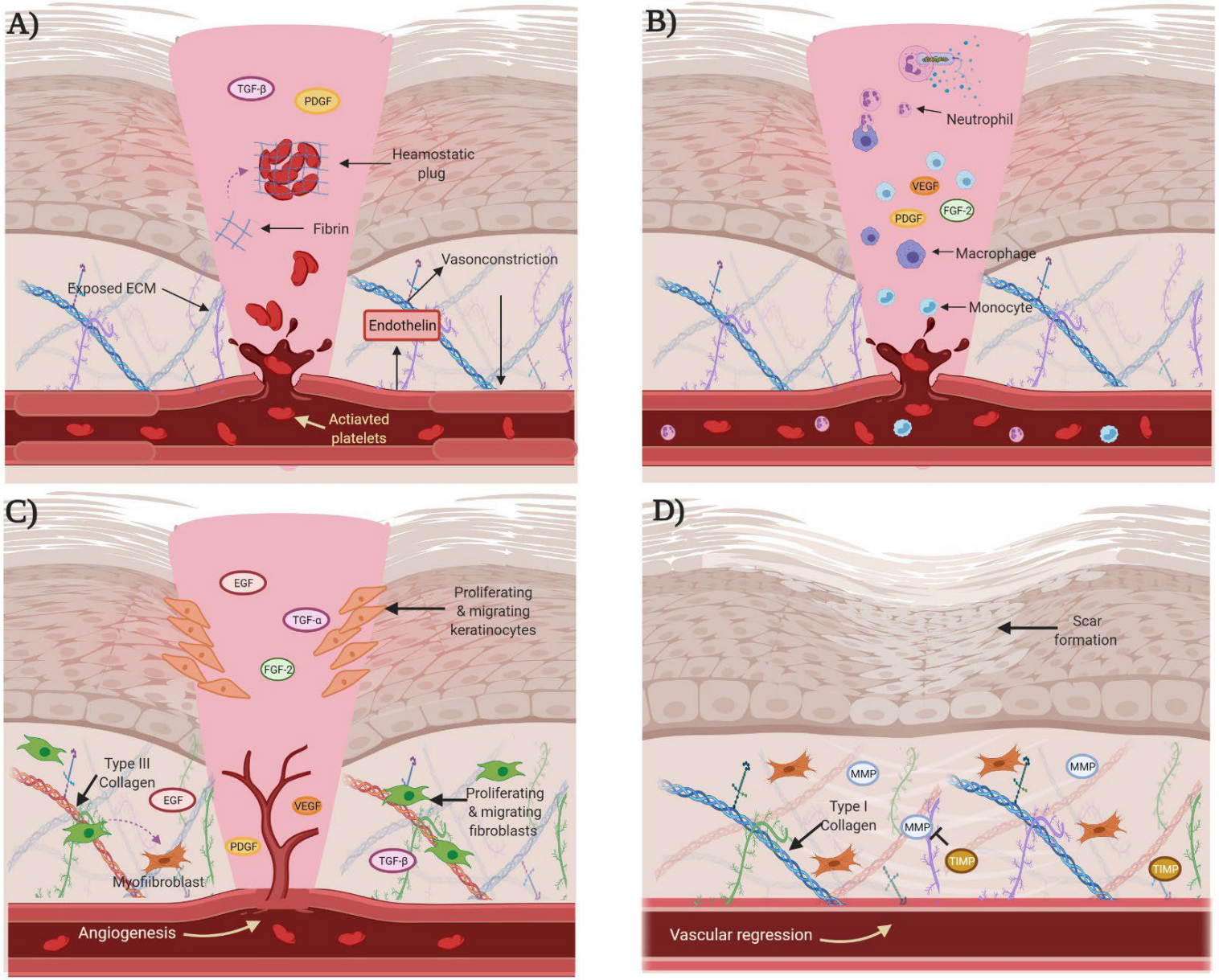
A)
TGF-β
PDGF
Heamostatic plug
Fibrin
Vasonconstriction
Exposed ECM
Endothelin
Actiavted platelets
B)
Neutrophil
VEGF
FGF-2
PDGF
Macrophage
Monocyte
C)
EGF
TGF-α
Proliferating & migrating keratinocytes
FGF-2
Type III Collagen
EGF
VEGF
PDGF
TGF-β
Proliferating & migrating fibroblasts
Myofiibroblast
Angiogenesis
D)
Scar formation
MMP
MMP
Type I Collagen
MMP
TIMP
TIMP
Vascular regression

Figure 1.1 Stages of wound healing.

(A) The first stage of wound healing is haemostasis. Upon injury, endothelin is released by damaged endothelial cells to cause vasoconstriction. This short-lived vasoconstriction is followed by vasodilation and the influx of platelets to the wound area to form a platelet plug. This platelet plug combines with fibrin to form a provisional ECM. **(B)** The next stage of wound healing is the inflammation stage which is initiated by the influx of neutrophils to the wound area. Neutrophils non-selectively destroy foreign bodies by releasing toxic granules. Next, monocytes are recruited to the wound area and differentiate into macrophages. Pro-inflammatory macrophages are responsible for phagocytosing pathogens and releasing inflammatory markers. Anti-inflammatory macrophages remove the neutrophils via efferocytosis and release VEGF-A and PDGF in preparation for proliferation. **(C)** The proliferation stage of wound healing involves epithelisation, angiogenesis, and fibroplasia. In this phase, keratinocytes proliferate and migrate in response to EGF, TGF- α, and FGF2 to form a new dermal skin layer. Simultaneously, endothelial cells respond to VEGF-A, FGF, and PDGF released by platelets and endothelial cells for angiogenesis. Fibroblasts also proliferate and migrate in response to growth factors such as PDGF, TGF- β1, EGF, and FGF. **(D)** The last phase of wound healing is wound maturation and vascular remodelling. In this stage the composition of ECM changes as type I collagen is replaced by type III collagen and new blood vessels form. Image adapted from thesis by Carla Maria Cannizzo, 2021, The University of Sydney.

1.2 Critical cell types in wound healing

1.2.1 Neutrophils

Neutrophils originate from promyelocytes in the bone marrow ; they are known as “the first responders” as they are the first immune cells recruited to the wound site in response to “find me” signals including damage-associated molecular patterns, hydrogen peroxide, lipid mediators, and chemokines released from the wound site [26]. Within the first 24 h post-wounding, neutrophils constitute 50% of all cells in the wound. Activated neutrophils release signals to prolong and amplify neutrophil recruitment. Neutrophils destroy infectious agents by releasing toxic granules to produce an oxidative burst which initiates phagocytosis and generates neutrophil extracellular traps [3].

One characteristic of neutrophils is the formation of unique primary and secondary granules containing toxic chemicals. The primary granules contain particles such as myeloperoxidase and proteases. The secondary granules contain antimicrobial proteins, dMMP-8. Proteases are the major component of these toxic granules and are important for both antimicrobial activity and break down of the ECM and basement membrane which allows further neutrophil infiltration [3].

Activated neutrophils also release neutrophil extracellular traps, chromatin filaments that extend into the extracellular space and are coated with histones, cytosolic proteins, and proteases for the capture and elimination of exogenous bacteria, fungi, and viruses [27]. In addition, neutrophils destroy cell debris and bacteria by phagocytosis, predominantly by fusing with their released granules [3].

1.2.2 Macrophages

Macrophages are one of the most critical immune cell types for normal wound healing and tissue regeneration. Wounding causes macrophage infiltration and accumulation at the wound site within the first 24-48 h [28]. Macrophages can be characterised by their surface markers. Common surface markers used to identify macrophages include $CD45^+/CD11b^+/F4/80^+$ in mice and $CD45^+/CD11b^+/CD66B^-$ in humans. Macrophages at the wound site are sourced from both tissue-resident macrophages and macrophages transformed from bone marrow-derived monocytes, the latter being the predominant source of active inflammatory macrophages at the wound site. Monocytes are recruited to the wound area in response to platelets and mast cell degranulation, hypoxia-induced factors, and chemokines [3]. Monocyte chemoattractant protein 1 (also known as CCL2) is one of the main chemoattractants released by macrophages in order to recruit additional monocytes to the wound area [29].

In the early inflammatory phase of wound healing, macrophages are microbicidal and pro-inflammatory in phenotype, expressing TNF-α, IL-1β and IL-6 [3]. In addition, these pro-inflammatory macrophages engulf pathogens, synthesise MMPs to digest the ECM, and clear neutrophils by efferocytosis [3]. With the resolution of inflammation, inflammatory macrophages within the wound transition to an anti-inflammatory phenotype. Anti-inflammatory macrophages have also been referred to as pro-vascular macrophages as they assist with new vessel formation during the resolution of inflammation by releasing growth factors such as VEGF-A [30].

During the proliferation phase of wound healing, a unique subset of macrophages ($CD206^+/CD301b^+$) actively signal to dermal fibroblasts to trigger a transition to myofibroblasts and increase collagen and α-smooth muscle actin deposition into the wound [31]. Interestingly, macrophages can also transition into fibrotic cells and deposit collagen and other ECM components. These macrophages are referred to as fibrocytes or M2a macrophages [32]. The

interaction between macrophages and other cell types in the wound area is crucial: failure of this communication can lead to complications such as fibrosis and delayed wound healing[3].

1.2.3 Keratinocytes

Keratinocytes are the most dominant cellular component of the epidermis and are in a state of constant renewal [33]. During the re-epithelisation phase of wound healing, keratinocytes migrate, proliferate, and differentiate to restore the epidermal barrier [34]. Injury and/or external pathogens activate the expression of a range of immune genes in keratinocytes. As a first line of defence, keratinocytes use pattern recognition receptors (PRRs) to detect the pathogen-associated molecular patterns expressed by bacteria and other microorganisms [34]. Keratinocytes express various PRRs including Toll-like receptors (TLRs), C-type lectin receptors, nucleotide-binding oligomerisation domain-like receptors and retinoic acid-inducible gene I- like receptors [34].

After injury, TLR activation is a critical component of initiating and amplifying inflammation. Keratinocytes express a range of TLRs including TLR-1, -2, -4, -5, and -6, and the endosomal TLR-3 and -9. After stimulation, TLRs activate the nuclear factor kappa-light-chain-enhancer of activated B cells (NF-kB) to induce the expression of a host of inflammatory cytokines and chemokines [34].

Active communication between keratinocytes and immune cells at different stages of wound healing is critical for successful healing. Keratinocyte-secreted pro-inflammatory cytokines and chemokines contribute to the recruitment of neutrophils and macrophages to the wound site. Neutrophils and macrophages also secrete inflammatory markers such as IL-1β, TNF-α and IL-6 which stimulate keratinocyte proliferation and increase the immune response [34]. Another important cell population which interacts with keratinocytes upon injury is Langerhans cells, a dendritic cell population [35]. The pro-inflammatory cytokines secreted by keratinocytes such as IL-1β, TNF-α, and granulocyte-macrophage colony-stimulating factor enhance the migration

of Langerhans cells from the skin to the drainage lymph nodes to prime naïve T cells, therefore bridging the innate and adoptive immune system [35].

1.2.4 Fibroblasts

Dermal fibroblasts are the major cell component of the dermis and consist of two distinct subpopulations – papillary fibroblasts and reticular fibroblasts [36]. While papillary fibroblasts are primarily involved in the immune response, reticular fibroblasts are responsible for cytoskeletal organisation and cell mobility during wound healing [37]. The communication between fibroblasts and immune cells, mast cells, and keratinocytes is integral to appropriate and timely wound healing.

The interaction between fibroblasts is stimulated by TGF-β and results in the release of connective tissue growth factors which promote collagen synthesis and fibroblast proliferation under non-pathological conditions [36]. Production of nitric oxide by dermal fibroblasts facilitates further collagen synthesis and increases fibroblast contractility [36]. During the inflammatory phase of wound healing, dermal fibroblasts interact with immune cells such as neutrophils and B-lymphocytes via the adhesion molecules intercellular cell adhesion molecule-1 (ICAM-1), β2 integrin, vascular cell adhesion molecule-1 (VCAM-1) and α4 integrin. This facilitates the passage of these cells through the fibroblast barrier [36].

Dermal fibroblasts also interact with natural killer cells via the TNF receptor on fibroblasts and membrane-bound TNF-α on fibroblasts to produce IL-6 and IL-8, two important inflammatory cytokines [36]. As natural killer cells are early immune responders, the expression of these pro-inflammatory cytokines by dermal fibroblasts is important in initiating the inflammation phase of wound healing [36]. The M2 macrophage-derived PDGF-CC accelerates the differentiation of wound fibroblasts into the myofibroblast phenotype which is essential for the proliferation phase of wound healing [36].

The interaction between fibroblasts and keratinocytes is important for strengthening tissue integrity, especially during the re-modelling phase of wound healing. Fibroblast-derived soluble factors such as keratinocyte growth factor, hepatocyte growth factor, granulocyte-macrophage colony-stimulating factor, IL-6, IL-19, and FGF-10, diffuse into the epidermis and affect both keratinocyte growth and differentiation [36]. Lastly, the presence of both fibroblasts and the ECM is required for the formation of new blood vessels during wound healing as fibroblasts are responsible for remodelling the ECM and delivery of several signalling molecules to facilitate angiogenesis. VEGF is released by dermal fibroblasts then binds to the VEGF receptor, VEGFR-1, on endothelial cells and activates intrinsic tyrosine kinases and signalling cascades that result in endothelial cell migration and proliferation, which are required for angiogenesis [36].

1.3 Chronic wounds

Some flexibility exists in the wound healing process to support imbalances within each step and sequence, however, if this carefully regulated system is disrupted too much it can lead to the development of a chronic non-healing wound. Chronic wounds are defined as wounds that fail to proceed through the normal wound healing phases in an orderly and timely manner [38]. In patients with diabetes, a wound is classified as 'chronic' if it does not heal within the first three months [39]. Chronic wounds can be classified as vascular ulcers (e.g. venous and arterial ulcers), diabetic ulcers, and pressure ulcers [38]. Some common features shared by chronic wounds include prolonged and persistent inflammation due to excessive pro-inflammatory stimuli, persistent infection, formation of drug-resistant microbial biofilm, and the inability of dermal and epidermal cells to respond to stimuli [38].

Repeated tissue injury in chronic wounds causes platelet-derived factors such as TGF-β1 and ECM growth factors to stimulate the constant influx of immune cells to the wound area. This creates an excessive and prolonged pro-inflammatory cytokine cascade that causes elevated levels of proteases [38]. As mentioned previously, in the proliferation phase of acute

wound healing, protease activity (e.g. MMPs) is tightly regulated by inhibitors (e.g. TIMPs). However, in chronic wounds the level of protease activity exceeds the level of the inhibitors which causes the destruction of the ECM and degradation of important growth factors and their receptors [38, 40]. Prolonged exposure of the wound tissue to pro-inflammatory cytokines stimulates further production of proteases such as MMPs and inhibition of their respective inhibitors, creating a vicious cycle [40]. The proteolytic destruction of the ECM prevents the wound from transitioning to the next wound healing stage whilst also attracting additional inflammatory cells, thereby amplifying the inflammation cycle (Figure 1.2)[38].

The other important imbalance in chronic wounds is the presence of excessive reactive oxygen species (ROS), due to a predominantly hypoxic and inflammatory wound environment [41]. In normal conditions, low concentrations of ROS provides an important defence against pathogens, however, in chronic wounds excessive ROS levels damage ECM proteins and cause cell damage [41].

Several studies have shown a senescent cell phenotype in chronic wounds for fibroblasts, keratinocytes, endothelial cells, and macrophages that have impaired proliferative and secretary capacities, making them unresponsive to typical wound healing signals [42, 43]. This senescent cell phenotype is believed to be due to excessive oxidative stress which leads to DNA damage-related cell cycle arrest [43]. For example, it is suggested that keratinocytes at non-healing edges of chronic wounds are hyper-proliferative but non-migratory and therefore fail to close the wound [34].

Another defect identified in chronic wound healing is the deficiency and abnormality of mesenchymal stem cells [44]. Mesenchymal stem cells play a critical role in wound healing as they are recruited into the circulation in response to an injury [44]. As an example, the timely clearance of neutrophils (a type of mesenchymal stem cell) is critical as their disappearance

marks the resolution of the inflammation phase [45]. Previous studies have shown failure of neutrophil clearance and their persistence as a characteristic of chronic wounds such as diabetic foot ulcers (DFU), pressure ulcers, and venous leg ulcers [45].

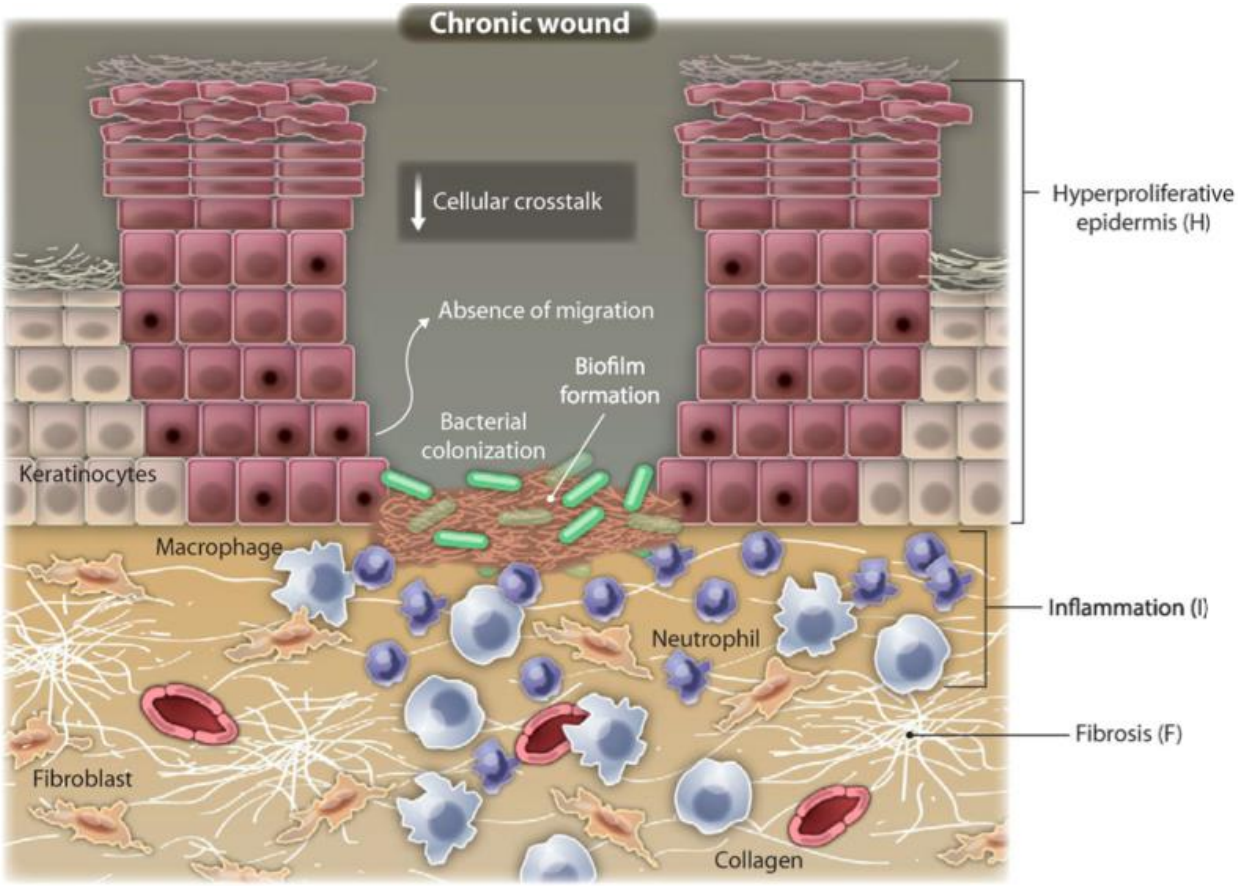

Figure 1.2 Cellular characteristics of chronic wounds.

Chronic wounds display characteristics such as: (1) hyperproliferative and non-migratory keratinocytes in the epidermis with reduced communication between epidermal cells; (2) increased levels of inflammatory cells such as neutrophils and macrophages producing pro-inflammatory cytokines and prolonged inflammation; (3) presence of infection, bacterial colonisation, and biofilm formation; (4) reduction in angiogenesis and recruitment of stem cells; and (5) impaired ECM remodelling compared to healthy wound healing. Image adapted from [46].

1.4 Diabetes

Diabetes is one of the most common metabolic disorders [47, 48]. The World Health Organisation reported 382 million diabetic people in 2013, with 592 million predicted by 2035 [47]. Diabetes is a condition characterised by chronic hyperglycaemia. Most diabetes diagnoses fall into two forms: type I and type II [49]. Type I diabetes is immune-based in nature, resulting from cellular-mediated autoimmune destruction of pancreatic β cells so they cannot secrete insulin [49]. Glucose uptake by cells is mediated by insulin; therefore a lack of insulin leads to an elevation in blood glucose levels [50]. Type I diabetes accounts for only 5-10% of diabetic people and their condition is managed by insulin therapy [49]. The main characteristic of type II diabetes is insulin resistance, defined as the resistance of cells to respond to insulin and a failure of a compensatory mechanism. Most patients with type II diabetes are obese, which is linked to insulin resistance [49]. Other risk factors include age, lack of physical activity, and genetic predisposition. Patients with type II diabetes are not initially insulin-dependent and are treated with oral hypoglycaemic agents, however, prolonged hyperglycaemia may result in β cell destruction and therefore insulin dependency [49].

The current gold standard guidelines for diagnosing type II diabetes in Australia are [51]:

- Haemoglobin A1c (HbA1c) ≥6.5% (≥48 mmol/mol)
- Non-fasting plasma glucose ≥200 mg/dL (≥11.1 mmol/L)
- Fasting plasma glucose ≥126 mg/dL (≥7.0 mmol/dL)
- Oral Glucose Tolerance Test 2 h glucose in venous plasma ≥200 mg/dL (≥11.1 mmol/L)

1.4.1 Diabetic complications

Generally, the complications associated with diabetes are categorised as either microvascular or macrovascular. Macrovascular complications include coronary artery disease, peripheral arterial disease (PAD), and stroke. Microvascular complications consist of diabetic nephropathy (damage to kidneys), neuropathy (nerve damage), and retinopathy (damage to the eyes) [52]. Additionally, the risk of impaired cutaneous wound healing is significantly elevated

in people living with diabetes and this leads to formation of DFU [52]. This thesis focuses on DFUs and the complications that lead to delayed wound healing in diabetes, such as PAD.

1.4.2 Peripheral arterial diseases (PAD)

Atherosclerosis is a progressive, immune-inflammatory disease characterised by the deposition of lipids within the sub-endothelial space of arteries [53]. Inflammation is the initiating driver for the development of atherosclerosis. Endothelial cells, leukocytes, and smooth muscle cells all contribute to the inflammatory response. PAD is a manifestation of atherosclerosis of the lower extremities [54]. Data from the Framingham heart study [55] have shown that 20% of symptomatic patients with PAD have diabetes. This, however, is likely to be an underestimation as many people with PAD are asymptomatic rather than symptomatic [54].

The most common symptom of PAD is intermittent claudication which is characterised by pain, cramping or aching in the calves, thighs or buttocks which is reproducible on walking and relieved by resting [54]. Advanced PAD is associated with more extreme presentations such as rest pain, gangrene or tissue loss which are collectively under the umbrella of chronic limb threatening ischaemia (CLTI)[54].

The link between PAD and diabetes is thought to be associated with pro-atherogenic changes that are exacerbated by diabetes such as increases in vascular inflammation and changes in the cellular components of the vessels [54]. One example of this is a diabetes-induced increase in C-reactive protein, which is strongly associated with the development of PAD [56]. The mechanisms underlying this include the ability of C-reactive protein to bind to endothelial cell receptors and promote apoptosis as well as co-localising with oxidised low-density lipoprotein (LDL) in atherosclerotic plaque [54].

1.4.3 Diabetes-related foot ulcers

Development of PAD and peripheral neuropathy are precursors for DFUs [57, 58]. Other risk factors include foot deformities, previous ulcerations, and impaired resistance to infection [59]. Approximately 25% of people living with diabetes develop a foot ulcer within their lifetime and it is estimated that 20% of patients with DFUs require amputation [57]. The five-year mortality rate for patients with diabetes and an existing DFU is 2.5 times higher than patients without diabetes [57, 60]. DFUs can be divided into two main groups: neuropathic and ischaemic/neuro-ischaemic [39].

More than 60% of DFUs are neuropathic ulcers [61]. Neuropathy in patients with diabetes is manifested in the motor, sensory, and autonomic components of the nervous system (Figure 1.3) [61]. Damage to the motor and sensory components of the nervous system causes an imbalance between the flexion and extension of intrinsic muscles in the foot as well as intrinsic muscle wasting. These complications result in anatomic foot deformities which creates bony prominences and pressure points that are prone to ulcer development [61]. In addition, damage to the sensory nervous system and loss of sensation in patients with diabetes makes them more vulnerable to developing DFUs due to unrecognised injury to the foot [61]. Autonomic neuropathy leads to attenuation of sweat and oil production by the skin, resulting in dry and callous skin susceptible to skin break down and ulcer formation [61].

Ischaemic ulcers are often seen on the margins of the foot, especially on the medial area of the first metatarsal joint and the lateral fifth toe area [62]. These ulcers develop as a result of diminished blood supply to the foot due to athero-occlusive PAD that is exacerbated by diabetes [63]. Restrictions in oxygen-carrying blood impairs wound healing in ischaemic ulcers and the rate of amputation is higher for these ulcers [64]. Regular non-invasive tests such as palpitation of pedal pulses and measurement of the ankle brachial index or toe pressures can be used for early detection of PAD.

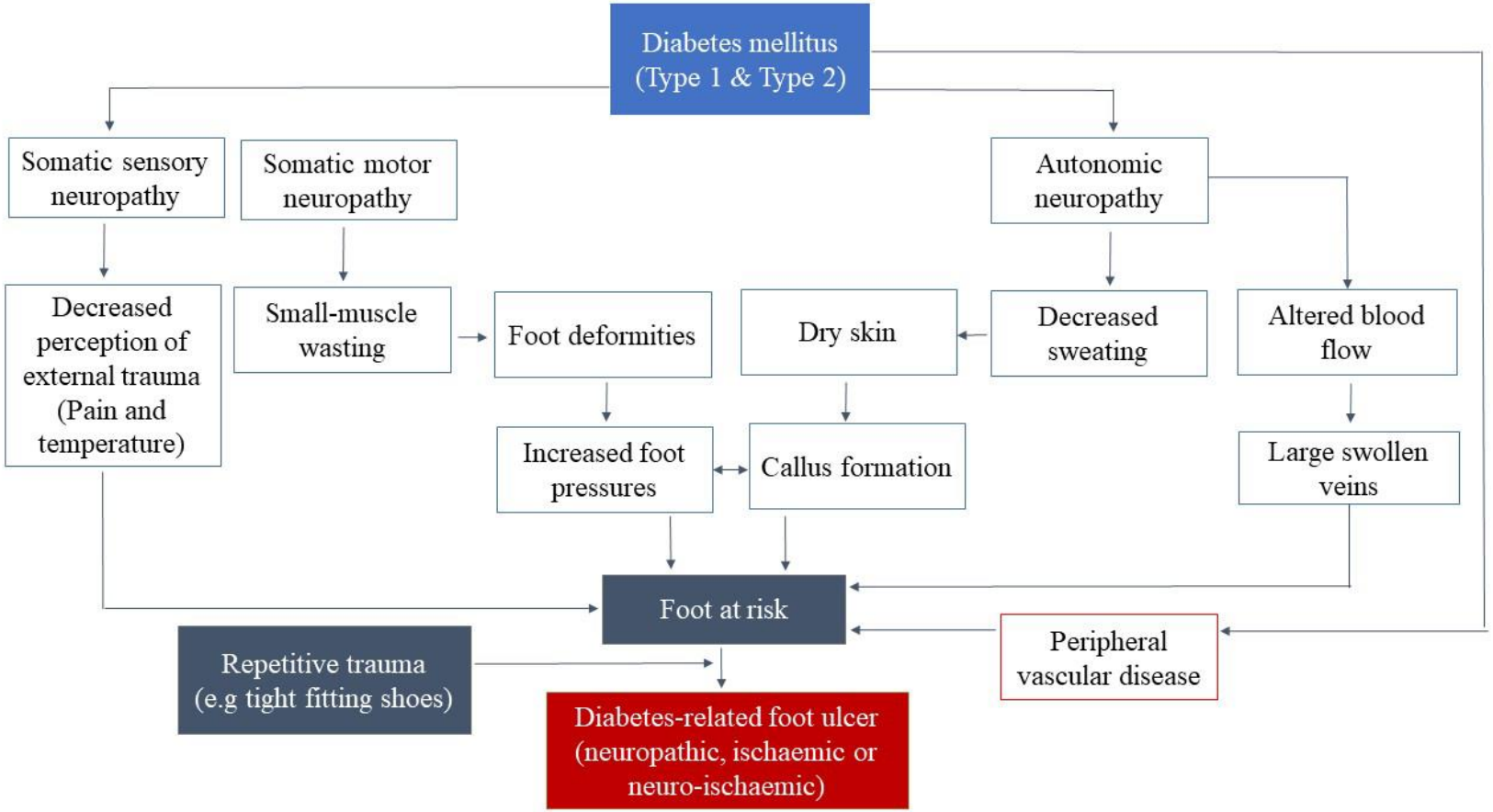

Figure1.3 Pathways leading to the formation of diabetic foot ulcers.

Diabetic foot ulcers may result from peripheral arterial diseases and/or peripheral neuropathy. Adapted from [65]

1.4.4 Diabetic complications at the molecular level

At the molecular level, diabetic hyperglycaemia causes multiple metabolic disruptions that cause cellular dysfunction including increased superoxide production, excessive production of advanced glycation end-products, enhanced aldose reductase activity, increased protein kinase C activity, increased hexosamine pathway flux, and overstimulation of the polyol pathway [66]. Under normal glucose conditions, the pyruvate produced from the glycolysis of glucose is converted into acetyl-CoA and enters the Krebs cycle where electron carriers are generated for use in the electron transport chain to make ATP for energy [67]. However, due to increased glucose oxidation in the hyperglycaemic environment more electrons are pushed into the electron transport chain which blocks complex III and causes electron accumulation on coenzyme Q [68]. Coenzyme Q then donates these electrons to damaging oxygen-generating superoxides [69].

Advanced glycoxidation (also termed advanced glycation or glycosylation) end products (AGEs) originate from 1-amino-1 deoxy ketose through the reaction between glucose and free amino groups [70]. It has been shown that hyperglycaemic conditions result in higher AGE production which interferes with normal ECM deposition through inappropriate cross-linking of matrix proteins, a key trigger of diabetes-related wound healing complications [71].

In addition, hyperglycaemic conditions cause excessive glucose to be converted to sorbitol by aldose reductase through the polyol metabolic pathway which requires reduced nicotinamide adenine dinucleotide phosphate (NADPH) [72]. This affects the normal synthesis of key antioxidant-reducing equivalents such as nitric oxide and glutathione [66]. NADPH levels are further reduced by the activation of the hexosamine biosynthesis pathway which inhibits the activity of glucose-6-phosphate dehydrogenase and consequently prevents the conversion of NADH to NADPH [73].

1.4.5 Prolonged inflammation in diabetic wounds

Diabetes causes substantial imbalances in each stage of the wound healing process. It is associated with persistent, non-resolving inflammation and defective tissue repair responses [74, 75]. For example, in hyperglycaemia neutrophils produce more superoxide and pro-inflammatory cytokines [76]. Neutrophils from patients with diabetes are also in a hyperactive state, indicated by increased expression of the activation marker CD11b [77]. Diabetes also increases the levels of circulating inflammatory C-reactive protein in foot wounds [78]. Diabetic wounds also have increased total numbers of inflammatory cells, paralleled by decreased concentrations of growth factors [79], which hinders the migration of the epidermis layer over the wound that is essential for healing [79]. Diabetes also causes alterations in wound structure and remodelling processes, causing a loss of heparan sulphate proteoglycans such as syndecan-4 [80] and increased degradation of the ECM [81].

Diabetes significantly prolongs wound inflammation and halts the normal sequence of the wound repair process; this includes disruption to wound macrophage regulation. The increased infiltration of inflammatory cells including neutrophils and macrophages into the wound area results in significantly higher levels of pro-inflammatory cytokines such as IL-1β and TNF-α, prolonging the inflammatory phase and delaying the healing process [46]. These inflammatory cytokines can lead to activation of NF-κB, a pivotal transcription factor that switches on further inflammatory gene expression, leading to an exacerbated inflammatory response. The NF-κB complex (which consists of two subunits, P50 and P65/RelA) is normally sequestered in an inactive state within the cytosol by the inhibitor of κB proteins (IκB) [82]. Stimulation by inflammatory cytokines such as IL-1β and TNF-α induces the activity of IκB kinase which phosphorylate IκB, resulting in its ubiquitination and consequent proteasomal degradation (Figure1.4). Degradation of IκB liberates the NF-κB dimer (p50/p65-RelA), allowing it to translocate to the nucleus where it initiates transcriptional activation of numerous target genes and creates an inflammatory response (Figure1.4).

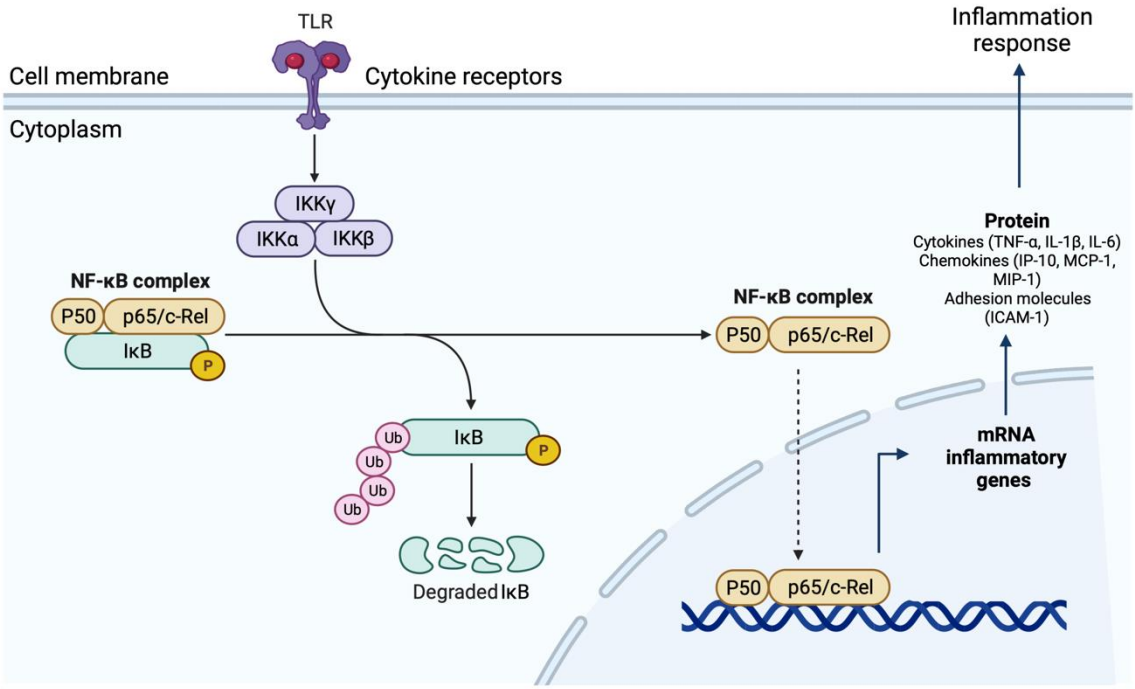

Figure 1.4 NF-κB signalling pathway in inflammation.

Inflammatory cytokines such as tumour necrosis factor α (TNF-α) and interleukin 1β (IL-1β) lead to activation of the inhibitor of the κB kinase (IKK) protein complex. This causes phosphorylation of IκB, which normally sequesters the NF-κB dimer that consists of p50 and p65 subunits within the cytoplasm. After IκB phosphorylation, IκB is targeted for ubiquitination and degradation, liberating the NF-κB dimer so that it can translocate to the nucleus and bind to NF-κB response elements and activate transcription of a range of inflammatory genes. Image created on Biorender.

A major inflammatory disruption in diabetic wound healing is a delay or failure of the phenotypic switch from pro-inflammatory macrophages to anti-inflammatory macrophages. When the skin is uninjured, the population of tissue-resident macrophages is higher than monocyte-derived macrophages. After injury, the influx of monocyte-derived macrophages results in a 2-fold increase in their number and an acute reduction in tissue-resident macrophages [12]. Shortly after injury and haemostasis, monocyte-derived macrophages enter the wound site and differentiate into pro-inflammatory (M1-like) macrophages which release inflammatory cytokines including IL-1β, TNF-α and IL-6 [83]. This is followed in the subsequent healing stages by polarisation into anti-inflammatory (M2-like) reparative macrophages, which release anti-inflammatory cytokines such as TGF-β and IL-10 and support tissue remodelling and fibrosis [83]. In pathological conditions such as diabetes, the transition from the M1 to the M2 phenotype is delayed, causing an increase in wound inflammation through excess M1-derived chemokine/cytokine expression. This persistent inflammation is likely to result in the development of a chronic wound [12].

In a study done by Mirza et al [74], macrophages isolated from the chronic wounds of patients with type 2 diabetes prominently exhibited a pro-inflammatory M1-like phenotype, expressing high levels of inflammatory cytokines including IL-1β and TNF-α as well as MMP-9 [74]. Furthermore, wound macrophages obtained from diabetic mice persisted as pro-inflammatory M1-like macrophages and failed to transition to the reparative M2-like phenotype [74]. Suppression of inflammation can, however, overcome these issues. For example, the use of an IL-1β blocking antibody improved wound healing, reduced M1-like macrophages, and increased the presence of M2-like macrophages in wounds [74]. It has also been observed that inflammatory cells from abnormal diabetic inflammatory wound areas escape apoptosis and hence persist within the wound environment [84].

High levels of TNF-α have been identified as a molecular predictive factor for failure of wound closure, and high levels of serum TNF-α have been identified in type 2 diabetes [85].

TNF-α is known to be involved in a positive feedback system and regulates its own secretion as well as the secretion of IL-1β (Figure 1.5) [84]. Excess TNF-α levels have been shown to reduce the wound tensile strength and to decrease type I and type III collagen expression [84]. In addition, TNF-α is responsible for enhanced T-lymphocyte adhesion to dermal fibroblasts via upregulation of dermal fibroblast ICAM-1 and VCAM-1, which bind to the leukocyte function-associated antigen 1 and very late antigen-4, respectively. These interactions contribute to the accumulation, retention, and activation of T-lymphocytes under chronic inflammatory conditions [36].

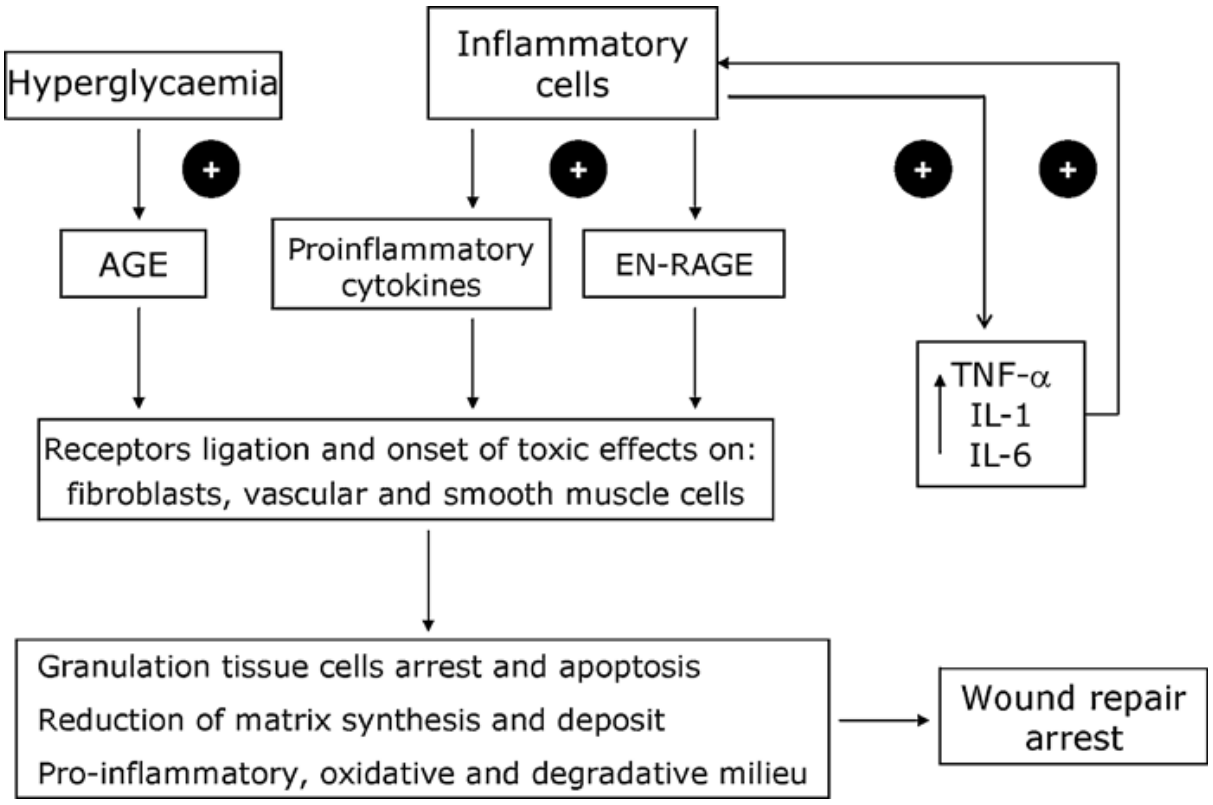

Figure 1.5 Role of pro-inflammatory mediators in wound healing failure.

The cytotoxic effect of pro-inflammatory cytokines and glycation products in the failure of diabetic wound healing. Hyperglycaemia stimulates the production of advanced glycation end products (AGE). Inflammatory cells stimulate the production of TNF-α, IL-1β and IL-6 which cause positive feedback with inflammatory cells. Inflammatory cells also stimulate the release of pro-inflammatory cytokines and extracellular, newly identified receptors for advanced glycation end products (EN-RAGE). Image adapted from [84].

1.4.6 Impaired angiogenesis in diabetic wounds

Angiogenesis is a physiological process which occurs in an orderly manner and requires coordination between several cells, growth factors, and chemokines. Diabetes leads to a significant impairment in this process via several mechanisms. Firstly, endothelial cells become dysfunctional when exposed to elevated systemic glucose concentrations leading to the loss of functional integrity and increased apoptosis [58]. Secondly, high serum glucose causes an imbalance in cytokine/chemokine and growth factor levels that disturbs normal angiogenesis. Studies have shown that the ability of VEGF-A to simulate the migration of monocytes within patients with diabetes is impaired when compared to monocytes from healthy individuals. This was despite higher levels of VEGF-A in diabetic plasma, suggesting this is due to a deficiency in VEGFR-2 activation. [86]. Furthermore, wounds in a diabetic murine model express significantly lower mRNA and protein levels of VEGF-A compared to healthy controls [87]. Higher levels of the anti-angiogenic growth factor pigment epithelium-derived factor [88] and low levels of the FGF-2 cell surface receptors syndecan-4 and glypican-1 [80] in patients with diabetes also lead to impaired angiogenesis. Furthermore, increases in anti-angiogenic molecules that cause proteolysis of VEGF-A have been observed in chronic venous ulcers [89, 90].

Impaired angiogenesis in diabetes also occurs because high glucose impairs angiogenic responses to wound ischemia, a result of low oxygen supply due to tissue injury or PAD [91]. Central to this is high glucose-induced destabilisation of HIF-1α, the key transcription factor that is activated in response to hypoxia/ischaemia to promote VEGF-A and angiogenesis [91]. Furthermore, there is a reduction in the recruitment of endothelial progenitor cells (EPCs) to the site of diabetic wounds. EPCs make significant contributions to wound vascularisation in response to ischaemia. In diabetes, the production of the chemokine stromal cell-derived factor (SDF)-1α (CXCL12) in the wound is reduced. SDF-1α normally facilitates the migration and recruitment of EPCs to the wound site and thus a reduction in its concentration leads to less

EPC recruitment and neovascularisation. In summary, diabetes leads to a multitude of events that cause a reduction in angiogenesis, an essential process for wound repair.

1.5 Current therapies for diabetic foot ulcers and their limitations

Based on guidelines prepared by *The International Working Group of the Diabetic Foot*, the most common treatment options for DFUs are limited to debridement of hypertrophic tissue surrounding the wound, application of appropriate dressings, and orthotic devices such as casting or shoe modifications to offload the pressure from the ulcer area [92]. In some cases, vascular reconstruction is required if macrovascular ischaemia is contributing to chronic wound development [92].

A recent comprehensive review evaluated all previous evidence supporting standard interventions and rated them based on the quality and level of evidence [93]. Interventions included debridement and wound bed preparation, antiseptics and dressing products, negative pressure wound therapy, growth factors and cellular products, placental-derived products, skin grafts, oxygen and other gases, and physical therapies [93]. When looking at debridement and wound bed interventions, which included sharp debridement [94], hydrodebridement [95], enzymatic debridement [96], and larval therapy [97], sharp debridement was the only intervention studied in a controlled manner and with adequate evidence to demonstrate benefit.

Previously studied topical interventions include antiseptics and antimicrobials [98], honey dressings [99], alginate and collagen dressings [100], sucrose octasulfate dressings [101], topical phenytonin [102], hydrogel dressings [103], and topical application of antibiotics such as tobramycin beads [104]. From these studies, the sucrose octasulfate dressing was found to be the most effective in a recent and well-controlled randomised multi-centre clinical trial across France, Spain, Italy, Germany, and the UK [101]. The sucrose octasulfate dressing demonstrated significant increases in wound closure in patients with non-infected neuro ischaemic DFUs. The mechanism of action is believed to be via inhibition of MMPs which are

found in higher concentrations in chronic wounds, increase inflammation and break down of the remodeling process [101]. The study, however, did not control for offloading devices to take away the pressure from the plantar surface of the foot between the multiple clinical centres. Other wound dressings have also revealed positive findings. One dressing incorporated autologous platelet-rich plasma and leukocytes [105]. Clinical testing showed improvement in wound healing [106], however, the weakness of the study was that it was not controlled appropriately. Another multilayered patch with a similar composition of autologous leukocytes, platelets, and fibrin was tested in a recent multi-center study. An increase in wound healing was reported in patients with 'hard to heal' ulcers but this dressing has the limitation of the high cost of preparing the autologous cells [105].

Negative pressure wound therapy (NPWT) used in parallel with best standard care has demonstrated promising benefits in clinical trials, especially when used after surgery [107]. However, for chronic wounds there is not enough evidence to establish whether NPWT has any benefit over and above standard care. NPWT is predominantly recommended for acute and larger wounds which have excess exudate that impacts wound healing.

Growth factors are essential for wound healing, particularly for promoting angiogenesis [93]. Numerous clinical trials have tested the topical application of growth factors including FGF, EGF, combined FGF-EGF, and others on diabetic wounds. Topical application of basal FGF in a spray format onto DFUs led to a 75% reduction in ulcer area, however, the analysis for this study was a per protocol analysis leading to bias [108]. Furthermore, a recent Phase III multicentre clinical trial using a spray form of recombinant human EGF found that it significantly improved wound healing in 167 patients with DFUs [109]. It must be noted that the studies that investigated the effect of growth factors have limitations in methodology, the inclusion of appropriate controls, details regarding the ulcer status (e.g. vascular supply) and poor statistical analyses leading to high bias and unclear outcomes. Further confounding the

translation of growth factor therapy is their lack of cost-effectiveness, a significant consideration.

In summary, despite the conduct of numerous clinical trials that have tested a wide variety of interventions, there is still no universally approved or effective therapy for diabetic wound healing which has been implemented to support the best standard of care. Most clinical interventions target only a single mechanism of action in the wound healing process. This may be insufficient to effectively heal mechanistically complex diabetic wounds. Agents that offer pleiotropic actions on the wound healing process are therefore more likely to be effective.

1.6 High-density lipoproteins

1.6.1 High-density lipoprotein structure and biology

High-density lipoprotein (HDL) is the smallest class of circulating endogenous lipoprotein particles. Mature HDL is a spherical biochemical compound composed of an outer monolayer of phospholipids, apolipoproteins, and unesterified cholesterol surrounding a hydrophobic core of cholesteryl esters and a small amount of triglyceride (Figure 1.6) [110]. HDL is the smallest and densest of the five main lipoproteins [111]. Circulating plasma HDL comprises a highly heterogeneous family of lipoprotein particles varying in density, size, surface charge, and lipid/protein composition [112]. When subjected to centrifugation, HDL is separated into two density subfractions: HDL_2 (1.063 - 1.125 g/mL) and the denser HDL_3 (1.125 - 1.12 g/mL). Gel electrophoresis can be used to distinguish HDL into five discrete populations by particle size ranging from 10.6 to 7.6 nm in diameter: two belong to the HDL_2 subclass and three belong to the HDL_3 subclass [113].

The main apolipoproteins found on the surface of HDL are apoA-I and apoA-II, which account for approximately 70% and 20% of total protein, respectively [114]. Another classification system for HDL is based on the presence of these two apolipoproteins: (1) A-I

HDL containing apoA-I but not apoA-II (less dense) is found in HDL_2, and (2) A-I/A-II HDL containing both apoA-I and apoA-II in a 2:1 molar ratio is found in HDL_3 [115]. ApoA-I is the most predominant apolipoprotein and AI-HDL is the most abundant lipoprotein, however, $HDL_{3,}$ in particular, is believed to be a subpopulation of HDL with superior anti-inflammatory effects [116].

There are a number of enzymes on the surface of HDL which catalyse reactions critical for the metabolism of HDL including lecithin: cholesterol acyltransferase (LCAT), cholesterol ester transfer protein (CETP) and phospholipid transfer protein [117]. HDL interacts with three key cell surface proteins: the cholesterol transporters ATP-binding cassette transporter 1 (ABCA1) and ABCG1, and the scavenger receptor SR-BI (SR-BI) [118]. A vast number of *in vitro*, *in vivo,* and epidemiological studies have demonstrated that HDL exhibits athero-protective, anti-thrombotic, antioxidant, anti-apoptotic, anti-inflammatory, anti-proteolytic, and pro-angiogenic properties [112].

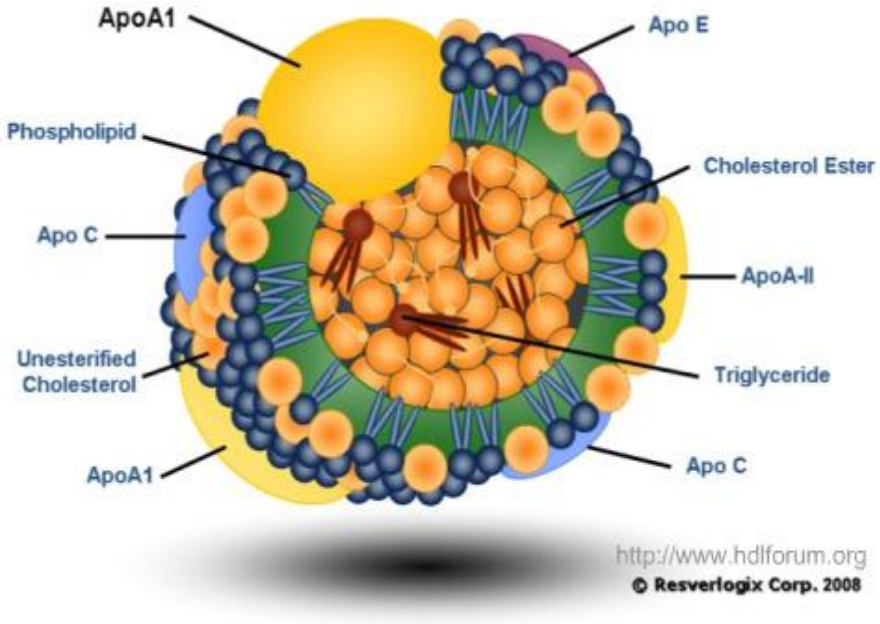

Figure 1.6 The structure of mature high-density lipoprotein.

A schematic diagram showing the typical structure of mature high-density lipoprotein (HDL), composed of an outer layer of phospholipids, unesterified cholesterol, and different apolipoproteins surrounding a core of triglycerides and cholesterol esters. The predominant apolipoprotein is apoA-I, however, other apolipoproteins such as apoA-II, apoC and apoE are present in certain subsets of HDL [119].

1.6.2 HDL metabolism and remodelling

A major role of HDL is known as reverse cholesterol transport which involves scavenging cholesterol from peripheral cells and tissues and transporting it back to the liver for metabolism or excretion. To initiate this process, apoA-I is synthesised in the liver and released into the plasma in a lipid-poor/lipid-free form [120]. Circulating apoA-I then immediately combines with phospholipids and unesterified cholesterol from cell membranes to form the earliest HDL particle which is discoidal in shape. The transfer of lipid from cell membranes to discoidal HDL is mediated by ABCA1 [121]. The main role of ABCA1 is to transport intracellular free cholesterol and phospholipids to extracellular apoA-I [122]. Discoidal A-I HDL is the preferred substrate for LCAT, a hydrophobic plasma enzyme that generates cholesteryl esters [123]. As cholesteryl ester is more hydrophobic than cholesterol, it immediately migrates to the centre of HDL giving rise to the spherical and mature but small/dense HDL_3. The function of LCAT is to create a concentration gradient to mediate the efflux of free cholesterol from the cell membrane to the core of HDL [124]. Small/dense HDL_3 particles develop into large/light HDL_2 particles through further cholesteryl ester formation or HDL particle fusion through the action of LCAT and phospholipid transfer protein enzymes [125].

Conversion of HDL_2 (small/dense) to HDL_3 (large/light) is mediated by CETP and hepatic lipase (HL) enzymes resulting in the release of lipid-free or lipid-poor apoA-I. The main function of CETP is to replace neutral lipids in HDL, such as cholesteryl esters, with triglycerides from LDL and low/very low density lipoproteins to form triglyceride-rich HDL [122]. The enrichment of HDL with triglycerides enhances the action of phospholipid transfer protein and generates a preferred substrate for HL. The HL-mediated hydrolysis of triglyceride reduces the size of the HDL core, especially in A-I HDL [122]. If the release of cholesteryl esters out of HDL is greater than the uptake of the triglycerides, the result is small/dense HDL which is HDL_3 [122].

While most of the lipids in HDL are transferred to other lipoproteins, a portion of cholesteryl esters are transferred to the liver and steroidogenic tissues via the action of the SR-BI receptor. SR-B1 regulates the transport of free cholesterol in cells in a bidirectional manner, depending on the gradient direction of cholesterol. In hepatocytes and steroidogenic cells, SR-B1 (as an HDL receptor) facilitates the selective uptake of cholesteryl ester in two steps: (1) combining HDL with SR-B1; and (2) diffusing cholesteryl ester molecules from the cell plasma membrane [122].

1.6.3 HDL in cardiovascular disease and diabetes

A large body of evidence supports a relationship between low circulating HDL-cholesterol levels and the risk of a cardiovascular events [126]. The first epidemiological study to discover this inverse relationship was the landmark Framingham study which found that for every 0.13 mmol/L decrement in serum HDL there was a 25% increased risk of myocardial infarction [127]. Consequently, several epidemiological studies have also established this relationship [128, 129]. More recently, epidemiological studies have also shown an inverse relationship between HDL cholesterol levels and the risk of developing diabetes. For example, levels of HDL_2 were found to be inversely correlated with the incidence of type 2 diabetes [130]. Interestingly, lower levels of HDL have been associated with an increased risk of diabetic neuropathy, an important contributing factor for DFU formation in both type 1 and type 2 diabetes [131].

Pharmacological elevation of circulating HDL-cholesterol levels using CETP inhibitors has not demonstrated benefit in reducing cardiovascular events [132, 133], but interestingly, CETP inhibitors delay the onset of type 2 diabetes mellitus, indicating an anti-diabetic effect [130]. Furthermore, there is increasing evidence that HDL *functionality* is a more accurate predictor of risk for cardiovascular disease rather than HDL *cholesterol concentrations*. HDL functionality is impaired in conditions such as diabetes and cardiovascular disease [134]. For example, in one study by Besler et al. [135], HDL obtained from patients with coronary artery

disease failed to stimulate endothelial nitric oxide production, a key atheroprotective function of HDL, which contrasted to HDL from healthy subjects. In another significant study, the cholesterol efflux capacity (CEC) of HDL from macrophages, a metric of HDL function, had a strong inverse relationship with both carotid intima-media thickness and the likelihood of angiographic coronary artery disease [136].

Individuals with diabetes are at greater risk of developing cardiovascular disease (CVD) compared to non-diabetic individuals, with approximately 60% of CVD-related deaths occuring in diabetic populations [137]. Type 2 diabetes and the collection of pathologies associated with this metabolic syndrome, including insulin resistance, obesity, and high plasma triglycerides are often associated with low HDL levels [138]. A hallmark of diabetes, as mentioned previously, is increased glycation end products which promote oxidative stress and oxidation of physiologically important biomolecules and increase inflammation, which can impact the functionality of HDL [138]. In the presence of high glucose levels, the apoA-I component of HDL can get glycated and there is a direct correlation between plasma glucose levels and extent of apoA-I glycation, which alters the structural integrity of HDL and consequently its function [139]. Non-enzymatically glycated apoA-I was shown to have a reduced ability to inhibit NF-κB activation and reactive oxygen species formation in a rabbit model of acute vascular inflammation [140].

As mentioned, cholesterol efflux is one of the main roles of HDL and is a measure of its functionality. The primary cause of decreased HDL-mediated cholesterol efflux is the oxidative modification of the HDL particle and its main protein component, apoA-I [141]. Given that apoA-I is the main component of HDL that removes of cholesterol from macrophages, particularly at the arterial wall, oxidative damage of apoA-I directly impairs HDL functionality [138]. Zheng and colleagues [142] showed that myeloperoxidase oxidation of HDL and apoA-I results in selective inhibition in ABCA1-dependent cholesterol efflux from macrophages

[142]. It has also been reported that high levels of non-esterified fatty acids in individuals with diabetes may inhibit ABCA1-mediated reverse cholesterol transport [138]. A clinical study found that both apoA-I and HDL_2-mediated cholesterol efflux were impaired in macrophages treated with albumin isolated from patients with type 1 diabetes, compared with non-diabetic albumin-treated cells. This observation was attributed to intracellular ABCA1 protein content, with the study showing that glycated albumin from poorly controlled type 1 diabetes mellitus in patients with type 1 diabetes alters macrophage gene expression and impairs ABCA1-mediated reverse cholesterol transport [143].

1.6.4 Anti-inflammatory properties of HDL in wound healing

Inflammation is important in the early stages of wound healing to combat infection; however, prolonged, inappropriate inflammation negatively affects wound healing at every step of the repair process. As discussed previously, diabetes exacerbates inflammation and substantially slows its resolution, causing multiple complications in wound biology and healing. Agents that suppress inflammation are, therefore, likely to have significant wound healing benefits. It is well-established that HDL has anti-inflammatory effects that include: (1) the suppression of endothelial cell inflammation and improved endothelial function; and (2) the reduction of monocyte/macrophage activation and recruitment to sites of inflammation [110]. These properties of HDL all have benefits on the wound healing process and the prevention of chronic wound development.

Endothelial cells play a key role in wound healing. They are the building blocks of wound neovessels that are essential for repair. Through their expression of adhesion molecules, chemokines, and cytokines, endothelial cells mediate the delivery of monocytes and macrophages to the wound site. Controlled endothelial cell inflammation is, therefore, critical for successful healing but when inappropriately prolonged or elevated leads to chronic wound development. HDL exhibits potent inhibitory effects on endothelial cell inflammation (Figure 1.7). For example, HDL reduces the expression of key cell adhesion molecules including ICAM-1, VCAM-1 and E-selectin both *in vitro* and *in vivo* [116]. One of the mechanisms for the anti-inflammatory

effects of HDL on endothelial cells starts with the interaction between HDL and the sphingosine-1-phosphate $(S1P)_3$ receptor. This results in the phosphorylation and activation of the phosphoinositide 3-kinase (PI3K)/Akt pathway, which leads to the activation of endothelial nitric oxide synthase and the production of nitric oxide. Whilst nitric oxide plays an important role in the promotion of wound angiogenesis and in maintaining endothelial function it also exhibits anti-inflammatory effects. Several previous studies have illustrated that HDL stimulates endothelial cell nitric oxide production [144]. Nitric oxide inhibits the TNF-α activation pathway via the suppression of inflammatory transcription factor NF-κB [116]. rHDL (apoA-I complexed with phospholipid) also suppresses endothelial cell chemokine expression including CCL2, CCL5, and CX_3CL1. This is mediated via interaction with SR-B1 resulting in the inhibition of downstream kinase signalling and suppression of NF-κB activation [145] (Figure 1.7).

Preclinical models of vascular inflammation have also demonstrated the anti-inflammatory effects of HDL. For example, in a rabbit model of carotid occlusion [146], systemic infusion of rHDL inhibited neutrophil infiltration, the expression of VCAM-1, ICAM-1, and the chemokine CCL2 [146]. HDL has also been reported to increase the anti-inflammatory enzyme platelet activating factor-acetyl hydrolase, which inactivates platelet-activating factor and promotes inflammation [147].

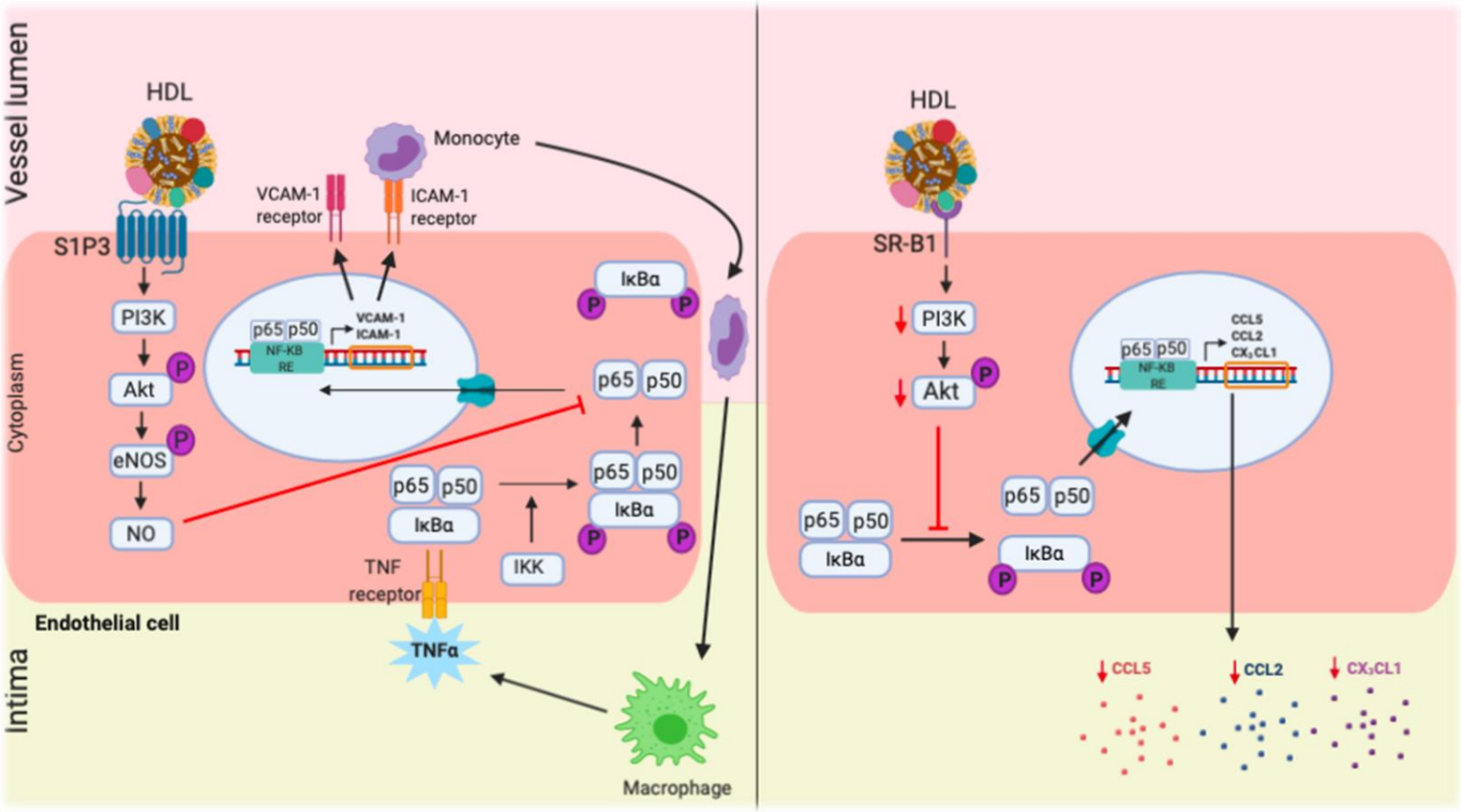
Vessel lumen
HDL
Monocyte
VCAM-1 receptor
ICAM-1 receptor
S1P3
PI3K
Akt
eNOS
NO
p65 p50
NF-KB RE
VCAM-1
ICAM-1
IκBα
TNF receptor
IKK
TNFα
Cytoplasm
Endothelial cell
Intima
Macrophage
SR-B1
CCL5
CCL2
CX3CL1

Figure 1.7 Mechanisms for the anti-inflammatory effects of HDL in endothelial cells.

Left panel: HDL increases formation of bioactive nitric oxide (NO) via interaction with the sphingosine-1-phosphate 3 (S1P3) receptor, which activates PI3K/Akt and leads to the inhibition in the action of NF-κB. This prevents the translocation of the NF-κB subunits p65/p50 to the nucleus where it binds to the NF-κB response elements in the promoter region of inflammatory genes including vascular cell adhesion molecule (VCAM)-1 and intercellular cell adhesion molecule (ICAM)-1. **Right Panel:** In an alternative pathway, HDL reduces the production of the inflammatory cytokines CCL2, CCL5 and CX_3CL1 via interaction with scavenger receptor (SR)-B1 that leads to suppression of downstream kinase signalling (PI3K/Akt) and inhibition of the NF-κB activation pathway. Image adapted from [148].

Macrophages are an important cell type for both the initiation and resolution of the inflammation phase of wound healing [12]. Multiple studies have demonstrated that HDL has anti-inflammatory effects on human monocytes and macrophages, which is likely to have substantial benefits on the wound healing process. For example, HDL prevents the activation of primary human monocytes by significantly decreasing the expression of CD11b [149]. In an *in vitro* study [149], HDL inhibited phorbol 12-myristate-13-acetate (PMA)-induced activation of monocyte CD11b in a dose-dependent manner [149]. Furthermore, when monocytes were pre-treated with HDL followed by stimulation with PMA, CD11b expression was significantly reduced [149].

HDL has also been shown to promote a shift from M1-like macrophages to M2-like macrophages. In a study by Sanson *et al*., [150] HDL suppressed both basal and IFN-γ-induced expression of M1 inflammatory markers such as iNOS, IL-6 and TNF-α. Furthermore, HDL caused a 10-fold increase in the expression of the M2-like markers Arg-1 and Fizz-1 [150]. It is important to note that both Arg-1 and Fizz-1 are likely to contribute to tissue remodelling in wound healing as they have been shown to mediate the deposition of ECM in animal models [151]. These findings further highlight the biological plausibility of utilising the anti-

inflammatory properties of HDL for wound healing. HDL also inhibits the production of inflammatory cytokines from monocytes. One mechanism by which HDL does this is via binding of the apoA-I component of HDL to the 'stimulating factor' on circulating stimulated T lymphocytes. This blocks the normal interaction between monocytes and stimulated T lymphocytes, thereby preventing cytokine release (e.g. IL-1β, TNF-α) from monocytes at sites of inflammation (Figure 1.8) [152]. ApoA-I has also been shown to inhibit the production of inflammatory cytokines such as IL-1β, TNF-α, and intercellular reactive oxygen species by blocking the interaction of T cell ligands to the leukocyte β2-integrin subunit [116]. Consistent with these findings, rHDL reduces the secretion of the chemokines CCL2, CCL5, and CX_3CL1 from monocytes and the expression of the chemokine receptors CCR2 and CX_3CR1 [145]

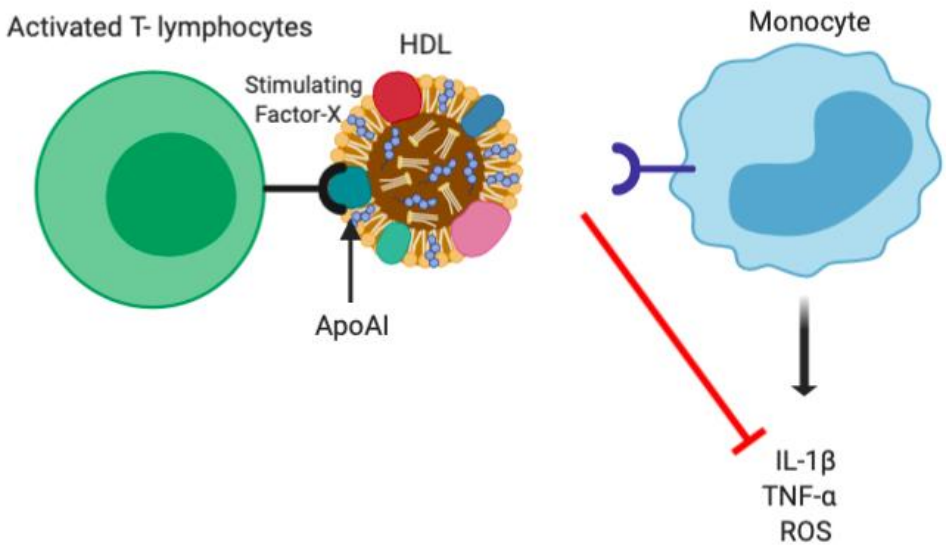

Figure 1.8 Anti-inflammatory effects of HDL on monocyte/macrophages.

HDL blocks the interaction between stimulated T lymphocytes and monocytes by interacting with 'stimulating factor X' on T lymphocytes. This reduces the interaction between stimulated T lymphocytes and monocytes which in turn reduces monocyte secretion of inflammatory cytokines and reactive oxygen species. Image created on Biorender.

HDL also suppresses TLR-induced expression of pro-inflammatory cytokines from macrophages [153]. For example, pre-treatment of bone marrow-derived macrophages with HDL reduced IL-6 and TNF-α secretion in response to a variety of TLR ligands. The mechanism for these effects of HDL was found to be via regulation of the activating transcription factor ATF3 that is downstream of the TLR. ATF3 is induced through TLR stimulation and acts through a negative feedback system to inhibit excessive production of pro-inflammatory cytokines. Interestingly, infusion of HDL into mice increased the level of ATF3 mRNA expression in the Kupffer cells (macrophages) of the liver. In the same study, HDL demonstrated an endothelial-protective effect by increasing re-endothelisation of carotid arteries after carotid injury, an effect that was not observed in Atf-3-deficient mice [153].

1.6.5 Pro-angiogenic properties of HDL in wound healing

A number of studies demonstrate a pro-angiogenic effect of HDL *in vitro* in response to hypoxia and in pre-clinical murine models of hind-limb ischaemia and wound healing [91]. *In vitro*, HDL has been shown to significantly induce proliferation, migration, and tubule formation of endothelial cells, which are critical for angiogenesis. Investigation of the intracellular mechanisms has revealed that these changes in endothelial cell function occur through the Src family kinases PI3K and mitogen-activated protein kinase (MAPK) with the involvement of SR-BI [154]. SR-BI has also been implicated as the receptor that mediates the augmentation of ischaemia-driven angiogenesis in *in vivo* murine models of hind-limb ischaemia and wound healing [155]. In SR-B1$^{-/-}$ mice, it was delineated that HDL activates the PI3K/Akt pathway via SR-BI, leading to increased levels of HIF-1α and the transcription and production of VEGF-A (Figure 1.9). Further investigation of the mechanisms of action revealed that in endothelial cells, rHDL stabilises HIF-1α in high glucose through an increase in the ubiquitin ligases Siah-1 and Siah-2 which then suppress the prolyl hydroxylase domain (PHD) proteins PHD-2 and PHD-3 that normally target HIF-1α for degradation [156]. There is also emerging evidence that rHDL stabilises HIF-1α and improves angiogenesis in diabetes by correction of impaired metabolic reprogramming responses to hypoxia [157].

VEGF-A is a potent pro-angiogenic growth factor that is under the control of HIF-1α. It activates numerous angiogenic cellular activities once bound to its receptor, VEGFR-2, on endothelial cells. Following binding, the extracellular signal-regulated kinase (ERK)1/2 and p38MAPK downstream signalling pathways are activated which are important for endothelial cell proliferation and cell migration, respectively. In a recent *in vitro* study, rHDL was shown to augment VEGFR-2 phosphorylation and activate ERK1/2 and p38MAPK in endothelial cells under hypoxic conditions, adding further mechanistic support to understanding the proangiogenic effects of rHDL [158].

S1P is a bioactive lipid mediator that regulates angiogenesis, vascular stability, and permeability [159]. HDL transports 60% of the S1P in the plasma making it the main acceptor and carrier of S1P. It has been reported that HDL-mediated angiogenesis involves activation of VEGFR-2 via the S1P3 signalling pathway [159]. This occurs via binding of the HDL/S1P to the S1P3 receptor which then phosphorylates/activates VEGFR-2 and promotes angiogenic functions including proliferation, migration, and tubule formation in endothelial cells [159]. The Ras-activated MAPK pathway was the reported intracellular mechanism of action for these HDL-S1P/S1P3 receptor-driven pro-angiogenic effects of HDL [160].

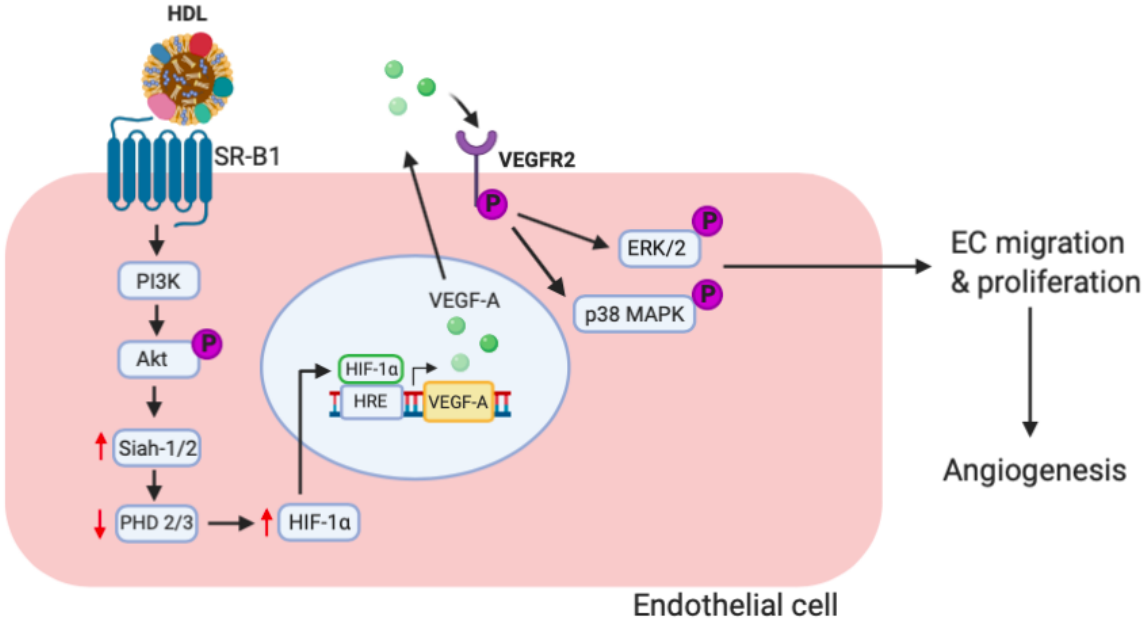

Figure 1.9 The pro-angiogenic effects of HDL in endothelial cells.

Following interaction with scavenger receptor (SR)-B1, HDL activates downstream PI3K/Akt signalling. This increases HIF-1α stabilisation through an increase in the ubiquitin ligases Siah-1 and Siah-1 which inhibits the prolyl hydroxylase domain (PHD) proteins PHD-2 and PHD-3 that normally target HIF-1α for degradation. With increased HIF-1α stabilisation it allows for elevated levels of HIF-1α translocation to the nucleus. In the nucleus, HIF-1α binds to HIF response elements (HRE) in the promoter regions of pro-angiogenic genes including VEGF-A that increases their expression. This increases the interaction between VEGF-A with its receptor VEGFR-2, leading to enhanced activation of ERK1/2 and p38 MAPK that promote endothelial cell migration and proliferation, respectively, and result in increased angiogenesis. Image adapted from [148].

1.6.6 Emerging role of topical HDL in wound repair

Accumulating evidence demonstrates that HDL displays significant wound healing benefits. For example, drop-wise topical application of rHDL to non-diabetic and diabetic wounds in a murine model of wound healing improves the rate of wound closure [155, 161]. Using Laser Doppler imaging, topical HDL was shown to increase wound angiogenesis in both non-diabetic and diabetic mice. This effect of rHDL was attenuated in SR-BI$^{-/-}$ mice, demonstrating that SR-BI, at least in part, mediates improved wound healing and wound angiogenesis by rHDL [155]. Daily topical application of HDL formulated in a 20% Pluronic F-127 gel (pH 7.2) also increased wound healing in atherosclerosis-prone apolipoprotein (apo)E$^{-/-}$ mice through an increase in granulation tissue formation and re-epithelisation [162]. Furthermore, a study in 24-month-old mice also found that topical rHDL promoted the rate of wound healing and wound angiogenesis [161].

1.6.7 Epidemiological evidence of a role for serum HDL in wound healing

Only one clinical study has specifically evaluated the relationship between endogenous HDL-cholesterol levels and diabetic wound healing outcome [163]. In 163 patients with an existing DFU in a single hospital in Japan, this study found an inverse correlation between circulating HDL-cholesterol levels and three endpoints: (1) minor amputation, or below the ankle amputation; (2) major amputation or amputation above the ankle; and (3) wound-related death (defined as a death with unhealed ulcer). This independently suggested that endogenous HDL-cholesterol is a predictor for lower extremity amputation.

1.7 Hypothesis and Aims

Wound healing is a complex and tightly regulated process. Some flexibility exists in the process to support imbalances within each step and sequence, however, if this carefully regulated system is disrupted too much it can lead to the development of a chronic non-healing wound. Multiple mechanisms are affected by diabetes including prolonged inflammation and impaired angiogenesis - two principal features of diabetes-impaired wound healing. Due to the complicated nature of diabetic wound healing, a successful therapy for DFU needs to exhibit pleiotropic actions. Currently there is no therapy with pleiotropic actions for DFU, highlighting a significant need for new wound healing treatments.

HDL exhibits anti-inflammatory, endothelial protective, and pro-angiogenic effects in response to ischaemia and therefore possesses significant wound healing therapeutic potential through regulation of multiple important wound healing mechanisms. Whilst topical rHDL has been shown to rescue diabetes-impaired wound healing by promoting angiogenesis [155], the anti-inflammatory effect of topical rHDL on wounds, including its effects on macrophage polarisation, is yet to be investigated. As mentioned previously, a recent epidemiological study found an inverse relationship between endogenous HDL-cholesterol levels and diabetic wound healing outcomes [163]. There is increasing evidence that HDL functionality is a better predictor of cardiovascular disease risk rather than HDL-cholesterol concentration. HDL functionality as a predictive factor for wound healing outcomes has not yet been explored.

Accordingly, the hypotheses of this thesis are that: (1) topical rHDL will have anti-inflammatory effects in diabetic murine wounds and (2) that HDL functionality will be predictive of wound healing success in people with DFU.

The aims this PhD thesis are:

Aim 1:

In a diabetic murine model of wound healing:

A) Assess the anti-inflammatory effects of topical rHDL in wound by measuring changes in key inflammatory mediators.
B) Assess the effect of topical rHDL on macrophage polarisation in wounds.
C) Track the fate of fluorescently labelled rHDL in wounds after topical application.

Aim 2:

In patients with and without diabetes and toe amputation/s:

1 Assess changes in the anti-inflammatory, pro-angiogenic and cholesterol efflux capacity of isolated HDL at the time of amputation, and one-month and six months post-amputation
2 Determine the relationship between HDL functionality indices and the rate of wound closure

CHAPTER 2 – GENERAL METHODS

2.1 Materials

Table 2.1 List of Reagents and Materials.

Reagent/Material (Product Code)	**Manufacturer**
1-Bromo-3-chloropropane (B9673)	Sigma-Aldrich, MO, USA
1-Palmitoyl-2-linoleoyl phosphatidylcholine (850458P)	Avanti Polar Lipids, AL, USA
2-Propanol (19516)	Sigma-Aldrich, MO, USA
^{3}H-Cholesterol NET 139 (NET139001MC)	PerkinElmer, MA, USA
Chloroform (AJA152-2.5L GL)	Ajax Finechem, NSW, Australia
Click-iT™ EdU Alexa Fluor™ 488 Flow Cytometry Assay Kit (C10420)	Life Technologies, CA, USA
DiO powder (D275)	Life Technologies, CA, USA
Dulbecco's Phosphate Buffered Saline (D1408-500ML)	Sigma-Aldrich, MO, USA
Dulbecco's Modified Eagle Medium (D5523)	Sigma-Aldrich, MO, USA
EDTA (E3889)	Sigma-Aldrich, MO, USA
Emulsifier-Safe (6013389)	PerkinElmer, MA, USA
Ethanol (E7023)	Sigma-Aldrich, MO, USA
Fluorescence Mounting Media (S3023802)	Dako, CA, USA
Foetal Bovine Serum (AU-FBS/PG)	CellSera, NSW, Australia
Guanidine hydrochloride (G4505)	Sigma-Aldrich, MO, USA
SsoAdvancedTM Universal SYBR® Green Supermix (1725275)	Bio-Rad Laboratories, CA, USA
iScript cDNA Synthesis Kit (1708841)	Bio-Rad Laboratories, CA, USA
Isopropanol (I9516)	Sigma-Aldrich, MO, USA
LabAssay™ Cholesterol kit (294-65801)	Wako Diagnostics, VA, USA
LabAssay™ Triglyceride kit (290-63701)	Wako Diagnostics, VA, USA

Matrigel® Growth Factor Reduced Basement Membrane Matrix (356231)	Corning Life Sciences, NY, USA
MesoEndo Cell Growth Medium (212-500)	Cell Applications Inc., CA, USA
Methanol (MA004)	Chem-Supply, SA, Australia
Nuclease-free water (P1193)	Promega, WI, USA
Paraformaldehyde (C004)	ProSciTech, QLD, AUS
Phosphatase Inhibitor Cocktail 2 (P5726)	Sigma-Aldrich, MO, USA
Pierce BCA Protein Assay Kit (23227)	ThermoFisher Scientific, MA, USA
Polyethylene glycol (P2139)	Sigma-Aldrich, MO, USA
Potassium bromide (PA006)	Chem-Supply, SA, Australia
Protease Inhibitor Cocktail (P8340)	Sigma-Aldrich, MO, USA
Sodium Azide (SA189)	Chem-Supply, SA, Australia
Sodium Chloride (71380)	Sigma-Aldrich, MO, USA
Sodium Cholate Hydrate (C6445)	Sigma-Aldrich, MO, USA
Sodium Citrate Tribasic Dihydrate (C8532)	Sigma-Aldrich, MO, USA
Tissue-Tek® O.C.T. compound (IA018)	ProSciTech, QLD, Australia
TRI® Reagent (T9424)	Sigma-Aldrich, MO, USA
Tris hydrochloride (T3253)	Sigma-Aldrich, MO, USA
Trypsin-EDTA (15400054)	ThermoFisher Scientific, MA, USA
Tumour Necrosis Factor-α Human (T0157)	Sigma-Aldrich, MO, USA
Trypan Blue solution (T8154)	Sigma-Aldrich, MO, USA
Tween®-20 (P9416)	Sigma-Aldrich, MO, USA
Vectashield® Antifade Mounting Medium with DAPI (H-1200)	Vector Laboratories, CA, USA

2.2 Preparation of participant HDL, discoidal rHDL, and DiO discoidal rHDL

2.2.1 Participant samples and HDL isolation

Blood samples were obtained from cohorts of men and women aged 46–79 years from groups classified as: Group 1 – patients with diabetes requiring toe/ray amputation (n=19), Group 2 – patients without diabetes requiring toe/ray amputation (n=6) and Group 3 - healthy aged and gender matched (n=20). For Groups 1 and 2, blood samples were collected at the time of surgery, 1-month post-amputation, and six-months post-amputation. This study was approved by the Central Adelaide Local Health Network (CALHN) Human Research Ethics Committee (Reference number: HREC/19/CALHN/349 and CALHN reference number: 11743). All study participants gave informed consent.

Whole blood (9 mL) was collected into two EDTA-treated tubes; the plasma was then collected by centrifuging the blood tube for 10 minutes at 1,000–2,000 g at 4°C using an Eppendorf refrigerated centrifuge 5145R (Eppendorf, Hamburg, Germany). To isolate HDL from plasma samples, 100–200 μL of plasma was incubated with equal volumes of polyethylene glycol (PEG600- 200 mg/mL in MilliQ water) at room temperature for 5 minutes to precipitate the apoB-containing lipoproteins. The samples were then centrifuged at 13,000 rpm for 5 minutes at 4°C. The supernatant (containing the HDL fraction) was collected, and filter sterilised using a 0.22 μm filter. The HDL concentration was determined using the Pierce™ BCA Protein Assay Kit, following manufacturer's instructions. Isolated participant HDL was used for subsequent cell culture studies to assess anti-inflammatory and angiogenic capacity.

2.2.2 Reconstituted discoidal HDL production

ApoA-I, the main protein component of native HDL, was isolated from pooled, autologously donated human plasma kindly provided by the Red Cross Blood Bank, Adelaide, South Australia, by ultracentrifugation and anion-exchange chromatography, as described previously

[164]. Approval was granted by the Sydney Local Health District Human Ethics Review Committee (HREC\EXECOR\15-06) and conformed to the Declaration of Helsinki, with informed consent obtained at the time of collection.

Purified lipid-free apoA-I was reconstituted in reconstitution buffer (100 mM Tris, 3 M guanidine hydrochloride, pH 8.2) then dialysed in Tris-buffered saline (TBS: 10 mM Tris, 150 mM NaCl, 4.6 mM NaN_3, 0.17 mM EDTA, pH 7.4) for 5 days, which was replaced daily. The molecular weight cut off for the dialysis tubing was 10,000 (Thermo scientific, USA). After dialysis, the apoA-I protein concentration was measured using the BCA Protein Assay Kit. Discoidal reconstituted HDL (rHDL) was prepared by complexing purified lipid-free apoA-I with the phospholipid 1-palmitoyl-2-linoleoyl-phosphatidycholine (PLPC) for 2 h at an initial PLPC: apoA-I molar ratio of 100:1. PLPC was added to glass tubes and dried to form a thin layer using a stream of nitrogen gas. The PLPC was lyophilised overnight, followed by incubation with 30 mg/mL sodium cholate in TBS. The tubes were vortexed every 15 mins until optically clear, then 2 mg apoA-I was added to each tube and allowed to complex with PLPC for 2 h on ice. The tube contents were pooled and dialysed against 5 × 1 L changes of TBS over 5 days, followed by dialysis against 3 × 1 L PBS. The rHDL was filter sterilised prior to use in all cell culture experiments and the final apoA-I concentration was determined using the BCA assay. The final PLPC: apoA-I molar ratio ~80:1.

2.2.3 DiO Discoidal rHDL

Fluorescently labelled discoidal rHDL was prepared by complexing the PLPC with DiO powder (Life Technologies, Eugene, USA) in a 100:1 ratio as previously described [165]. The details of DiO-rHDL preparation are discussed in Chapter 3.

2.3 Cell culture

Human coronary artery endothelial cells (HCAEC; Cell Applications Inc., San Diego, CA, USA) were cultured at 37°C and 5% CO_2 in Meso Endo Cell Growth Medium and used for experiments at passage 4. To harvest HCAECs for experiments, cells were washed twice with PBS then incubated with 0.05% (w/v) trypsin-EDTA in PBS for 5 min at 37°C, typically 5 mL per T-75 culture flask. After checking for complete cell detachment, the trypsin was inactivated by adding an equal volume of MesoEndo. The cell suspension was then transferred to clean tubes before centrifugation at 2,500 rpm for 5 min at room temperature. After removing the supernatant, the cells were resuspended in MesoEndo and counted on a haemocytometer after mixing 1:1 with Trypan Blue solution to identify non-viable cells.

HCAECs were subsequently seeded at the required density and exposed to either: (i) unstimulated controls, (ii) inflammation, or (iii) glucose conditions. To mimic an inflammatory milieu *in vitro*, HCAECs were incubated in MesoEndo containing TNFα. For the glucose conditions, cells were incubated in either normal (5 mM) or high (25 mM) supplemented with D-glucose MesoEndo media. Further details regarding cell culture for the *in vitro* experiments are provided in Chapter 5.

2.4 Real-time polymerase chain reaction

2.4.1 RNA extraction

At the conclusion of the cell culture studies, the media was removed, and the cells were washed twice with cold PBS. RNA was isolated from HCAECs and murine wound tissue using TRI reagent before transferring the lysates to autoclaved Eppendorf tubes. Then 50 μL of 1-bromo-3-chloropropane was added to each sample and the tubes were vigorously vortexed for 15 seconds to ensure complete mixing of both aqueous and organic phases. Samples were then centrifuged at 14,000 rpm for 15 min at 4°C. The top aqueous layer was transferred to a separate autoclaved tube containing 250 μL of isopropanol prior to storing at –20°C at least overnight.

The samples were then briefly vortexed and centrifuged at 14,000 rpm for 15 min at 4°C. The supernatant was carefully removed, and the remaining cell pellet was washed with 250 µL ice-cold 70% (v/v) ethanol. The samples were vortexed and centrifuged again at 14,000 rpm for 10 min at 4°C. The ethanol wash was removed, and the pellet allowed to air-dry in a fume hood for 5–10 min prior to dissolution in 20 µL of nuclease-free water pre-warmed to 60°C. To facilitate complete dissolution, samples were further agitated in a ThermoMixer (Eppendorf, Macquarie Park, NSW, Australia) at 300 rpm for 5 min at 60°C. The extracted RNA was kept on ice or stored at 80°C prior to quantitation.

2.4.2 RNA quantification

The quantity of RNA in each sample was determined using a spectrophotometer (NanoDrop 2000, ThermoFisher Scientific, CA, USA). Absorbance was measured at 260 nm (*A*260) and 280 nm (*A*280), and the purity of the extracted RNA was determined from the absorbance ratio (*A*260/*A*280), with a value between 1.6–2.0 considered acceptable purity. RNA concentration was calculated from the *A*260, corrected using a conversion factor according to the formula: (RNA) = *A*260 x 40. All RNA samples were normalised to a concentration of 100 ± 5 ng/µL and stored at –80°C until further use.

2.4.3 Complementary DNA synthesis

Complementary DNA (cDNA) was synthesised by reverse transcription of 400 ng total RNA from each sample using the iScript cDNA Synthesis Kit (Bio-Rad Laboratories, Hercules, CA, USA), performed in triplicate as per the component volumes outlined in Table 2.2. The reactions were performed using a T100 Thermal Cycler (Bio-Rad) using a pre-set protocol for first-strand cDNA synthesis: annealing at 25°C for 5 min, extension at 42°C for 30 min, and inactivation at 95°C for 5 min. Triplicate cDNA samples were pooled and diluted 1:3 in nuclease-free water, then stored at –20°C until further use.

Table 2.2 Reverse transcription reaction mix.

Component	Volume (µL)
5x iScript Reaction Buffer	2.0
Nuclease-Free Water	4.0
Normalised RNA	4.0
Total	10.0

2.4.4 Quantitative real-time PCR

The mRNA expression levels of the genes of interest, *CCL2*, *IL-6*, *RELA*, *TGF- β1*, *CCL5*, *VCAM-1*, *ICAM-1* and *CX3CL1*, as well as the reference housekeeper gene, human β2-microglobulin, were measured in triplicate by quantitative real-time PCR (qPCR) using the SsoAdvanced SYBR® Green SuperMix in a QuantStudio™ 7 Flex Real-Time PCR System (Table 2.3). All amplicons were amplified according to the reaction mix outlined in Table 2.4, with 40 pmol of forward and reverse primers (primer sequence details are noted in the relevant chapters). The PCR protocol used was as follows: initial activation step at 95°C for 3 minutes then a 3-step cycling protocol of 95°C for 15 seconds, 58°C for 30 seconds, and 72°C for 30 seconds (40 cycles). Dissociation (melting) curve analysis of the PCR products was also performed: 95°C for 10 seconds and 65.0°C – 95.0°C in increments of 0.5°C/s for 15 seconds.

Table 2.3 Primer sequences for qPCR. Supplier: Sigma-Aldrich.

Gene	Sequence	
	Forward	**Reverse**
B2M	5'-CATCCAGCGTACTCCAAAGA-3'	5'-GACAAGTCTGAATGCTCCAC-3'
RELA	5'-GTTCACAGACCTGGCATCC-3'	*5'-TGTCACTAGGCGAGTTATACG-3'*
CX3CL1	*5'-TGCCCTAACTCGAAATGGCG-3'*	5'-GGCTCCAGGCTACTGCTTTC-3'
CCL2	5'-TCATAGCAGCCACCTTCATT-3'	5'-TCGGAGTTTGGGTTTGCTT-3'
CCL5	5'-CAGTCGTCCACAGGTCAAGG-3'	5'-CTTCTCTGGGTTGGCACACA-3'
VCAM-1	5'-GGACCACATCTACGCTGACA-3'	5'-TTGACTGTGATCGGCTTCCC-3'
ICAM-1	5'-CAAGGCCTCAGTCAGTGTGA-3'	5'-TCTGAGACCTCTGGCTTCGT-3'

Table 2.4 Quantitative real-time PCR reaction mix.

Component	**Volume (µL)**
SsoAdvanced SYBR® Green SuperMix	5.0
Forward Primer (10µM)	0.4
Reverse Primer (10µM)	0.4
Nuclease-Free Water	1.7
cDNA sample	2.5
Total	10.0

2.4.5 PCR data analysis

Relative changes in mRNA expression were calculated using the standard $^{\Delta\Delta}Ct$ method [166] normalised to *β2-microglobulin* and unstimulated controls. Specifically, this involved determining the difference between the mean threshold cycle (*Ct*) values of the gene of interest and the reference gene, *β2-microglobulin*, for each sample. The mean *Ct* difference for the experimental control was then subtracted from that of each experimental treatment and the fold

change in expression (relative to the control) for each sample was then calculated by taking the inverse of base 2 raised to the power of these values. These were averaged to determine the fold change in mRNA for each treatment as a percentage of the control.

2.5 Protein analysis

2.5.1 Protein extraction

To digest wound tissue for protein analysis, 300 µL of cell lysis buffer (0.1 M Tris HCl, 0.1 M NaCl, 0.05 M NaF,0.005 M Na4P2O7, 1 mL Triton-X 100, pH 7.4) containing phenylmethanesulfonyl fluoride solution (1:100 dilution) and protease inhibitor cocktail (PIC; 1:100 dilution) were added to the homogenisation tube containing the wound tissue. Tissues were homogenised at 6,000 rpm for 30 seconds for up to four-times using a Precellys homogeniser (Bertin Technologies, France) with a quick spin between homogenisations. After tissue homogenisation, samples were centrifuged at 14,000 rpm for 1 min at 4°C and the supernatant was then transferred to autoclaved Eppendorf tubes and stored at -80°C until further use.

2.5.2 Protein estimation

An estimate of protein concentration for each sample was determined using the Pierce BCA Protein Assay Kit. To construct a standard curve, various standard solutions were prepared by diluting 2 mg/mL bovine serum albumin (BSA) stock in MilliQ water according to Table 2.4. In a 96-well plate, 5 µL of each standard solution was loaded in duplicate wells along with 5 µL of each sample in single wells. BCA reagent mix was prepared by combining 50 parts reagent A with 1 part reagent B (copper (II) sulphate); 195 µL of this was added to each standard or sample well. The plate was incubated at 37°C for 30 min, after which the absorbance of each well was measured at 595 nm using a microplate reader (GloMax® Discover Multimode Microplate Reader spectrophotometer; Promega). The standard curve was constructed by linear

regression in Microsoft Excel and the unknown protein concentrations of each sample was interpolated from this standard curve.

Table2.5 Standard BSA solutions used in BCA assay.

BSA (mg/mL)	BSA stock (μL)	MilliQ water (μL)
0	0	300
0.25	37.5	262.5
0.5	75	225
0.75	112.5	187.5
1	150	150
1.25	187.5	112.5
1.5	225	75
2	300	0

2.5.3 ELISA

To measure the protein expression of IL-6, TGF-β1, and CCL2 in murine wound tissues, enzyme-linked immunosorbent assay (ELISA) kits (R&D systems, Minneapolis, USA) were used: 50 – 100 mg of total protein was added to the relevant assay plate with assay diluent and incubated for 2 h. The wells were then washed and rinsed with wash buffer four-times before adding the mouse conjugate and incubating for 2 h. A second round of washes were performed before incubation with the substrate solution for 30 minutes. At the end of this incubation period, the stop solution was added, and the absorbance was recorded at 450 nm.

2.6 Statistical analysis

Data were analysed using GraphPad Prism software (version 9, Software MacKiev, California, USA) and SPSS (version 27). GraphPad Prism (version 9) and SPSS (version 27)

were used for graph preparation. Normal distribution of data was determined using the Shapiro–Wilk test. All results are expressed as mean ± standard error of the mean (SEM). All data were compared using either an unpaired t-test, one-way analysis of variance (ANOVA) or two-way ANOVA, followed by *post hoc* analysis using Bonferroni's multiple comparison tests, where appropriate. Statistical significance was set at a two-sided $P<0.05$.

CHAPTER 3 – THE EFFECT OF TOPICAL RECONSTITUTED HIGH-DENSITY LIPOPROTEINS ON WOUND INFLAMMATION AND MACROPHAGE POLARISATION IN DIABETIC MURINE WOUNDS

3.1 Introduction

As described in Chapter 1, wound healing is a dynamic and complex process consisting of four continuous yet overlapping phases characterised by haemostasis, inflammation, proliferation, tissue maturation and vascular remodelling [3]. Some flexibility exists in the wound healing process to support imbalances within each step and sequence, however, excessive disruption to this carefully regulated system, as caused by diabetes, can lead to the development of chronic non-healing wounds such as DFU. Approximately 25% of people living with diabetes develop DFU during their lifetime. It is estimated that 20% of patients with a DFU require minor amputations [57] and patients with an existing DFU are at 2.5-times higher risk of death than patients with diabetes and without an ulcer over 5 years [57, 60].

Prolonged inflammation prevents successful wound healing and is a key mechanism that causes impaired wound healing in patients with diabetes [148]. Inflammation is important in the early stages of wound healing by preventing infection, however, prolonged, inappropriate inflammation has negative effects on the healing process [12]. Despite the significant clinical demand for an effective DFU treatment, there are no treatments that actively improve DFU wound healing.

HDL has been shown to exhibit potent anti-inflammatory properties in pre-clinical studies [167, 168]. Our team has previously shown that topical application of rHDL rescues diabetes-impaired murine wound healing by enhancing wound angiogenesis [155]. The pro-angiogenic effects of rHDL were shown to be mediated by increases in VEGF-A/VEGFR-2 production and signalling and enhanced endothelial nitric oxide synthase activity [155].

It is well-established that HDL has anti-inflammatory properties which have been demonstrated *in-vitro* and *in-vivo* [145, 146]. These properties include the ability to suppress cytokine and chemokine expression from endothelial cells [169], smooth muscle cells [170], and monocytes/macrophages [171]. HDL has also been shown to increase the transition of pro-inflammatory (M1-like)

macrophages to anti-inflammatory reparative (M2-like) macrophages [150] . Whether HDL exhibits anti-inflammatory properties in diabetic wounds, in which these same mechanisms are important for successful healing, is currently unknown.

Whilst rHDL has been applied topically to full-thickness murine wounds in several studies [155, 172] its fate and uptake into wound cells has never been tracked. This information is important for understanding the required frequency of application and to support its future translation. Accordingly, this Chapter will assess the anti-inflammatory effect of topical rHDL in a diabetic murine model of wounding by measuring (1) key inflammatory mediators in the wounds, (2) changes in pro-inflammatory (M1-like) and anti-inflammatory (M2-like) macrophage populations, and (3) tracking the fate of fluorescently labelled rHDL.

3.2 Methods

3.2.1 Reconstituted Discoidal HDL

ApoA-I, the main protein component of native HDL, was isolated by ultracentrifugation and anion-exchange chromatography, as described previously [164], from pooled samples of plasma donated by healthy humans (Australian Red Cross; Supply Agreement 14-02NSW-04). Purified lipid-free apoA-I was reconstituted in reconstitution buffer (100 mM Tris, 3 M guanidine hydrochloride, pH 8.2) then dialysed against TBS (10 mM Tris, 150 mM NaCl, 4.6 mM NaN3, 0.17 mM EDTA, pH 7.4) for 5 days, which was replaced daily. After dialysis, the apoA-I protein concentration was measured using the BCA Protein Assay Kit. Discoidal rHDL was prepared by complexing purified lipid-free apoA-I with PLPC for 2 h at an initial PLPC: apoA-I ratio of 100:1. PLPC was initially added to glass tubes and dried to form a thin layer using a stream of nitrogen gas. The PLPC was lyophilised overnight, followed by incubation with 30 mg/mL sodium cholate in TBS. The tubes were vortexed every 15 mins until optically clear; 2 mg apoA-I was then added to each tube and allowed to complex with PLPC for 2 h on ice. The tube contents were pooled and dialysed against 5 × 1 L changes of TBS over 5 days, followed by dialysis against 3 × 1 L PBS. The rHDL was filter-sterilised prior to use in all cell culture experiments and the final apoA-I concentration was determined using the BCA assay. The final PLPC: apoA-I molar ratio was ~80:1.

3.2.2 DiO Discoidal rHDL

Preparation of fluorescent DiO-rHDL was similar to above (section 3.2.1) with the exception that the PLPC was first complexed with DiO powder (Life technologies, Eugene, USA) in a 100:1 ratio, as previously described [165]. To protect the fluorescent signal from light (photo-bleaching), the samples were always covered with aluminium foil.

3.2.3 Animal Studies

Mice were housed in specific pathogen-free conditions in the animal facility at South Australian Health and Medical Research Institute (SAHMRI). All experimental protocols were approved by the SAHMRI Animal Ethics Committee (SAM301). Six- to eight-week-old male C57BI/6J mice were rendered diabetic by a single high-dose intraperitoneal injection of streptozocin (165 mg/g; Sigma Aldrich). Hyperglycaemia was confirmed 2-weeks post-streptozocin injection with non-fasting blood glucose concentrations of ≥ 15.0 mmol/L.

Table3.1 weight and blood glucose levels of mice for the inflammation study.

Macrophage study	Body weight (gr)		Blood glucose (mmol/L)	
	Diabetic Mice	Non-Diabetic Mice	Diabetic Mice	Non-Diabetic Mice
Day0	21.97 ± 0.67	26.54 ± 0.59	26.88 ± 2.98	11 ± 1.98
Day1	21.88 ± 0.67	25.24 ± 0.32	NA	NA
Day2	21.94 ± 0.64	26.12 ± 0.45	NA	NA
Day3	21.74 ± 0.44	26 ± 0.40	NA	NA
Day4	21.65 ± 0.67	26.764 ± 0.45	NA	NA
Day5	22 ± 0.69	25.24 ± 0.32	NA	NA
Day6	21.8 ± 0.64	25.24 ± 0.32	NA	NA
Day7	21 ± 0.56	25.24 ± 0.32	NA	NA

Table3.2 weight and blood glucose levels of mice for the macrophage characterisation study.

Inflammation study	Body weight (gr)		Blood glucose (mmol/L)	
	Diabetic Mice	Non-Diabetic Mice	Diabetic Mice	Non-Diabetic Mice
Day0	23.27 ± 1.03	26.54 ± 0.59	26.60 ± 1.96	10 ± 1.98
Day1	22.75 ± 1.13	25.24 ± 0.32	NA	NA
Day2	23.34 ± 0.83	26.12 ± 0.45	NA	NA
Day3	23.37 ± 0.78	26 ± 0.40	NA	NA

3.2.4 Murine Model of Wound Healing

The murine model of wound healing is illustrated in Figure 3.1A [173]. The wound healing surgery occurred after the mice for the diabetic group were confirmed to be diabetic. For the purpose of the wound healing surgery, the mice were anaesthetised using 5% isofluorane in 100% oxygen (flow rate 1 L/min) and then maintained under anaesthesia using 2.5% isofluorane. The fur was then removed using clippers followed by light application of depilatory cream to ensure no hair was present for the surgery. Two full-thickness wounds (4 mm in diameter) were created on the either side of the mouse's sub-flank area, followed by adhering and suturing a silicone splint (10mm diameter circle with 6 mm inner circle cut) around the wound area to prevent the wound contraction that occurs in rodents, more closely replicating wound healing in humans. For each mouse, one wound received rHDL (50 μg/wound/day) and the other received PBS by topical application. A transparent occlusive dressing (Opsite^{TM}) was applied. Two cohorts of diabetic and non-diabetic mice (n=9-10 mice/group) were used to track the changes in wound inflammation at 24 h (early inflammation) and Day 3 (mid inflammation) post-wounding Figure3.1B. An additional cohort was used at Day 7 post-wounding for assessment of wound macrophages. Excised skin tissues collected at the time of surgery were used for baseline measurements (i.e. 0 h post-wounding). Wound areas were measured daily to track wound closure and were calculated from the average of three diameter measurements along the x-, y- and z-axes using a micro-calliper. Wound closure is expressed as a percentage of initial wound area at day 0.

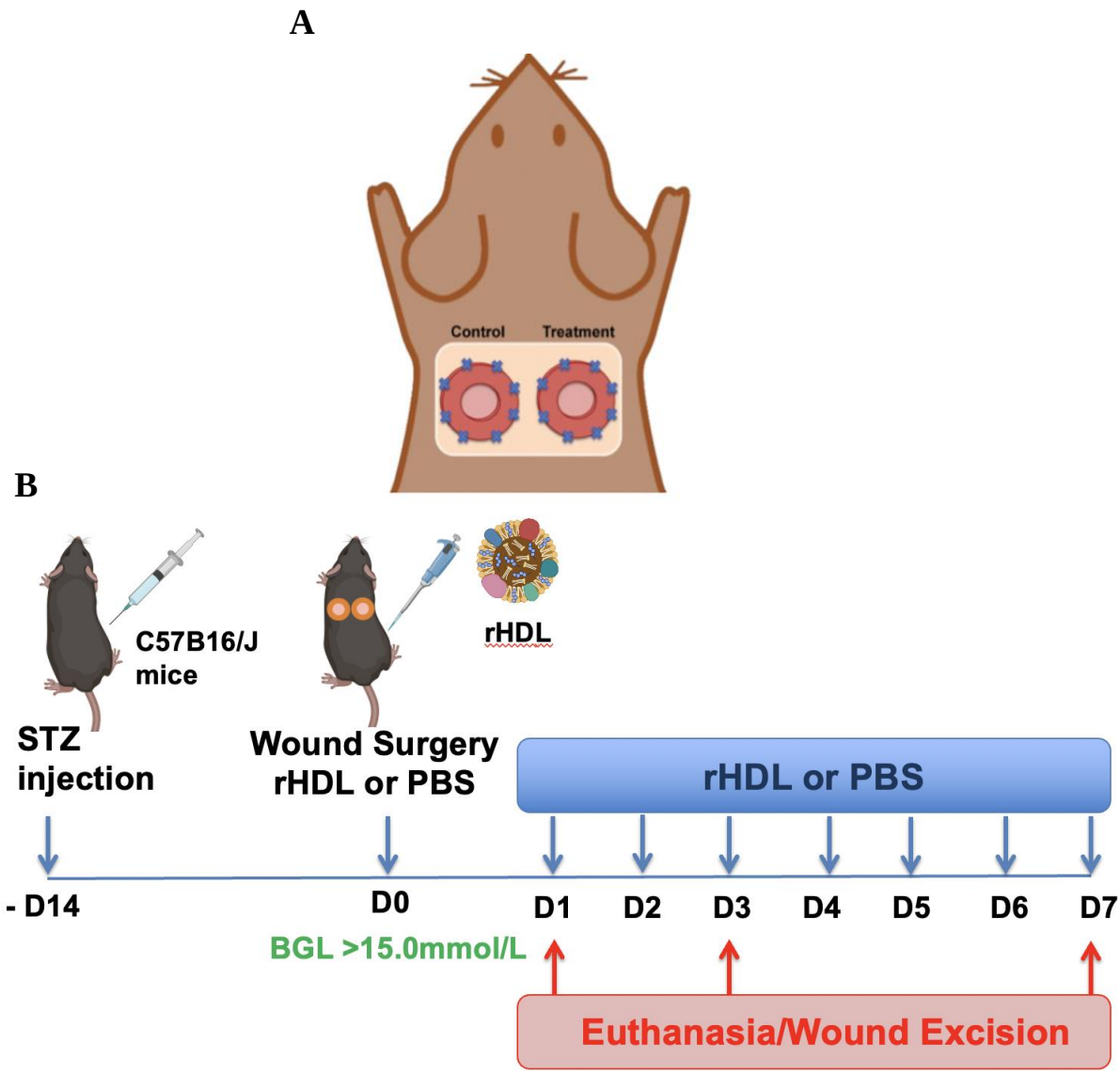

Figure 3.1 (A) Schematic representation of the murine surgical wound healing model. Full-thickness wounds were created on either side of the midline, allowing each mouse to serve as their own control. Silicon splints were adhered and sutured to the wound perimeter to prevent wound contraction to replicate human wound healing. Image from [173]. **(B) Timeline for inflammation and macrophage studies using diabetic murine model of wound healing.** STZ injection was performed 14 days prior to the wound healing surgery to render mice diabetic. Following wound healing surgery, one wound was treated with rHDL (50 μg/wound), and the control wound was treated with PBS daily. The mice were euthanised on day1 and day3 post-surgery for inflammation study and on day 7 for characterising macrophage population.

3.2.5 Quantitative real-time PCR and ELISA

Total RNA from murine wound tissue was isolated using TRIzol reagent (Sigma, USA) as per the manufacturer's instructions. RNA concentration was quantified using the NanoDrop 800 spectrometer (Thermo fisher Scientific) and reverse transcribed to produce cDNA using the iScript RT Supermix (BioRad). Transcription levels of murine *Rela, Ccl-2, Il-6 and Tgf-β1* were evaluated via quantitative PCR using SYBR Green master mix (Biorad) and the relative changes in gene expression were normalised using the $^{\Delta\Delta}$CT method to murine β-actin. For the purpose of protein extraction for ELISA, wound tissues were snap frozen on dry ice after dissection and stored at -80°. Skin tissues were lysed in 1 x RIPA sample buffer on ice for 20 minutes, homogenised and clarified by centrifugation for 15 minutes at 4°C. Supernatants were collected to determine protein concentration using the Pierce BCA Protein Assay Kit (Thermo scientific, USA).

3.2.6 Preparation of wound cells for flow cytometry

Mice were euthanised 7 days post-wound surgery. The wound tissues were collected, stored and washed with PBS. Wound tissues were then incubated for 2 h in 37°C in a solution containing Liberase TM (50 μg/mL) (Roche Applied Science, Mannheim, Germany). Disaggregates were then neutralised with Iscove's Modified Dulbecco's Medium (Sigma Aldrich) supplemented with 10% foetal calf serum (FCS) (Cell Sera, Australia). Cells were then immunostained for flow cytometry as described below.

3.2.7 Flow cytometry

Cell suspensions from skin tissue were resuspended in aliquots of $\leq 10^6$ cells in 100 μL BD stain buffer (BD Biosciences). After blocking for 15 minutes at 4°C, cells were incubated for 30 minutes with fluorochrome-conjugated anti-mouse monoclonal antibodies to different

surface markers. For non-conjugated antibodies, after blocking for 15 minutes at 4°C, cells were incubated for 30 minutes at 4°C with primary antibodies. Cells were then washed with stain buffer and incubated with a fluorophore-conjugated secondary antibody for 30 minutes at 4°C. All samples were then washed and fixed in BD fixation buffer (BD Biosciences). A complete list of antibodies used for flow cytometry is provided in Table 3.3. All samples were run on a BD LSRFortessa™ X-20 Analyser (BD Biosciences) and list mode data files were analysed with FlowJo™ version 10.5.3 software. Gating was performed based on light scatter morphology to exclude cell debris and expression thresholds were set at fluorescence intensities of unstained and fluorescence minus one control. A sequential gating strategy was used to identify populations expressing specific markers: total macrophages ($CD11b^+$ $F4/80^+$), M1-like macrophages ($CD11b^+$ $F4/80^+$ $CD86^+$) and M2-like macrophages ($CD11b^+$ $F4/80^+$ $CD206^+$). Percentage of total macrophages was calculated from the total cell population and percentage of M1 like and M2 like macrophages were calculated from the total macrophage population.

Table 3.3 List of fluorochromes used to label wound tissues for flow cytometry throughout the study.

Antigen	Fluorochrome	Concentration (µg/µL)	Supplier
CD11b	PE	3	BD Bioscience
F4/80	FitC	5	BD Bioscience
CD206	APC	2.5	BD Bioscience
CD86	BV650	2.5	BD Bioscience
DiO	GFP	2	Invitrogen

3.2.8 *In vivo* imaging system (IVIS) imaging

Mice were anaesthetised using 5% isofluorane in 100% oxygen (flow rate 1 L/min) before being placed in the IVIS chamber and maintained under anaesthesia using 2.5% isofluorane inside the IVIS chamber. DiO rHDL or PBS were applied to the wound site while the mice were under anaesthesia. The fluorescent signal was acquired using the excitation/emission

range of 484/501 nm. The images were captured immediately, 5, 10, 20, 40, 60, 75, 90 mins and 4, 24 and 48 h post DiO application. The average wound radiance (Avg Radiance [p/s/cm≤/sr]) was calculated using Live Image (version 4.4) software.

3.2.9 Wound section preparation for DiO-treated wounds

The whole wound area was excised and cut in half through the centre of the wound. The wound was carefully placed into Tissue-Tek cryomolds (USA), fully submerged in OCT (ProSciTech, QLD, Australia) and then immediately placed on dry ice for OCT to solidify. Five μm sections were cut using a Cryostat then mounted onto Super Frost slides. Sections were air-dried for at least 30 minutes at room temperature and kept overnight at 4°C in the dark. The wound sections were then washed three times with PBS + 0.05% Tween for 5 mins between each wash. The wound sections were then covered with antifade mounting media with DAPI (to visualise nuclei) and imaged using Axio Scan. Z1 (Zeiss).

3.2.10 Statistical analysis

Data were analysed on GraphPad Prism software (v9.0, Software MacKiev, California, USA). All results are expressed as mean ± standard error of the mean (SEM). All data were compared using either paired student t-test, one-way analysis of variance (ANOVA) or Two-way ANOVA, followed by post hoc analysis using Bonferroni's multiple comparison tests, with $P<0.05$ considered statistically significant.

3.3 Results

3.3.1 Topical rHDL rescues diabetes-impaired wound healing

We first sought to determine the effect of topical rHDL on the rate of wound closure in a diabetic murine model of wound healing. Figure 3.2 shows that PBS-treated wounds from mice with diabetes (grey line) had significantly impaired wound closure at Day 5, Day 6, and Day 7, when compared to non-diabetic PBS-treated (black line) control wounds (Day 5: 93.6%, $P<0.001$; Day 6: 69.1%, $P<0.05$; Day 7: 79.6%, $P<0.001$). Daily topical application of rHDL rescued diabetes-related impairment in wound closure back to the level of non-diabetic control wounds. When compared to the PBS-treated diabetic wounds (grey line), topical rHDL in diabetic mice (navy line) significantly increased wound closure at Day 6 and Day 7 (Day 6: 287.8%, $P<0.01$; Day 7: 639.3%, $P<0.0001$). rHDL treatment in non-diabetic mice (light blue line) also significantly increased the rate of wound closure at Day 5, when compared to PBS-treated non-diabetic wounds (30.4%, $P<0.05$).

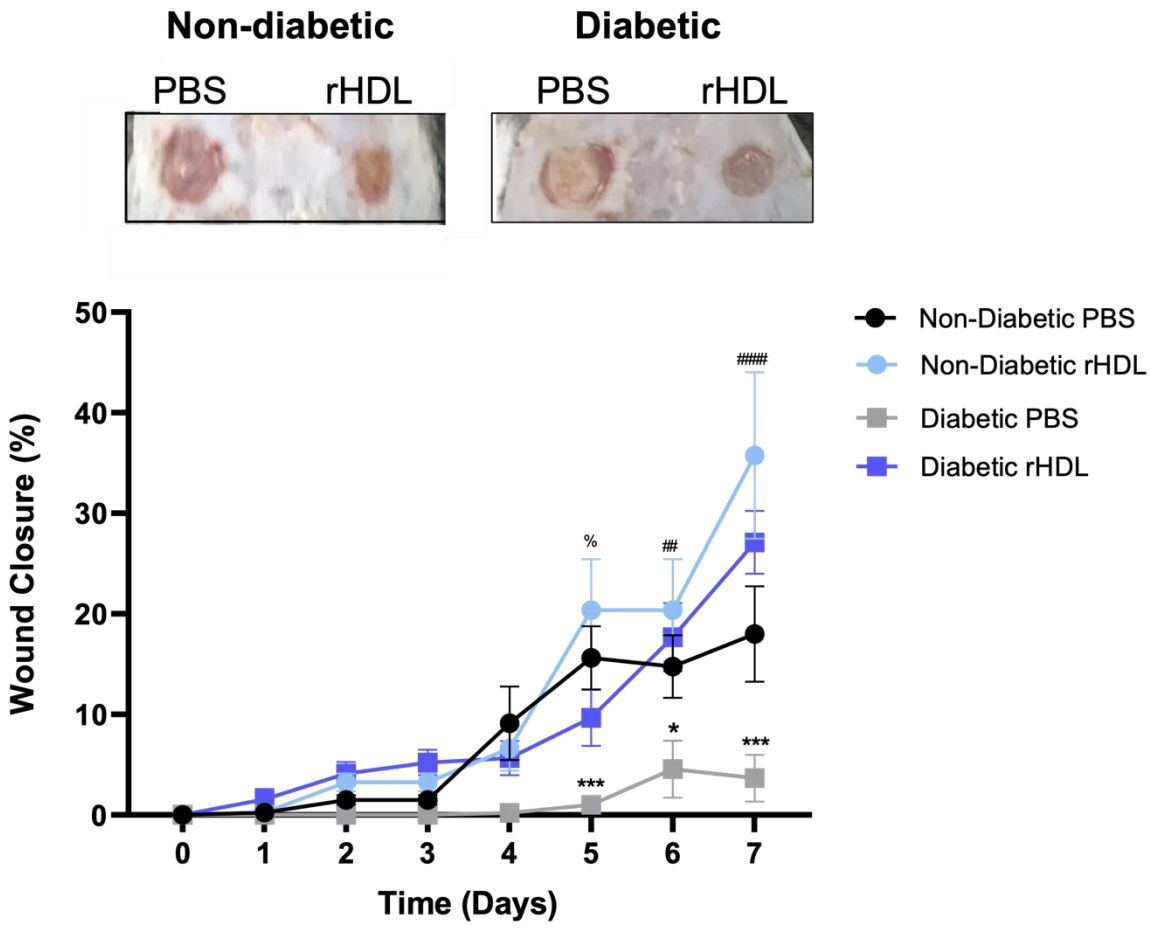

Figure 3.2 Topical rHDL rescues diabetes-impaired wound closure in a murine model of wound healing. Full-thickness wounds were created on the back flanks of non-diabetic and diabetic C57BI/6J mice (n=9-10 mice/group). Mice received daily topical application of rHDL (50 μg/wound) or PBS (vehicle) for 7 days. Wound area was calculated from the average of three daily diameter measurements along the x-, y- and z-axes; wound closure was expressed as a percentage of initial wound area at Day 0. Black circles: non-diabetic PBS-treated; Grey squares: diabetic PBS-treated; Navy squares: diabetic rHDL-treated; Light blue circles: non-diabetic rHDL treated. All data are expressed as mean ± SEM. **P*<0.05, ****P*<0.001 vs. non-diabetic PBS; $^{\#\#}$P<0.01, $^{\#\#\#\#}$P<0.0001 vs diabetic PBS; % vs. diabetic rHDL.

3.3.2 Topical rHDL has no effect on wound macrophages

Macrophages are recruited early post-wounding to fight infection. In the early post-wound stage, macrophages are predominantly the M1-like inflammatory phenotype. In healthy wounds, M1-like macrophages differentiate into M2-like anti-inflammatory reparative macrophages in the mid-stage of healing as the wound enters the remodelling phase. We evaluated the effect of topical rHDL on total wound macrophages and changes in M1-like and M2-like macrophage populations at Day-7 post-wounding. Through prior optimisation studies we determined this was the best timepoint to capture macrophage transition in diabetic mice and ensure both populations were present.

The total number of wound macrophages ($CD11b^+F4/80^+$), 7 days post-wounding, was significantly higher in diabetic wounds for both PBS-treated and rHDL-treated wounds (PBS: 77.6%, $P<0.001$; rHDL: 101.5%, $P<0.001$; Figure 3.3), when compared to non-diabetic wounds. Topical application of rHDL did not, however, significantly change the total number of wound macrophages. When examining the M1-like ($CD86^+$) and M2-like ($CD206^+$) wound macrophage populations, no changes were found with the induction of diabetes or the application of rHDL (Figure 3.3B and 3.3C).

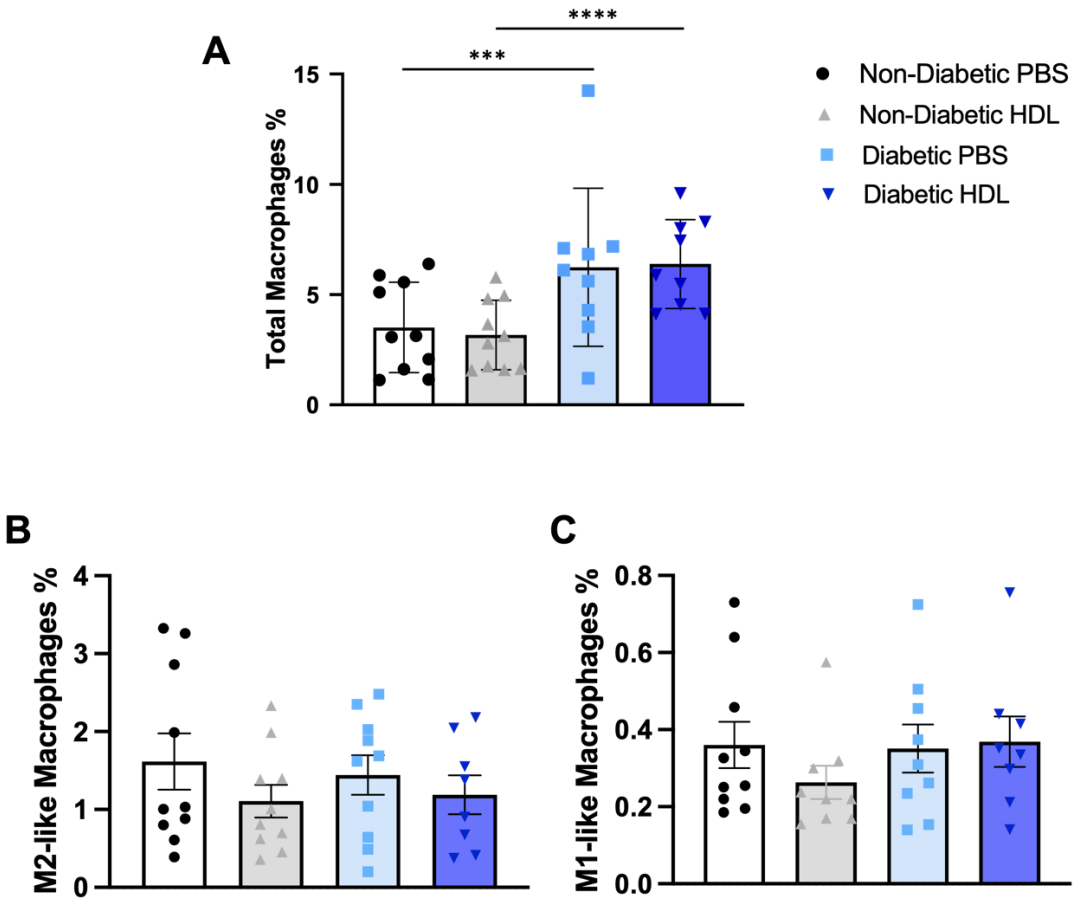

Figure 3.3 Topical application of rHDL does not change wound macrophages on Day 7 post-wounding. Full-thickness wounds were created on the back flanks of non-diabetic and diabetic C57BI/6J mice (n=9-10 mice/group). Mice received daily topical application of rHDL (50 μg/wound) or PBS (vehicle) for 7 days. Wound tissues were digested and stained with antibodies against macrophage (CD11b, F4/80) and polarity markers (CD86, M1-like; CD206, M2-like). Flow cytometry was used to measure: **(A)** $CD11b^{+}F4/80^{+}$ total macrophages; **(B)** $CD206^{+}$ M2-like macrophages and **(C)** $CD86^{+}$ M1-like macrophages. All data are expressed as mean ± SEM. ***P<0.001 vs. non-diabetic PBS; ****P<0.0001 vs. non-diabetic rHDL.

3.3.3 Topical application of rHDL decreases inflammatory mediators *Rela* and *Ccl2* in diabetic mice 72 h post-wounding

We examined the effect of topical rHDL on the expression of inflammatory mediators in diabetic murine wounds, which were tracked from the time of wounding to 72 h post-wounding. *Rela* is the gene that transcribes the p65 subunit of NF-κB, a pivotal transcription factor that activates a host of inflammatory genes. There were no changes in *Rela* mRNA levels between treatment groups at Baseline (0 h) or 24 h post-wounding. At 72 h post-wounding *Rela* mRNA levels were significantly higher in the diabetic PBS-treated wounds (152.6%, $P<0.01$), when compared to the non-diabetic PBS-treated wounds (Figure 3.4A, inset using paired t-test analysis). Topical administration of rHDL for 72 h prevented the induction of *Rela* mRNA. rHDL-treated diabetic wounds had significantly lower *Rela* mRNA levels (65.4%, $P< 0.05$) (Figure 3.3A). We also assessed the rHDL:PBS ratio of *Rela* mRNA levels over time in diabetic mice (Figure 3.3B). Data points below the 100% PBS treatment (dotted line) represent a decrease in *Rela* mRNA levels with rHDL treatment in which we found a significant reduction at 72 h (56.3%, $P<0.05$).

CCL2, also referred to as monocyte chemoattractant protein 1, recruits monocytes to the wound. There was a significant elevation in wound *Ccl2* mRNA levels in diabetic mice (both PBS and rHDL-treated, ~30-fold and ~28-fold, respectively, $P<0.001$; Figure 3.4C) 24 h post-wounding compared to PBS-treated non-diabetic mice. This elevation declined 72 h post-wounding, when compared to the 24 h group. Interestingly, the application of topical rHDL further decreased this decline at the 72 h timepoint where a significant reduction in *Ccl2* mRNA levels was observed in diabetic wounds treated with rHDL, when compared to the PBS-treated diabetic wounds (58.8%, $P<0.05$; Figure 3.4C, inset using paired t-test analysis). The inhibitory effect of topical rHDL on *Ccl2* mRNA expression in diabetic wounds was also demonstrated by the rHDL:PBS ratio in which there was a significant reduction below the 100% PBS as a result of rHDL treatment (81.9%, $P<0.05$; Figure 3.4D). A similar pattern was observed with wound Ccl2 protein levels where a

significant elevation in Ccl2 protein was observed 24 h post-wounding, when compared to baseline (Figure 3.4E). At 72 h there was a decline in Ccl2 protein and, when comparing the diabetic wounds, those treated with rHDL had lower Ccl2 protein levels than PBS-treated controls, however, this decrease did not reach significance.

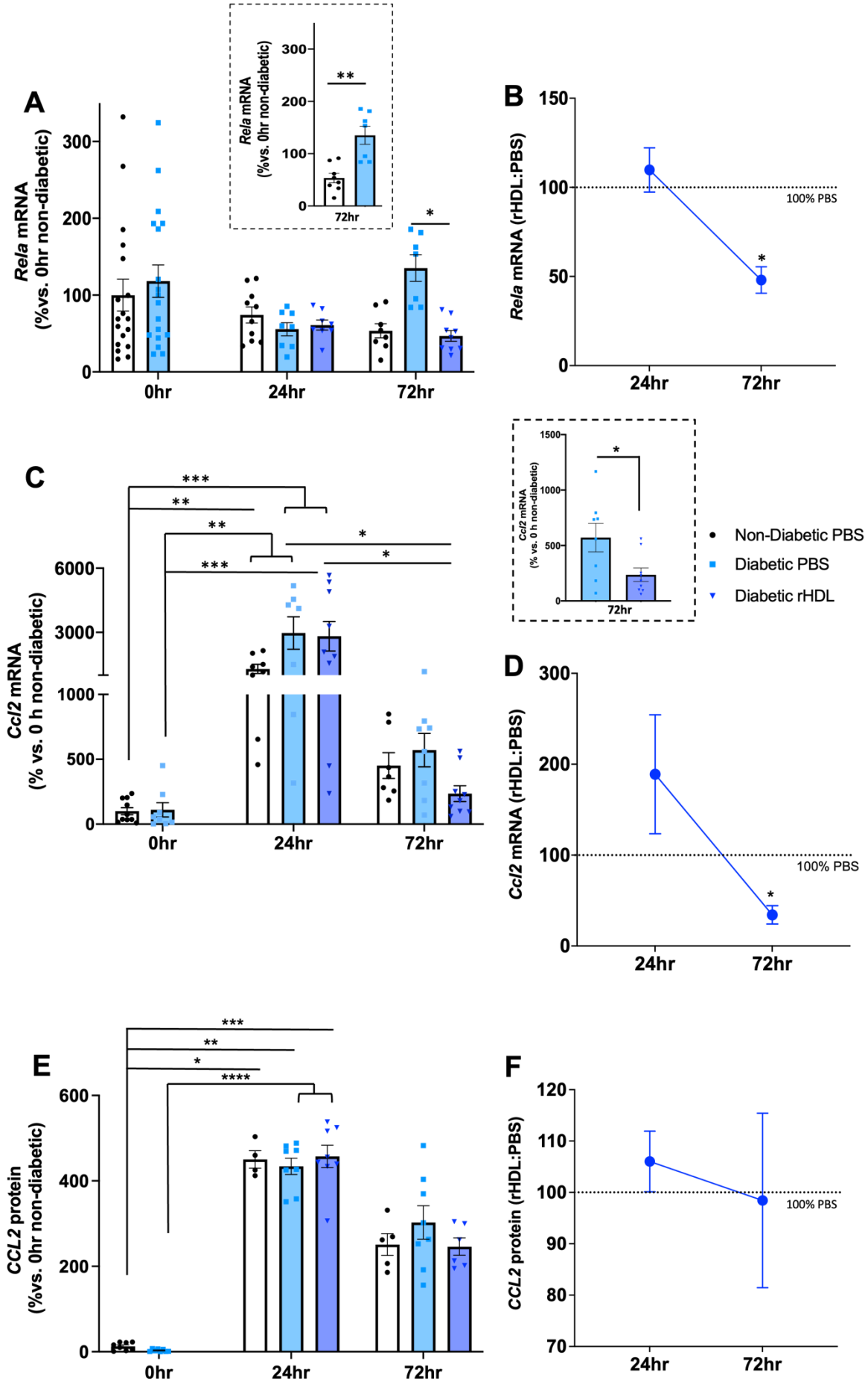
A
Rela mRNA (%vs. 0hr non-diabetic)
0hr
24hr
72hr
B
Rela mRNA (rHDL:PBS)
100% PBS
C
Ccl2 mRNA (% vs. 0 h non-diabetic)
D
Ccl2 mRNA (rHDL:PBS)
E
CCL2 protein (%vs. 0hr non-diabetic)
F
CCL2 protein (rHDL:PBS)
Non-Diabetic PBS
Diabetic PBS
Diabetic rHDL

Figure 3.4 Topical application of rHDL decreases inflammatory mediators *Rela* and *Ccl2* in diabetic mice 72 h post-wounding. Two full thickness wounds were created on the back flanks of non-diabetic and diabetic mice (n=9-10 mice/group). Mice received a daily topical rHDL (50 µg/wound) or PBS (vehicle) until euthanasia. RNA isolated from wound tissues was subjected to qPCR analyses for the measurement of: **(A)** *Rela* mRNA levels; inset: *Rela* mRNA levels at 72 h post-wounding **(B)** *Rela* mRNA levels expressed as a ratio of rHDL:PBS in diabetic wounds; **(C)** *Ccl2* mRNA levels; inset: *Ccl2* mRNA levels at 72 h post-wounding **(D)** and expressed as a ratio of rHDL:PBS in diabetic wounds. Using ELISA, wound **(E)** Ccl2 protein levels were measured and **(F)** expressed as a ratio of rHDL:PBS in diabetic wounds. All data are expressed as mean ± SEM. **P*< 0.05, ***P*<0.01, ****P*<0.00. One-way ANOVA test with Tukey's multiple comparison and paired t-test.

3.3.4 Effects of topical rHDL on wound cytokine levels

The mRNA levels of inflammatory cytokines *Tgf-β1* and *Il-6* were next tracked in diabetic and non-diabetic wounds. No changes were found in wound *Tgf-β1* mRNA levels between diabetic or non-diabetic mice or with rHDL treatment over time (Figure 3.5A). When assessing the treatment effect of topical rHDL in each mouse, it was noted that in diabetic mice there was an initial elevation in *Tgf-β1* mRNA levels at 24 h followed by a decline after 72 h (P=0.06; Figure 3.5B). At baseline, TGF-β1 protein levels were significantly lower in diabetic mouse wounds than non-diabetic wounds (82.9%, $P<0.05$; Figure 3.5C, inset;). TGF-β1 protein levels then increased significantly at both 24 h and 72 h post-wounding across all groups. No significant differences were noted in TGF-β1 wound protein levels with topical rHDL treatment (Figure 3.5C). This was also evident when investigating the effect of topical rHDL in each mouse (Figure 3.5D).

Il-6 mRNA levels were significantly higher in diabetic mouse wounds compared to non-diabetic wounds at baseline (470.8%, $P<0.01$; Figure 3.5D, inset). Otherwise, no differences were found in wound *Il-6* mRNA levels between diabetic and non-diabetic mice or with topical rHDL treatment (Figure 3.5E). Whilst there was a trend for a reduction in wound *Il-6* mRNA levels over time from 24 h to 72 h with rHDL treatment, this was not significant (Figure 3.5F). IL-6 protein levels were significantly higher in diabetic wounds at 24 h when compared to baseline levels for both PBS- and HDL-treated wounds (~26-fold, $P<0.01$ and ~38-fold, $P<0.001$, respectively, Figure 3.5G). Otherwise, no changes were observed in IL-6 protein levels with rHDL treatment across the different groups over time. Similar with *IL-6* mRNA levels, we observed a reduction in IL-6 protein levels over time from 24 h but this did not reach significance (Figure 3.5H).

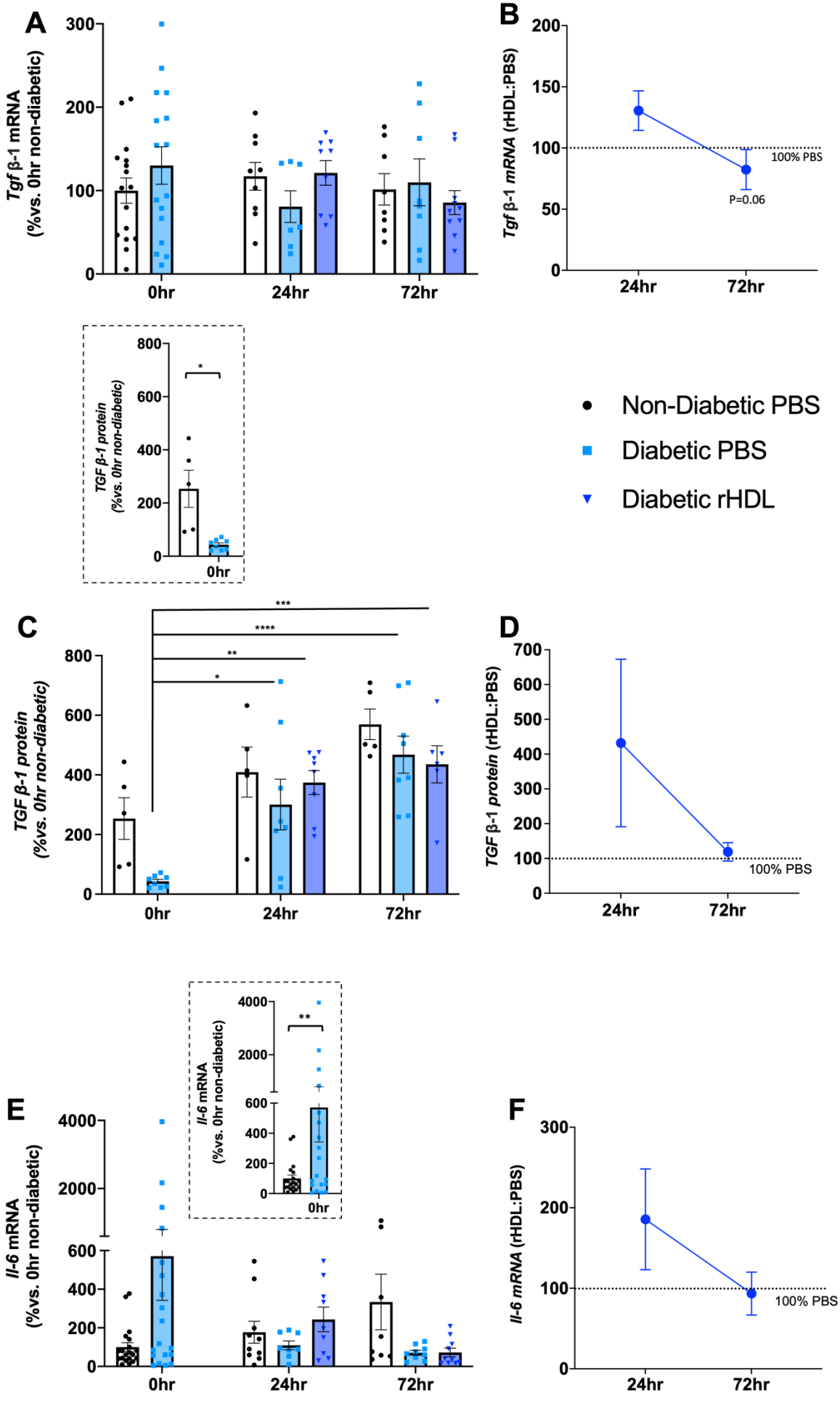
A
Tgf β-1 mRNA (%vs. 0hr non-diabetic)
0hr
24hr
72hr
B
Tgf β-1 mRNA (rHDL:PBS)
100% PBS
P=0.06
TGF β-1 protein (%vs. 0hr non-diabetic)
*
Non-Diabetic PBS
Diabetic PBS
Diabetic rHDL
C
TGF β-1 protein (%vs. 0hr non-diabetic)
***
****
**
*
D
TGF β-1 protein (rHDL:PBS)
100% PBS
E
Il-6 mRNA (%vs. 0hr non-diabetic)
**
F
Il-6 mRNA (rHDL:PBS)
100% PBS

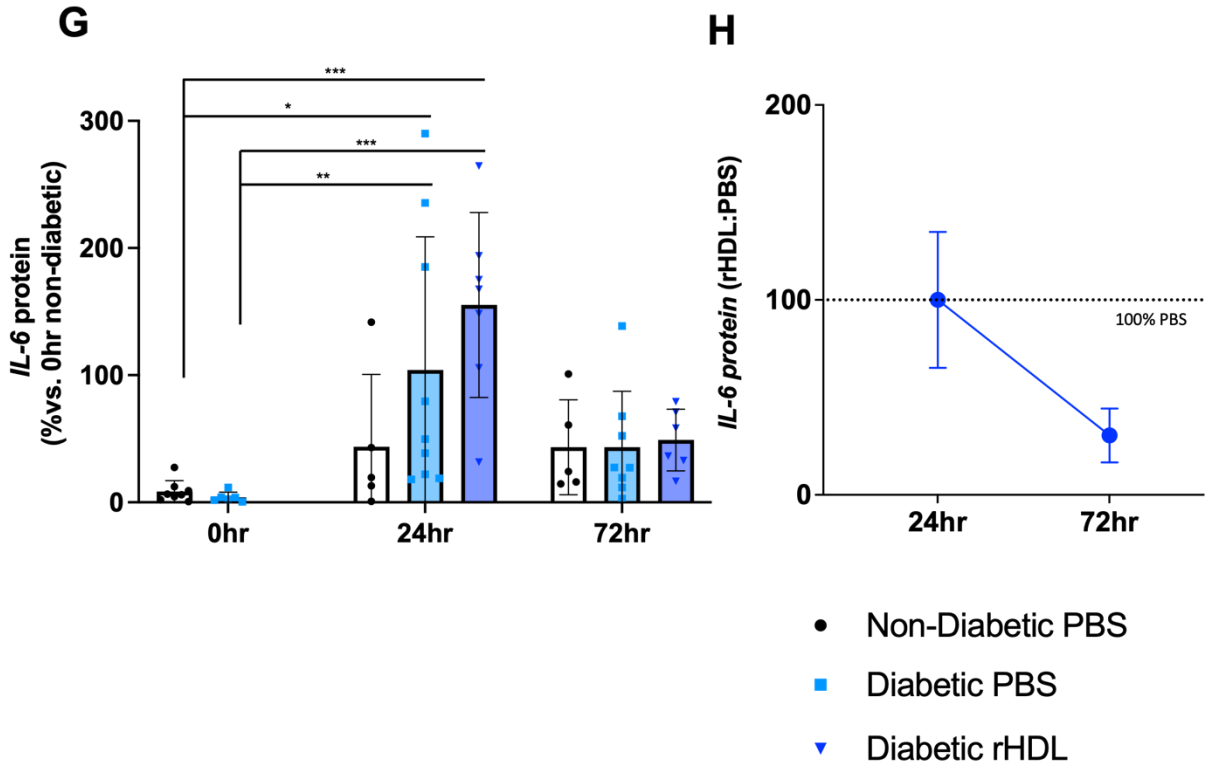

Figure 3.5 Effect of topical rHDL on wound cytokines. Two full thickness wounds were created on the back flanks of non-diabetic and diabetic mice (n=9-10 mice/group). Mice received a daily topical dose of rHDL (50 µg/wound) or PBS (vehicle). Wound lysates were subjected to qPCR and ELISA analyses for: **(A)** *TGF- β1* mRNA levels and **(B)** expressed as a ratio of rHDL:PBS, **(C)** TGF- β1 protein, inset: TGF- β1 protein levels at 0hr **(D)** TGF- β1 protein expressed as a ratio of rHDL:PBS **(E)** *IL-6* mRNA, inset: *IL-6* mRNA levels at 0hr **(F)** *IL-6* mRNA levels expressed as ratio of rHDL:PBS. **(G)** Il-6 protein and **(H)** expressed as a ratio of rHDL:PBS**.** All data are expressed as mean ± SEM. **P*< 0.05, ***P*<0.01, ****P*<0.00. One way ANOVA test with Tukey's multiple comparison and paired t-test.

3.3.5 Topical rHDL is retained in mouse wounds

Fluorescently labelled rHDL was prepared using DiO (DiO-rHDL) and used to detect the fate of topically applied rHDL on non-diabetic murine wounds. To validate the uptake and fluorescence detection of DiO-rHDL in cells, DiO-rHDL was first incubated in culture with immortalised bone marrow-derived macrophages (iBMDMs). The uptake of DiO-rHDL by iBMDMs was clearly visualised using fluorescent microscopy (Figure 3.6A) and confirmed using flow cytometry (Figure 3.6B). Using whole-body fluorescence imaging by IVIS, the radiance was 101.74-fold higher in DiO-rHDL-treated wounds when compared to PBS control-treated wounds. This radiance declined by 36.1% over the first 20 mins (0.3 h; Figure 3.6D). Radiance then remained constant until a further decline was measured between 4 h and 24 h (58.2%) but remained stable until the 48 h timepoint. Using fluorescent microscopy on wound sections, the DiO-rHDL signal was also detected in wounds treated with DiO-rHDL, but not in PBS-treated wounds (Figure 3.6E).

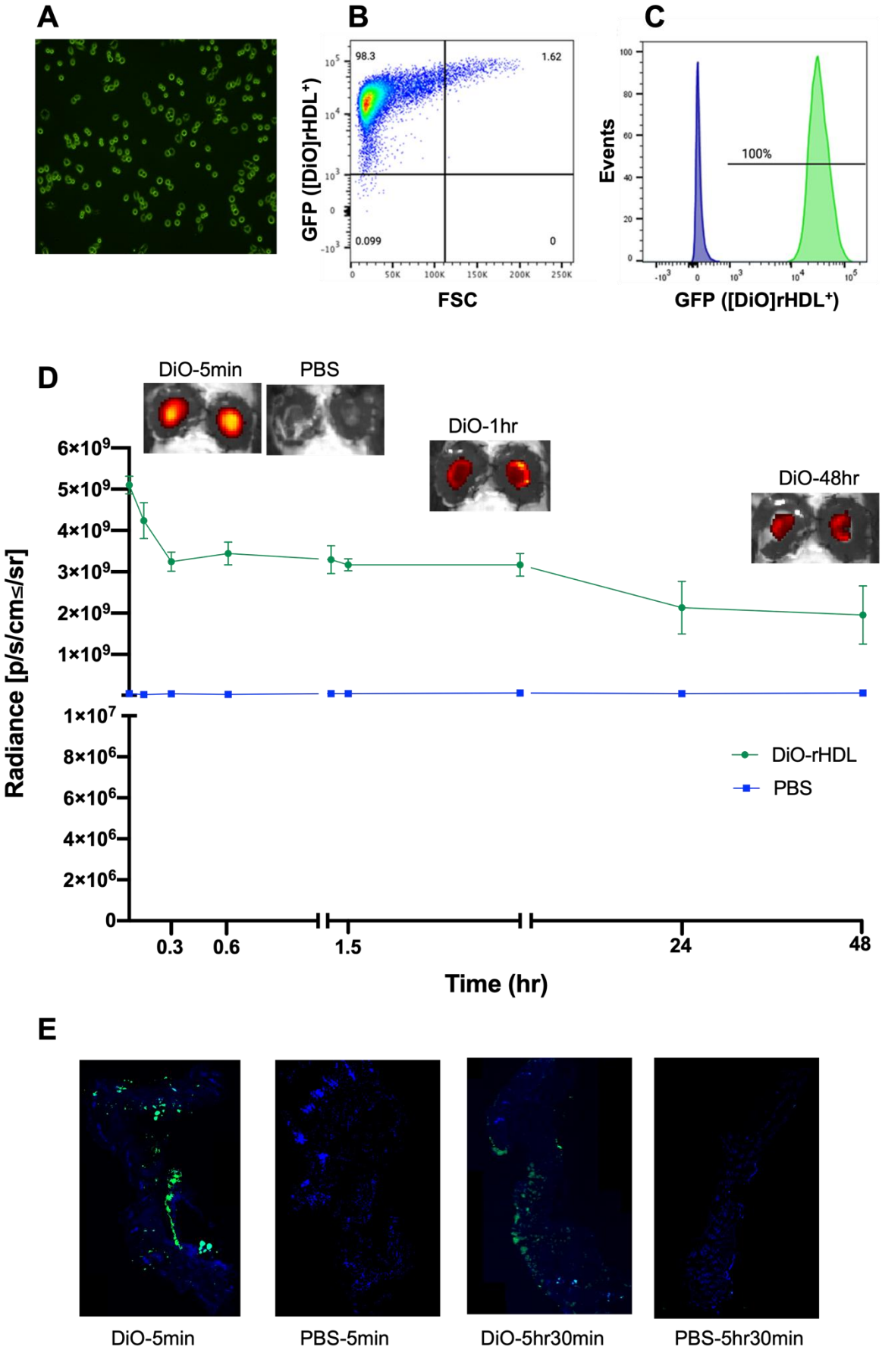
A
B
C
98.3
1.62
0.099
0
GFP ([DiO]rHDL+)
FSC
Events
100%
GFP ([DiO]rHDL+)
D
DiO-5min
PBS
DiO-1hr
DiO-48hr
Radiance [p/s/cm≤/sr]
6×10^9
5×10^9
4×10^9
3×10^9
2×10^9
1×10^9
1×10^7
8×10^6
6×10^6
4×10^6
2×10^6
0
0.3
0.6
1.5
24
48
Time (hr)
DiO-rHDL
PBS
E
DiO-5min
PBS-5min
DiO-5hr30min
PBS-5hr30min

Figure 3.6 Detection of fluorescently labelled DiO-rHDL *in-vitro* and *in-vivo*. rHDL fluorescently labelled with DiO dye (DiO-rHDL) was incubated with immortalised bone marrow-derived macrophages for 2 h for: **(A)** visualisation using fluorescence microscopy at 484 nm, 20X magnification; and **(B-C)** detection by flow cytometry at 484 nm. DiO-rHDL or PBS was applied topically to 5-day wounds (n=3) and changes in radiance were tracked using IVIS. **(D)** Average wound radiance value for topically applied DiO-rHDL and PBS. **(E)** Fluorescence microscopy images of mouse wound sections from DiO-rHDL and PBS-treated wounds.

3.4 Discussion

Inflammation is critical in the early stages of wound healing to combat infection, however prolonged and inappropriate inflammation prevents the progression of wound healing and results in non-healing, chronic wounds. Diabetes, in particular, is associated with persistent and non-resolving inflammation leading to the formation of DFU [58, 75, 148]. rHDL has been shown to rescue diabetes-impaired wound healing through the promotion of angiogenesis [155]. Despite well-established anti-inflammatory properties, the effect of topical rHDL on diabetic wound inflammation has not been previously explored. In this Chapter we found that topical application of rHDL significantly increased the rate of wound closure with no effect on macrophage number or polarity, yet significantly reduced inflammatory markers *Rela* and *Ccl2* in diabetic wounds 72 h post-wounding. Using DiO-rHDL, we found rHDL was retained in the wound for a prolonged period. Our findings add to the known wound healing benefits of rHDL by showing reductions in key inflammatory markers in the early- to mid-stages of diabetic wound healing.

rHDL has well-established anti-inflammatory properties that have been demonstrated *in-vitro* in endothelial cells, monocytes/macrophages, and smooth muscle cells all of which are key in the wound healing process. The anti-inflammatory properties of rHDL have also been demonstrated *in-vivo* in vascular inflammation models [116]. The central mechanism for the anti-inflammatory effects of rHDL is driven by its ability to inhibit the activation of the pivotal inflammatory transcription factor NF-κB. NF-κB controls the regulation of inflammatory chemokines (CCL2) and cytokines (TGF-β, IL-6) [145]. Our study showed that *Rela* (the gene that transcribes the p65 subunit of NF-κB) mRNA levels were significantly higher in diabetic murine wounds compared non-diabetic wounds. However, daily topical application of rHDL to wounds reduced wound *Rela* and *Ccl2* mRNA levels and CCL2 protein levels in diabetic mice 72 h post-wounding. This finding confirms previous studies showing the reduction of *Rela* and *Ccl2* following rHDL treatment. We did not, however, observe changes in IL-6 and TGF-β in

diabetic wounds at either the mRNA or protein level. One possible explanation for this is that transcription of *Ccl2* is primarily driven by NF-κB [174]. However, the transcriptional regulation of the *Il-6* gene is more complex and involves at least four different transcription factors, including NF-κB, activator protein-1, CCAAT/enhancer binding protein, and cAMP response element-binding protein) [175]. There is no evidence that these additional transcription factors are affected by rHDL and may explain why rHDL did not elicit a change in *Il-6* gene expression.

The reduction in wound *Rela* and *Ccl2*/CCL2 was observed 72 h after daily topical application of rHDL. Using fluorescently labelled rHDL (DiO-rHDL) we demonstrated that rHDL was retained in the wound for a prolonged period following application, predominantly for the first hour but it could be visualised by fluorescence microscopy in wound tissue sections after 5.5 h and was even retained at low levels out to 48 h, as detected by IVIS. This suggests that rHDL does not enter the circulation immediately and can interact with the wound cells. The requirement for an anti-inflammatory effect appears to be three repeat daily doses over 72 h. *In vitro* studies with rHDL that investigated its anti-inflammatory properties predominantly used incubation periods of 16 – 24 h. This is perhaps an equivalent accumulative time frame to our *in vivo* application in wounds when taking into consideration the loss of rHDL retained in the wound over time. Furthermore, a reduction in inflammation at 72 h post-wounding is perhaps an optimal time point because it follows the early stage of wound healing when inflammation is needed to fight infection and to prevent excessive inflammatory cell accumulation in the mid-stage that risks development of a chronic non-healing wound. Supporting this is our finding of an increased rate of wound closure in rHDL-treated diabetic and non-diabetic wounds.

Our study showed a significant increase in the total macrophage population in diabetic wounds compared to non-diabetic wounds 7 days post-wounding, consistent with previous literature [46]. There were, however, no changes in the total number of wound macrophages in

rHDL-treated wounds or in the M1-like or M2-like macrophage populations in non-diabetic and diabetic mice. Based on our data showing that topical rHDL reduced diabetic wound inflammation it may have been anticipated that there would also be fewer wound macrophages. *CCL2* is an important chemokine that recruits monocytes from the circulation into the neighbouring wound tissues. However, other chemokines can also perform this function including *CCL5* and *CX_3CL1* which are released by endothelial cells, suggesting that the inflammatory response was exerted primarily by other cell types such as endothelial cells rather than monocytes/macrophages [145].

It may have been expected that rHDL would increase the transition from M1-like to M2-like macrophages in diabetic wounds. A previous *in vitro* study by Sanson *et al* [150] found that rHDL caused a significant shift from M1-like to M2-like macrophages, with a 10-fold increase in the expression of the M2-like markers *Arg-1* and *Fizz-1* [150]. It is important to note that this shift of macrophage phenotype by rHDL was seen in *in-vitro* settings, whereas our findings were in a murine model of wound healing. However, in contrast, another *ex-vivo* study found HDL did not influence macrophage polarisation in human monocyte-derived macrophages [176]. It is possible, therefore, that in a biologically complex *in vivo* environment with diverse cell types that co-habit the wound with macrophages, that the macrophage polarisation properties of rHDL are diluted and less effective. Alternatively, our timepoint of 7 days post-wounding may not have captured the transition. It may have occurred later, especially in diabetic wounds.

Several studies have examined topical rHDL application to full-thickness murine wounds [155, 172], however, to our knowledge, no study has tracked its uptake, retention, and fate. Determining the uptake and fate of topically applied rHDL provides integral information required for future translational studies such as the required frequency of application. In our study, we successfully labelled rHDL with the fluorescent dye DiO, which has previously been

used intravenously to track the biodistribution of [S]-rHDL in murine atherosclerosis models [177]. We were also able to show robust uptake of DiO-rHDL by macrophages *in vitro* and in murine wound tissue. These findings will provide critical information to help interpret both the mechanism of action of rHDL in wounds and to facilitate its future translation.

In conclusion, the studies described in this Chapter showed that topical application of rHDL rescues diabetes-impaired wound healing. We found topical rHDL reduced the inflammatory markers *Rela* and Ccl2/CCL2 in diabetic wounds 72 h post-wounding. Despite this, we did not observe changes in wound macrophages with rHDL treatment. Using fluorescently labelled rHDL (DiO-rHDL) we confirmed rHDL is retained in the wound for a prolonged period. The combined anti-inflammatory and pro-angiogenic properties of topical rHDL in diabetic wound healing present rHDL as an effective pleiotropic treatment option for DFU.

CHAPTER 4 – THE RELATIONSHIP BETWEEN HDL-CHOLESTEROL AND WOUND HEALING IN PATIENTS WITH AND WITHOUT DIABETES AND WITH TOE AMPUTATIONS

4.1 Introduction

Patients with diabetes have a predisposition for the development of PAD and peripheral neuropathy, both of which are precursors for the development of DFU [57]. It is estimated that approximately 25% of patients with diabetes will develop DFU in their lifetime. Peripheral neuropathy includes motor neuropathy, sensory neuropathy, and autonomic neuropathy which lead to formation of foot deformity, loss of protective sensation, and dry skin, respectively [57]. These factors all contribute to the formation of callous or dry skin which can result in DFU. Repetitive minor trauma or injuries can cause ulcer formation. Poor vascular supply which could lead to the formation of non-healing wounds may result in amputation of part of the foot or above the ankle. It is estimated that approximately 20% to 25% of moderate or severe DFU fail to heal and require amputation [57].

There is currently no universally approved treatment for wound management of DFU and evidence-based management options focus on pressure off-loading, infection control, surgical debridement, and revascularisation [178]. As discussed in Chapter 1, multiple aspects of wound healing are impaired in diabetes, therefore, optimal treatment would seek to correct multiple deficiencies of the wound healing process (i.e. a therapy that exhibits pleiotropic properties). Previous studies have demonstrated that topical rHDL is a promising can1didate as it has been shown to rescue diabetes-impaired wound closure, wound angiogenesis, and capillary density in a diabetic *in-vivo* model of wound healing [155]. Additionally, the work presented in Chapter 3 confirms the anti-inflammatory properties of topical rHDL in diabetic wounds. rHDL therefore displays both pro-angiogenic and anti-inflammatory properties, thus addressing two key processes for successful wound closure in DFU.

There is a well-established inverse relationship between circulating HDL-cholesterol levels, the risk of a cardiovascular event, and the development of type 2 diabetes [126, 130]. There is, however, emerging evidence that HDL *functionality* rather than HDL-cholesterol *levels* provide

a better biomarker of the relative protective properties of HDL. Indices of HDL functionality include its ability to efflux (remove) cholesterol from cells (particularly macrophages), its anti-inflammatory properties, and its pro-angiogenic effects. Only one clinical study has evaluated the relationship between HDL-cholesterol levels and diabetic wound healing outcomes. That study found an inverse correlation between the levels of circulating HDL-cholesterol and the risk of minor (defined as amputation below the ankle) and major amputation (defined as amputation above ankle) as well as wound-related death (defined as death with an unhealed ulcer) [179]. The relationship between HDL functionality and wound closure is currently unknown.

Accordingly, this Chapter aimed to identify the relationship between circulating HDL-cholesterol levels and functionality with the rate of post-amputation wound closure in patients with/without diabetes requiring toe amputations as a result of non-healing foot ulcers. In this Chapter we also present clinical data of study participants, report longitudinal wound closure data and measures of the cholesterol efflux capacity of participant HDL.

4.2 Methods

4.2.1 Experimental timeline and design

Eighteen diabetic participants (Group 1) and eight non-diabetic participants (Group 2) admitted to the Royal Adelaide Hospital (RAH) Vascular Surgery Department, Adelaide, SA, for a minor amputation (e.g., excision of toe/s) due to non-healing wound/tissue necrosis associated with diabetes or peripheral vascular disease, consented to join the study (Human Research Ethics Committee Reference Number: HREC/19/CALHN/349; Central Adelaide Local Health Network Reference Number: 11743) (Figure 4.1). Potential study participants were identified from the elective or emergency vascular surgical list at RAH and were approached before the surgery. After obtaining consent, the first blood sample was collected, and clinical data recorded. At 24-72 h post-amputation surgery, baseline wound areas were measured using a 3D camera (WoundVue, LBT Innovations). Wound areas were measured every 2-weeks during clinical visits until wound healing was complete. Blood samples were also collected at 4-weeks and 6-months post-amputation for measurement of HbA1c, full blood count, erythrocyte sedimentation rate, C-reactive protein, and lipid profiles (total cholesterol, LDL-cholesterol HDL-cholesterol, non-HDL-cholesterol, triglyceride). Twenty healthy and aged-matched participants were also enrolled in the study (Group 3) as the control group and provided a single blood sample.

4.2.2 Inclusion and exclusion criteria

Inclusion criteria

Group 1 (diabetic participants): diagnosis of diabetes (types I and II), HbA1c<12%, eGFR >15 mL/min/1.73m^2 and not on dialysis with recent ray amputation. Group 2: non-diabetic participants with recent ray amputation. Group 1 and Group 2 participants were eligible for recruitment if there were no signs of active infection and there was evidence of adequate

perfusion (>40 mm/Hg toe cuff pressure). Lipid-lowering drugs (e.g. statins, ezetimibe) were allowed. Group 3: age-matched, non-diabetic participants with no ulcers.

Exclusion criteria

Elevated liver enzymes (>50 units AST, >56 units ALT), stroke or transient ischaemic attack within the previous three months, heart failure, cancer with ongoing treatment or prognosis of <5 years, active infection, history of pancreatitis, deep vein thrombosis or pulmonary embolism, organ transplant, steroid therapy, hyperbaric treatment, dialysis, negative pressure wound therapy; and not deemed likely to require major leg amputation within four weeks or any obstacle to regular follow-up.

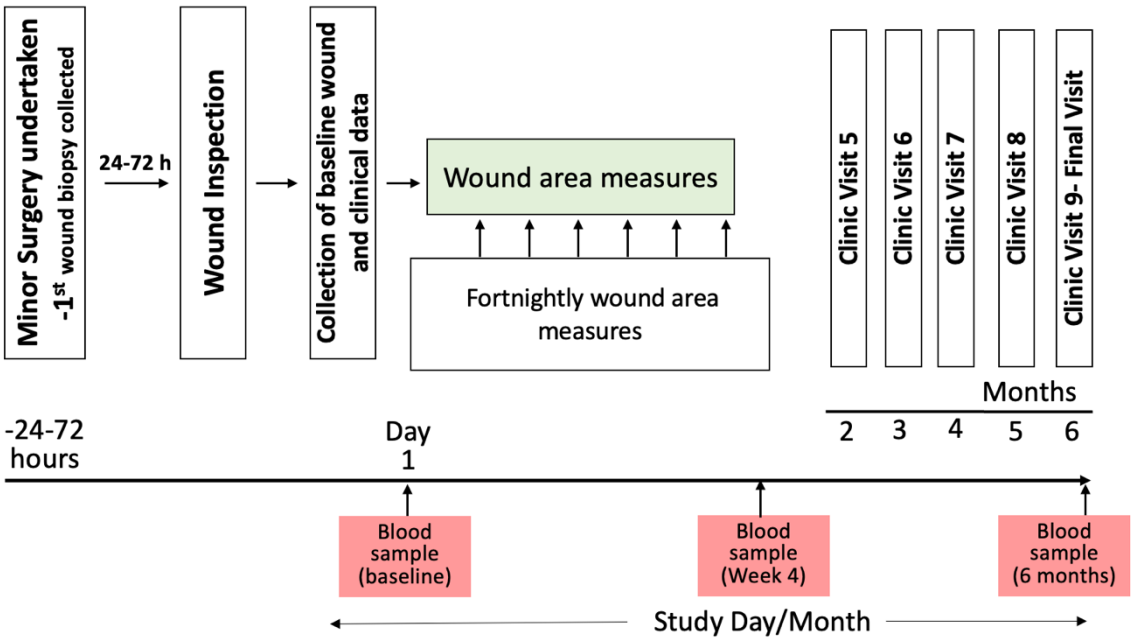

Figure 4.1 Clinical study protocol. Group 1 (diabetic) and Group 2 (non-diabetic) participants were admitted to the Royal Adelaide Hospital for toe/s amputation. The post-amputation wounds were inspected and if there was no major infection the participants were recruited into the study. The first image of the wound was captured immediately post-amputation followed by fortnightly visits until wound closure. Blood was collected from Group 1 and Group 2 participants at Baseline, four weeks, and six months post-amputation. Blood was collected from Group 3 (healthy controls) participants at baseline.

4.2.3 Blood analysis and clinical parameters

Whole blood was collected in two 9 mL EDTA tubes. One tube was sent to SA Pathology for analysis of C-reactive protein, HbA1c, full blood count, and erythrocyte sedimentation rate. The percentage of glycosylated haemoglobin (% of HbA1c) in the blood reflects the average blood sugar levels over the preceding 2-3 months. An HbA1c levels of 6.5% is recommended as the cut point for diagnosing diabetes, however a value less than 6.5% doesn't exclude diabetes diagnosed using glucose tests. The second tube was used in the lab to measure lipid profiles (total cholesterol, LDL-cholesterol, HDL-cholesterol, non-HDL-cholesterol, triglycerides) and to isolate HDL for use in functional assays. Total cholesterol, HDL-cholesterol and triglycerides were determined enzymatically using the LabAssay^{TM} Cholesterol and LabAssay^{TM} Triglyceride kits. The Friedwald equation: LDL-cholesterol = (total cholesterol - HDL-cholesterol) – (total triglycerides/2.2) was used to calculate LDL-cholesterol [180].

4.2.4 Cholesterol efflux assay

Immortalised bone marrow derived macrophages [181] (passage 3-10) were plated at $1x10^5$ cells/well and incubated for 24 h. The cells were then loaded with [^{3}H] radiolabelled cholesterol (2 μCi/mL, 24 h). Cells were incubated with 0.2% BSA-DMEM for 18 h to equilibrate labelled cholesterol among intracellular cholesterol pools. After aspiration, cells were incubated with 300 μL of baseline control (0.2% BSA-DMEM) or the cholesterol acceptors: rHDL and isolated patient HDL (25 μg/ml). Movement of radiolabelled cholesterol from cells to media containing isolated HDL/rHDL was quantified using the Tri-Carb 4810TR scintillation counter (PerkinElmer) and expressed as a percentage of total cell [^{3}H] cholesterol content.

4.2.5 Calculating the rate of wound healing

To monitor the rate of wound healing in participants with toe amputations (Groups 1 and 2), a 3D camera "WoundVue" (LBT technologies, Adelaide, Australia) was used to capture the wound area [182]. The rate of wound healing was calculated by subtracting the wound area

(mm^2) at the first reading (baseline) from the wound area at each of the subsequent time points (mm^2), divided by the number of days between the readings to obtain the rate (mm^2/day).

4.2.6 Statistical analysis

GraphPad Prism (version 9) and SPSS (version 27) were used for graph preparation and data analysis. Inter-group comparisons were performed using either one-way ANOVA with post hoc Tukeys test or paired and unpaired two-group t-tests. The association of efflux capacity with clinical and HDL-related variables was assessed using linear correlation test in SPSS, with wound size at Baseline adjusted. P value of 0.05 indicated statistical significance.

4.3 Results

4.3.1 Characteristics of the study cohort

The study cohort was composed of patients with diabetes (Group 1; N=18), predominantly with type 2 diabetes mellitus, and patients without diabetes (Group 2; N=8) with a mean age of 68 and 77, respectively, (Table 4.1). Group 1 and 2 participants were admitted to the Vascular Department at the Royal Adelaide Hospital for amputation of toes due to non-healing ulcers or wet gangrene. The majority of participants were male in both Group 1 (94%) and Group 2 (75%) (Table 4.1).

Some participants were unable to complete all follow-up appointments due to post-amputation complications including use of negative pressure wound therapy, need for unplanned additional surgical wound debridement, below knee amputation and suturing of the wound. Four participants in Group 1 (22%) and one participant in Group 2 (5.5%) required negative pressure wound therapy to facilitate exudate clearance from the wound, which excluded them from further participation. Two participants in Group 1 (11.1%) and two in Group 2 (25%) required below knee amputations due to infected wounds post-amputation. Furthermore, three Group 1 participants (16.6%) and two Group 2 participants (25%) had their wounds sutured during the surgery, limiting our ability to track wound closure; only baseline wound areas and blood samples could be collected from these participants.

As expected, the level of HbA1c (a measure of glycaemic control) was significantly higher in the diabetic group (Group 1) than both the non-diabetic group (Group 2; 54% increase, $P<0.05$) and healthy controls (Group 3; 45% increase, $P<0.0001$) at baseline (Table 4.1). HbA1c levels remained higher at the four-week timepoint post-amputation in the diabetic group (Group 1; 42.3% increase, $P<0.01$, Table 4.1), compared to the non-diabetic group (Group 2). Furthermore, the levels of C-reactive protein, a clinical biomarker for systemic inflammation,

were significantly higher in the diabetic group compared to healthy group at baseline (55.3±63.3 mg/L, P<0.001, Table 4.1).

Table 4.1 Demographic characteristics and the biochemistry measures of study cohort.

Variable	**Group 1** Patients with diabetes and minor amputation/s (N=18)	**Group 2** Patients without diabetes and with minor amputation/s (N=8)	**Group 3** Healthy controls (N=20)
Age (years ± SD)	68 ± 10	77 ± 13	67±10
Male sex -number (%)	17 (94.4)	6 (75)	18 (90)
Female sex -number (%)	1 (5.5)	2 (25)	2 (10)
Post-amputation Complications			
Negative pressure wound therapy- number (%)	4 (22.2)	1 (5.5)	NA
Below knee amputation - number (%)	2 (11.1)	2 (25)	NA
Wound sutured - number (%)	3 (16.6)	2 (11.1)	NA
Biochemistry			
HbA1c (%± **SD**) at Baseline	**8 ± 1.9 ****, ##**	**5.2 ± 0.5**	**5.52 ± 0.3**
HbA1c (%± **SD**) 4-weeks post-amputation	**7.4 ± 0.9 ##**	**5.2 ± 0.5**	NA
HbA1c (%)± **SD** 6-months post-amputation	7.6 ± 1.6	5	NA
ESR at Baseline (mm/h± **SD**)	55 ± 49.5	1	6.8 ± 5.6
ESR 1-month post-amputation (mm/h± **SD**)	41.3 ± 23.3	89.5 ± 27.5	NA
ESR 6-months post-amputation (mm/h± **SD**)	28.6 ± 24.4	1	NA
CRP at Baseline (mg/L± **SD**)	**57.4 ± 68****	**22.5 ± 17.7**	**2.1 ± 4.7**
CRP 1-month post-amputation (mg/L± **SD**)	14.8 ± 24.9	14.85 ±14.5	NA
CRP 6-months post-amputation (mg/L± **SD**)	18.3 ± 27.6	5.6	NA

Participants requiring a minor amputation(s) were recruited to the study. Healthy controls without amputation were also included. Blood was taken at the time of surgery (baseline), 1-month and 6-months post-amputation. A single blood sample was collected from the healthy controls. Haemoglobin A1c (HbA1c) with normal range of less than 6%. Erythrocyte sediment rate (ESR) with normal range of less than 10 mm/hr for men and less than 12 mm/h for women. C-reactive protein (CRP) with normal range of 0.0-8.0mg/L. Data are expressed as mean ± SD

and inter-group comparisons were made by one-way ANOVA (Tukey's post hoc comparison t-test) and unpaired t-test. Unpaired t-test. **P<0.01 and ****P<0.0001 compared healthy group. $^{\#}$P<0.05, $^{\#\#}$P<0.01 compared to non-diabetic.

4.3.2 Medications

Details of current medications were obtained (Table 4.2). All Group 1 (diabetic) participants were on anti-diabetic medication and 67% were on lipid-lowering medications. The non-diabetic group with amputation (Group 2) and the healthy controls (Group 3) were on far fewer medications overall.

Table 4.2 Participant medications.

Medication Class	**Group 1** Patients with diabetes and minor amputation/s (N=15)	**Group 2** Patients without diabetes and minor amputation/s (N=6)	**Group 3** Healthy controls (N=20)
Lipid-Lowering (Statins) – Total	**10 (67%)**	**2 (33%)**	**3 (15%)**
Rosuvastatin	6 (40%)	1 (16.6%)	1 (5%)
Atorvastatin	2 (13%)	1 (16.6%)	2 (10%)
Ezetimibe	1(6%)		
Simvastatin	1(6%)		
Anti-Diabetic- Total	**15 (100%)**	**Nil**	**Nil**
Insulin	7 (47%)		
Metformin	7 (47%)		
Linagliptin	2 (13.3%)		
Glucagon	1 (6.7%)		
Dulaglutide	1 (6.7%)		
Sitagliptin	2 (13.3%)		
Gliclazide	2 (13.3%)		
Empagliflozin	1 (6.7%)		
Antibiotic- Total	**6 (40%)**	**4 (67%)**	
Ciprofloxacin		1 (16.6%)	
Flucloxacillin	1 (6.7%)	1 (16.6%)	
Vancomycin		1 (16.6%)	
Pristinamycin	1 (6.7%)		
Amoxicillin- Clavulanic Acid	4 (26%)		
Cefalexin		1 (16.6%)	
Other			
Aspirin	3 (20%)	2 (33.3%)	1 (5%)
Beta-blocker	4 (26%)	1 (16.6%)	1 (5%)
Blood Pressure	10 (66.7%)	3 (50%)	3 (15%)

4.3.3 Blood cell counts of study participants

Full blood count data was obtained for all samples. Neutrophil numbers were significantly higher in both diabetic (2.3±1.4 x10^9/L, 59.9%, P<0.05) and non-diabetic (3.3±3.1 x10^9/L, 83.7%, P<0.05) groups, when compared to healthy controls (Table 4.3). Despite the significantly higher neutrophil levels in the diabetic and non-diabetic groups they were still within the normal range of 1.80-7.50 x10^9/L (close to the upper threshold). White cell counts were also significantly higher in both diabetic (2.6±1.4, 40.1%, P<0.01) and non-diabetic (3.1±2.6, 48.1%, P<0.05) groups, compared to healthy controls. Basophil levels were significantly lower in the diabetes group compared to healthy controls (-0.02 x10^9/L, 33.3%, P<0.01) but within the normal range of <0.10 x10^9/L.

Haemoglobin levels were significantly lower in both diabetic (24.8±12.8, 17.3%, P<0.001) and non-diabetic (26.9±12.8, 18.8%, P<0.01) patients, compared to the healthy controls (Table 4.4). Red blood cells were also significantly lower in diabetic (0.6±0.6, 13.0%, P<0.01) and non-diabetic (0.82±0.78, 17.45%) groups compared to the healthy controls. Lastly, red cell distribution width, which measures the differences in the volume and size of red blood cells, was significantly higher in diabetic (1.18±0.8, 9.25%, P<0.05) and non-diabetic (2.24±0.24, 17.55%, P<0.001) groups compared to the healthy controls.

Table 4.3 Full blood cell counts of study participants.

Variable	**Group 1** Patients with diabetes and minor amputation/s (N=18)	**Group 2** Patients without diabetes and minor amputation/s (N=8)	**Group 3** Healthy controls (N=20)
Neutrophils *-*x10^9/L	**6.27 ± 2.48***	**7.2 ± 4.14***	**3.92 ± 1.04**
Lymphocytes *-*x10^9/L	2.0 ± 0.75	1.42 ± 0.32	1.81 ± 0.57
Monocytes *-* x10^9/L	0.66 ± 0.29	0.65 ± 0.2	0.55 ± 0.13
Eosinophils *-* x10^9/L	0.20 ± 0.21	0.30 ± 0.18	0.16 ± 0.12
Basophils *-* x10^9/L	**0.04 ± 0.02****	**0.06 ± 0.02**	**0.06 ± 0.02**
Haemoglobin (g/L)	**118.7 ± 18.97*****	**116.6 ± 18.97****	**143.5 ± 6.21**
White cell count *-* x10^9/L	**9.11 ± 2.64****	**9.63 ± 3.8***	**6.5 ± 1.2**
Platelet count *-* x10^9/L	263.6 ± 132	347.2 ± 176.7	232.5 ± 54.13
Red blood cells *-* x10^{12}/L	**4.09 ± 0.77***	**3.88 ± 1.0***	**4.7 ± 0.22**
Packed cell volume (L/L)	0.36 ± 0.05	0.36 ± 0.07	0.65 ± 0.96
Mean cell volume (g/L)	87.59 ± 6.65	93.56 ± 6.14	84.52 ± 21.93
Mean cell haemoglobin (pg)	29.28 ± 2.71	30 ± 1	30.68 ± 1.12
Red cell distribution width (%)	**13.94 ± 1.7***	**15 ± 0.62****	**12.76 ± 0.86**
Mean platelet volume (fL)	10.61 ± 1.12	10.98 ± 1.21	10.32 ± 0.85

Full blood cell count was undertaken on participant samples by SA Pathology. Normal ranges: neutrophils, 1.80-7.50 x10^9/L; lymphocytes, 1.10-3.50 x10^9/L; monocytes, 0.20-0.80 x10^9/L; eosinophils, 0.02-0.50 x10^9/L; basophils, ≤ 0.10 x10^9/L; haemoglobin, 135-175 g/L; white cell count, 4.00-11.00 x10^9/L; platelet count, 150-450 x10^9/L; red blood cells, 4.50-6.00 x10^{12}/L; packed cell volume, 0.40-0.50 L/L; mean cell volume, 80.0-98 fL; red cell distribution width, 12.0-15.0%; mean platelet volume, 9.50-13.00 fL. Data are expressed as mean ± SD and inter-group comparisons were made by one-way ANOVA (Tukey's post hoc comparison t-test). *P<0.05, **P<0.01 and ***P<0.001 compared to healthy control group.

4.3.4 Lipid levels of study participants

Blood collected from healthy controls (baseline) and the diabetic/non-diabetic groups (baseline, 1-month and 6-months) was used to measure total cholesterol, HDL-cholesterol, triglycerides, and HDL-triglyceride levels (Table 4.4).

Interestingly, the level of total cholesterol at the time of surgery was significantly lower in both the diabetic (1.5± 0.13, 35.9%, P<0.0001) and non-diabetic groups (1.3, 32.1%, P<0.01) compared to healthy controls. HDL-cholesterol at the time of the surgery was also significantly lower in both diabetic (0.9±0.01, 46.2%, *P*<0.0001) and non-diabetic groups (0.5±0.01, 27.6%, *P*<0.01) when compared to healthy controls.

There were no changes in total cholesterol and HDL-cholesterol between the diabetic and non-diabetic groups at 1-month and 6-months post-amputation. No changes were observed in LDL-cholesterol across groups, nor were there changes in total and HDL triglyceride levels between diabetic, non-diabetic, or healthy controls at baseline.

We also compared changes in lipids between groups over time post-amputation and present them graphically in Figure 4.2A. Total cholesterol levels were significantly lower in the diabetic and non-diabetic groups than the healthy controls at Baseline, but no further changes were noted at the later timepoints.

Except for lower HDL-cholesterol levels at baseline in the diabetic and non-diabetic groups, no further changes were noted throughout the 6-month follow-up period in these two groups (Figure 4.2B). The level of total triglyceride was not significantly higher in the diabetic group compared to the healthy (at baseline) and non-diabetic groups (baseline, 1-month, and 6-months) (Figure 4.2C). Furthermore, there was no significantly higher HDL triglyceride levels

in the diabetic group compared to the non-diabetic group at baseline and 1-month post-amputation (Figure 4.2D).

Table 4.4 The lipid profile of study participants at baseline, 1-month, and 6-months post-amputation.

Variable	**Group 1** Patients with diabetes and minor amputation/s (N=18)	**Group 2** Patients without diabetes and minor amputation/s (N=8)	**Group 3** Healthy controls (N=20)
Lipid levels (mmol/L)			
Total Cholesterol at Baseline	**2.69 ± 0.9******	**2.85 ± 1.03****	**4.2 ± 1.03**
Total Cholesterol 1-month post amputation	3.51 ± 1.32	2.48 ± 0.85	NA
Total Cholesterol 6-months post amputation	3.96 ± 1.28	2.42 ± 0.49	NA
HDL-Cholesterol at Baseline	**1.06 ± 0.37******	**1.43 ± 0.37****	**1.97 ± 0.39**
HDL-Cholesterol 1-month post amputation	1.30 ± 0.35	1.57 ± 0.21	NA
HDL-Cholesterol 6-months post amputation	1.52 ± 0.48	1.26 ± 0.35	NA
Total Triglyceride at Baseline	1.89 ± 0.78	1.23 ± 0.83	1.22 ± 0.73
Total Triglyceride 1-month post amputation	2.55 ± 1.51	1.7 ± 0.85	NA
Total Triglyceride 6-months post amputation	2.57 ± 2.68	1.26 ± 0.16	NA
HDL Triglyceride at Baseline	0.16 ± 0.10	0.22 ± 0.05	0.18 ± 0.09
HDL Triglyceride 1-month post amputation	0.19 ± 0.09	0.23 ± 0.12	NA
HDL Triglyceride 6-months post amputation	0.26 ± 0.13	0.21 ± 0.05	NA
LDL at Baseline	0.78 ± 0.70	0.86 ± 0.86	1.92 ± 0.76
LDL 1-month post amputation	1.1 ± 0.87	0.14 ± 0.69	NA
LDL 6-months post amputation	1.27 ± 1.57	0.58 ± 0.06	NA

Total cholesterol, HDL-cholesterol, and triglyceride concentrations were determined enzymatically on plasma. Data are expressed as mean ± SD and inter-group comparisons were made by one-way ANOVA (Tukey's post hoc comparison t-test) and unpaired t-test. NA donates not applicable. **P<0.01 and ****P<0.0001 compared to healthy control group. High-density lipoprotein (HDL), low-density lipoprotein (LDL).

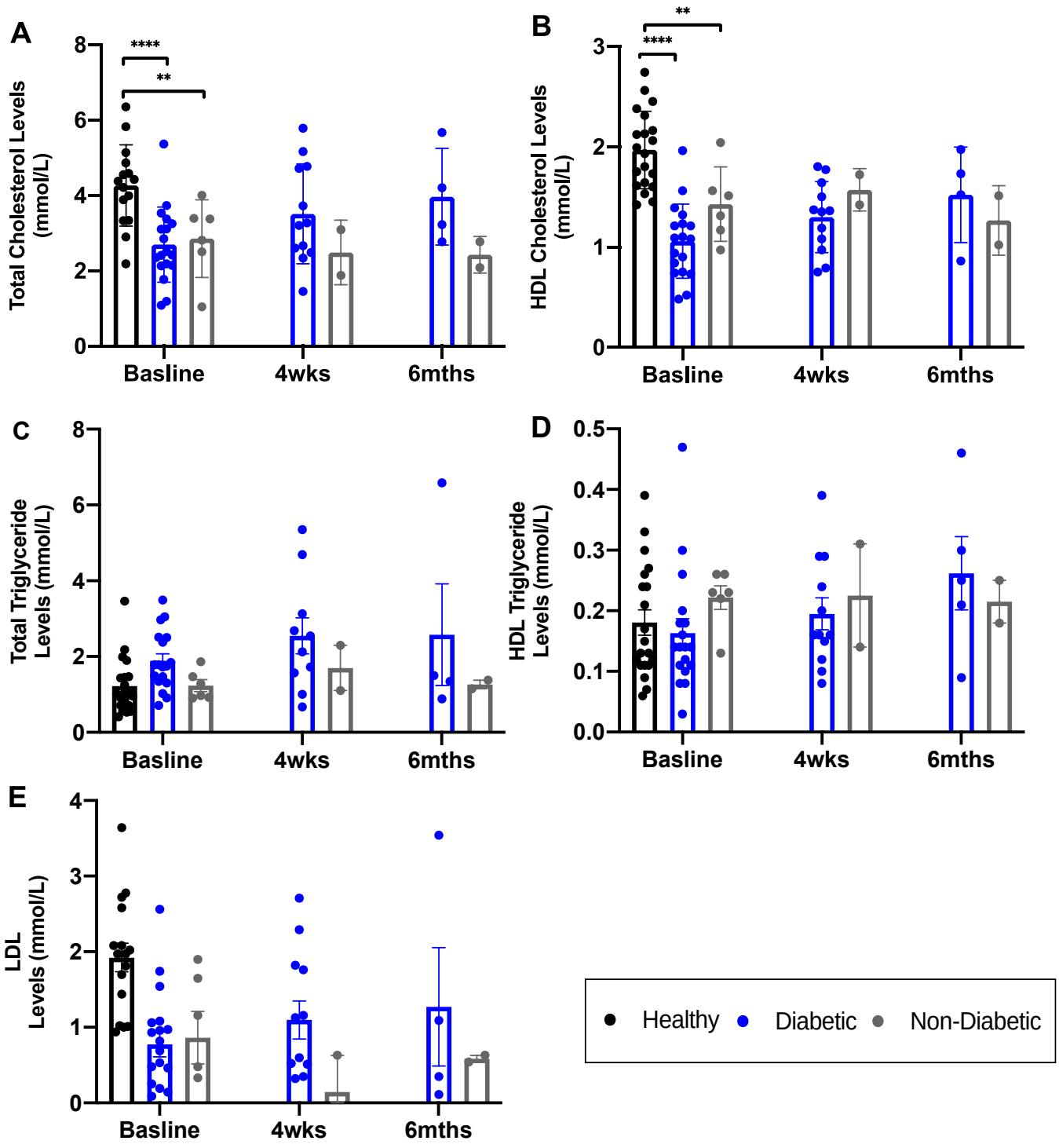

Figure 4.2 Lipid levels over time post-amputation. (A) Total cholesterol levels (mmol/L); **(B)** HDL cholesterol levels (mmol/L); **(C)** total triglyceride levels (mmol/L); **(D)** HDL triglyceride levels (mmol/L); **(E)** LDL levels (mmol/L) in healthy controls, diabetic and non-diabetic participants with toe amputation. Data are expressed as mean ± SD and inter-group

comparisons were made by unpaired t-test. **P<0.01 and ****P<0.0001 compared to healthy control group.

4.3.5 Wound closure

The percent wound closure from baseline over time until complete healing for each participant was calculated from wound images (Figure 4.3A). Except for participant #9, whose healing did not progress over 5 weeks (i.e., negative wound closure), required further debridement and did not continue in the study; all other participant wounds healed. The time for complete wound closure for participants with toe amputations ranged from 5 to 14 weeks from the time of amputation.

When comparing the time required for complete wound closure in diabetic and non-diabetic participants, we found that despite a low *n* number for non-diabetic participants, diabetic wounds took longer to completely heal than wounds in non-diabetic participants (approximately 6 weeks longer) (Figure 4.3B). This is consistent with previous research showing delayed wound healing in patients with diabetes [183].

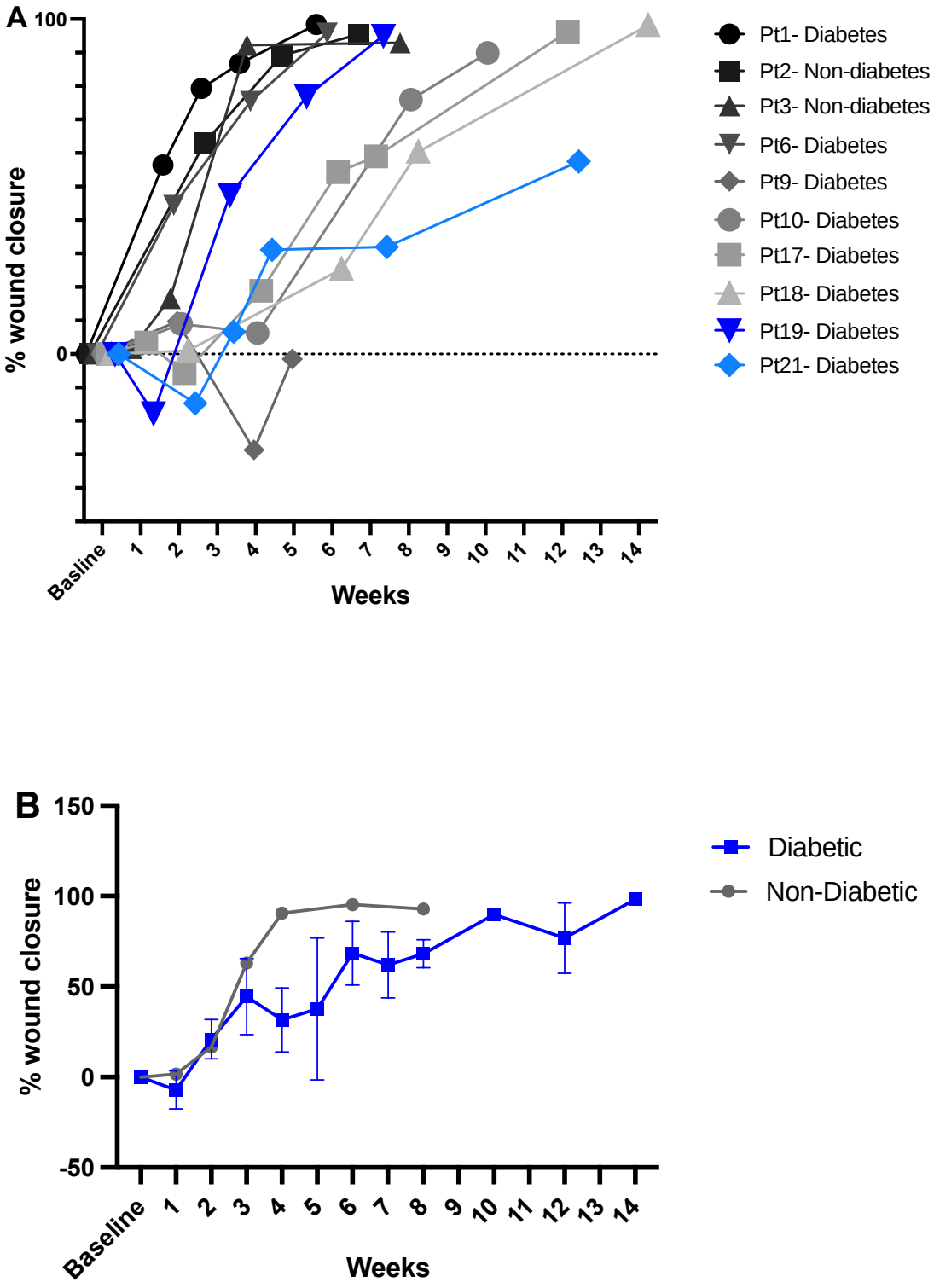

Figure 4.3 Wound closure post-amputation. Wound area was captured by a 3D camera (WoundVue) and analysed using WoundVue software. Wound closure is expressed as a percentage of baseline wound area after amputation. **(A)** The percentage of wound closure from

baseline for each patient. Each line represents a different participant. **(B)** The percentage of diabetic wound closure compared to non-diabetic wound closure.

4.3.6 HDL-cholesterol efflux capacity is impaired in diabetic participants

One of the most important functions of HDL is its ability to efflux cholesterol from macrophages. Recently, HDL functionality rather than concentration is thought to more accurately predict its atheroprotective effects [184]. We measured the cholesterol efflux capacity of HDL isolated from participant blood samples from all three groups (Figure 4.4A).

Our rHDL positive control elicited the greatest cholesterol efflux (8.0% ± 2.4) from [^{3}H]-cholesterol-loaded macrophages that was significantly higher than healthy control HDL at baseline (233.2%; P<0.0001; Figure 4.4B). At baseline no differences were evident in the cholesterol efflux capacity of HDL isolated from healthy controls, diabetic or non-diabetic participants. However, the cholesterol efflux capacity of HDL from diabetic participants was significantly lower than HDL from non-diabetic participants at 1-month (37.8%; 2.9 ± 0.1, *P*<0.05) and 6-months (45.5%; 3.9 ± 0.8) post-amputation.

A

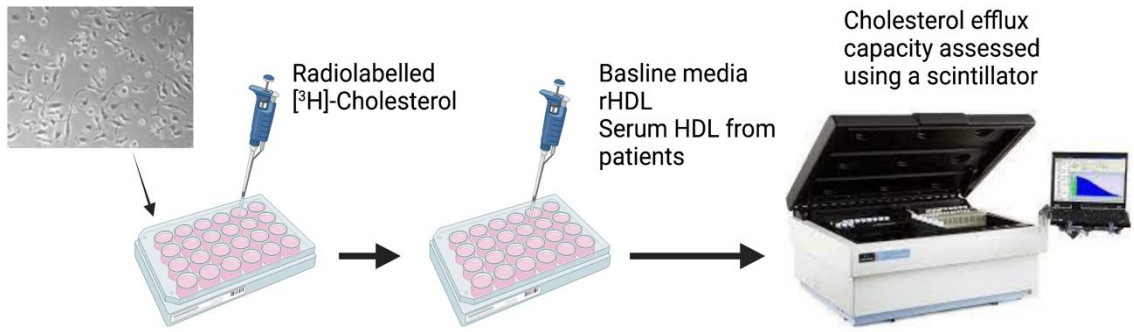
Radiolabelled
[3H]-Cholesterol
Basline media
rHDL
Serum HDL from
patients
Cholesterol efflux
capacity assessed
using a scintillator

B

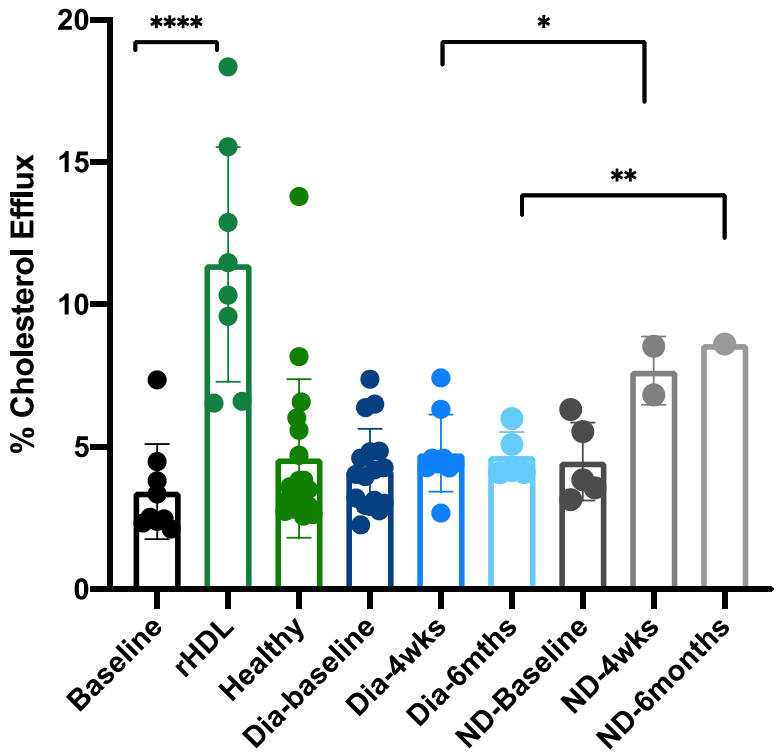
% Cholesterol Efflux
20
15
10
5
0
****
*
**
Baseline
rHDL
Healthy
Dia-baseline
Dia-4wks
Dia-6mths
ND-Baseline
ND-4wks
ND-6months

C

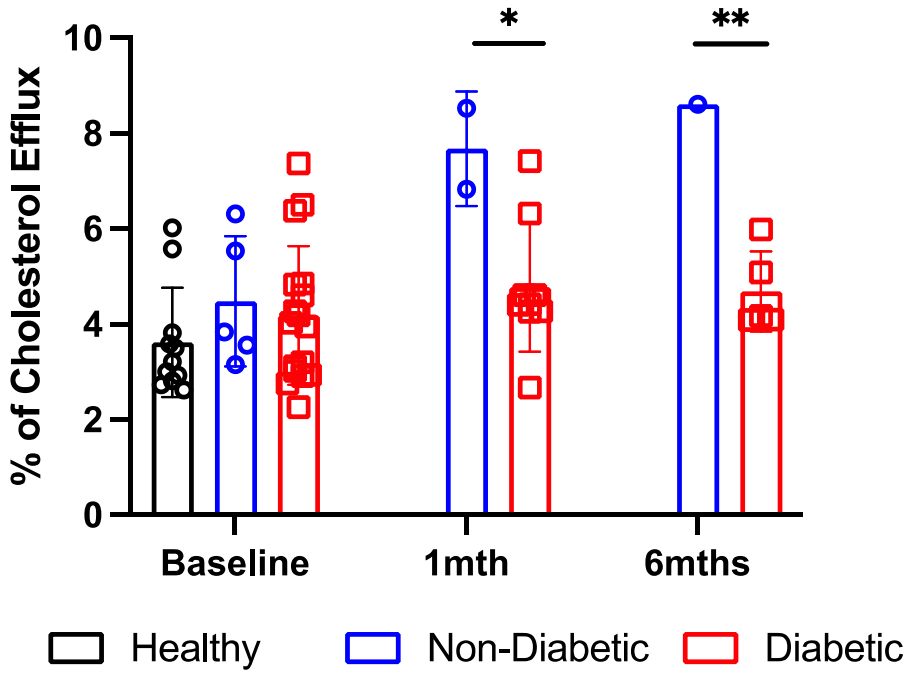
% of Cholesterol Efflux
10
8
6
4
2
0
*
**
Baseline
1mth
6mths
Healthy
Non-Diabetic
Diabetic

Figure 4.4 Cholesterol efflux capacity of participant HDL. (A) Immortalised bone marrow-derived macrophages were loaded with [^{3}H]-radiolabelled cholesterol (2 μCi/ml) for 24 h then incubated in serum-free medium to equilibrate labelled cholesterol among all intracellular cholesterol pools. Cells were then incubated with participant HDL and rHDL (25 μg/mL, positive control) and the movement of [^{3}H]-cholesterol from cells to media containing HDLs was quantified by scintillation counting. **(B)** Cholesterol efflux of PBS, rHDL, and participant HDL. Data are expressed as mean ± SD. Comparison between diabetic and non-diabetic groups was determined by unpaired t-test. *P<0.05, **P<0.005 and ***P<0.001 by unpaired t-test.

4.3.7 Relationship between HDL-cholesterol levels and the rate of wound closure

HDL-cholesterol levels have a well-established inverse association with the risk of myocardial infarction. [127]. Only one study has reported an inverse association between HDL-cholesterol levels and wound outcomes [163]. We first sought to determine the relationship between HDL-cholesterol concentration and the rate of wound healing in diabetic participants 1-month post-amputation. We found a significant positive correlation between HDL-cholesterol levels (mmol/L) and the rate of wound closure (% of change in mm^2/days) at 1-month post-amputation ($r^2 = 0.65$, P=0.03, Figure 4.5).

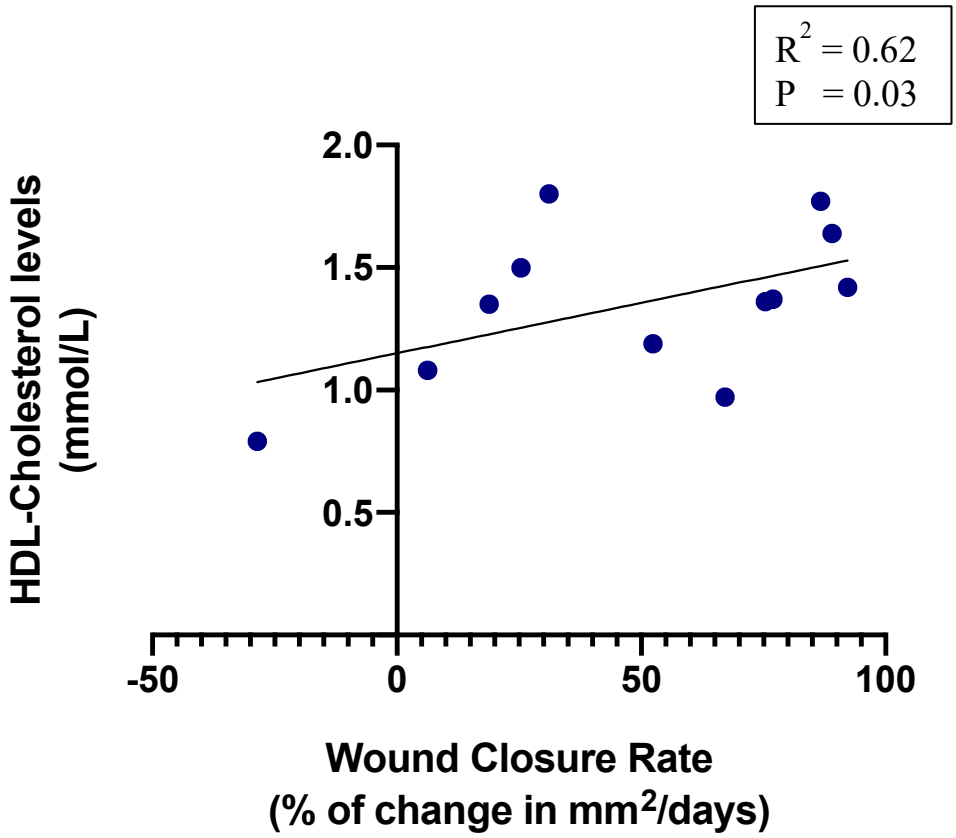

Figure 4.5 HDL-cholesterol levels associate with the rate of wound closure in diabetic participants 1-month post-amputation. Scatter plots showing the correlation between the levels of HDL-cholesterol (mmol/L) and the rate of wound closure (mm^2/days). Linear correlation by SPSS with Bootstrapping. Data were considered statistically significant at P<0.05; r value is the correlation coefficient.

4.3.8 No relationship between HDL-cholesterol levels or the rate of wound closure with HDL-cholesterol efflux

A significant positive correlation between the HDL cholesterol efflux capacity and HDL-cholesterol levels has been reported previously [136]. However, there was no correlation between HDL-cholesterol levels (mmol/L) and HDL-cholesterol efflux in patients with diabetes 1-month post-amputation ($R^2 = 0.04$, P=0.87; Figure 4.6A).

We also assessed the relationship between HDL cholesterol efflux capacity and the rate of wound closure (% of change in mm^2/days) in patients with diabetes 1-month post-amputation. We found no association ($r^2 = 0.339$, P = 0.615; Figure 4.6B), suggesting that the HDL functionality measure of HDL cholesterol efflux does not predict wound closure post-amputation.

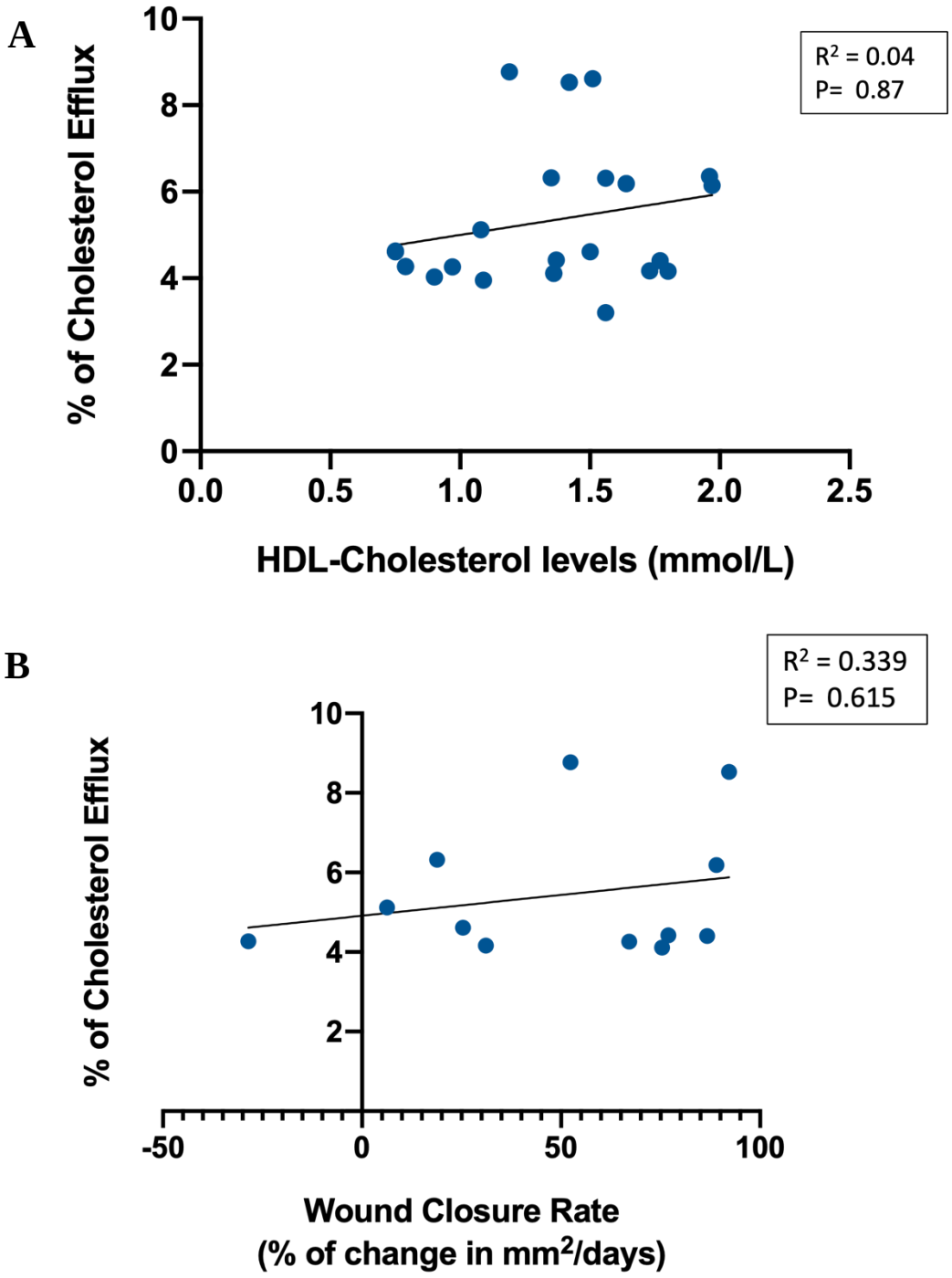

Figure 4.6 No association between HDL-cholesterol efflux and HDL-cholesterol levels or wound closure rate in diabetic participants 1-month post-amputation. Scatter plot showing the correlation between **(A)** the levels of HDL-cholesterol (mmol/L) with percentage of cholesterol efflux, and **(B)** the percentage of cholesterol efflux with the rate of wound closure (% of change in mm^2/days). Linear correlation by SPSS with Bootstrapping. Data were considered statistically significant at $P<0.05$; r value is the correlation coefficient.

4.3.9 No association between HbA1c levels, the rate of wound closure or HDL cholesterol efflux capacity

HbA1c is the most widely used parameter for assessment of glycaemic control. We determined the relationship between HbA1c and the rate of wound healing (% of change in mm^2/days) in diabetic participants 1-month post-amputation. Despite our observation that complete wound closure in the diabetic group took longer than in patients without diabetes, there was no correlation between HbA1c levels and the rate of wound healing ($r^2 = 0.33$, $P = 0.94$, Figure 4.8A).

We also investigated the correlation between HbA1c levels and the HDL cholesterol efflux capacity in diabetic participants 1-month post-amputation. We observed a non-significant negative correlation ($r = -0.46$, $R^2 = 0.2$, $P = 0.17$; Figure 4.8A). This trend suggested that higher levels of HbA1c (poorer management of diabetes) were weakly associated with lower HDL efflux capacity in the diabetic group post-amputation.

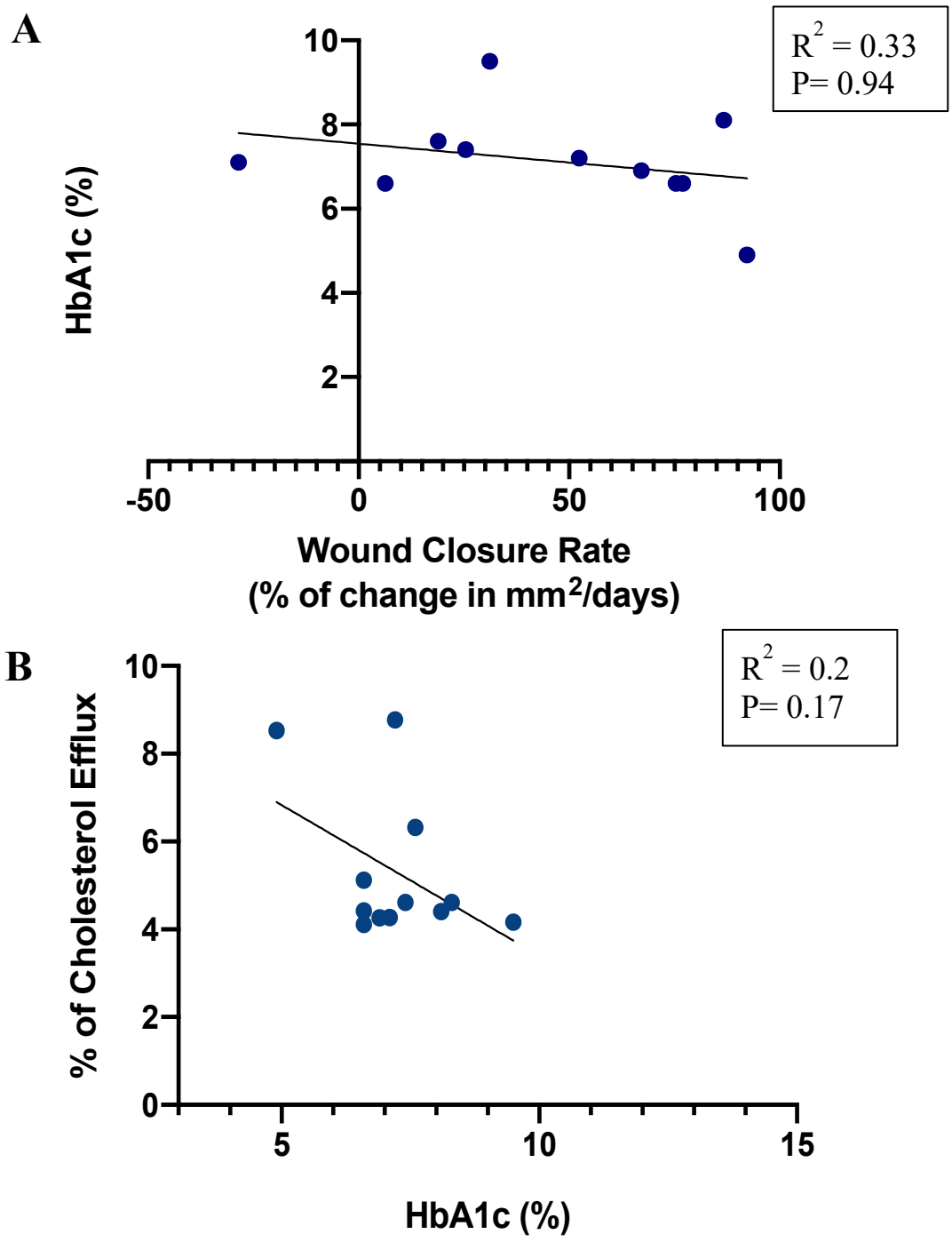

Figure 4.8 HbA1c does not associated with the rate of wound closure or HDL cholesterol efflux capacity. Scatter plot showing the correlation between **(A)** the rate of wound closure (mm^2/days), and **(B)** the percentage of cholesterol efflux capacity and HbA1c levels (%). Correlation analyses performed using Pearson Correlation. Linear correlation by SPSS with Bootstrapping. Data were considered statistically significant at $P<0.05$; r value is the correlation coefficient.

4.4 Discussion

There is a clear inverse correlation between the risk of myocardial infarction and HDL-cholesterol concentration. The Framingham study showed a 25% increased risk of myocardial infarction for every 0.13 mmol/L decrement in HDL [127]. Despite this, recent large-scale HDL-raising trials failed to show benefit in reducing cardiovascular events [132]. This highlighted that the biology of HDL was more complex than first thought and shifted the focus to HDL functionality as a more accurate predictor of cardiovascular risk. The studies reported in this Chapter aimed to determine the relationship between wound closure in diabetic and non-diabetic participants post-amputation together with HDL-cholesterol and HDL-cholesterol efflux, an important function of HDL. We report the following key findings: (1) the rate of wound closure post-amputation was delayed in the diabetic group compared to the non-diabetic group; (2) there was a significant positive correlation between HDL-cholesterol levels and the rate of wound closure in participants with toe/s amputation, 1-month post-amputation; (3) HDL obtained from diabetic participants 1-month and 6-months post-amputation have impaired cholesterol efflux; and (4) no association was found between the cholesterol efflux capacity of HDL and the rate of wound closure in participants with toe amputation/s.

Our study found a significant positive correlation between the levels of HDL-cholesterol and the rate of wound closure, demonstrating that diabetic and non-diabetic participants with higher levels of HDL-cholesterol had a faster rate of wound closure. This observation is in line with findings from a clinical study in Japan involving 163 patients with existing DFU that reported an inverse correlation between HDL-cholesterol levels and three wound healing outcomes: (1) minor amputation or below ankle amputation; (2) major amputation or above ankle amputation; and (3) death as a result of an unhealed ulcer. The findings from the Japanese study suggest that HDL-cholesterol levels are a predictive factor for lower extremity amputation [163]. Whilst the sample size for the Japanese study was 10-times higher than the sample size of this study, that study was a longitudinal historical cohort study and lipid levels

were not tracked over time, unlike our study. Nevertheless, both studies demonstrated a correlation between the level of HDL-cholesterol and wound healing outcomes.

We found that the cholesterol efflux capacity of HDL in all three groups (diabetic, non-diabetic, and healthy controls) was not significantly different baseline but was significantly higher in the non-diabetic group (Group 2) at 1-month and 6-months post-amputation compared to the diabetic group (Group 1). This suggests a recovery of non-diabetic HDL functionality over time post-amputation. In contrast, the cholesterol efflux capacity of HDL from the diabetic group failed to recover over time and remained significantly lower than the cholesterol efflux capacity of HDL from the non-diabetic group. Impaired HDL functionality (such as its efflux capacity) in conditions such as diabetes has been observed in previous studies [138]. One of the hallmarks of diabetes is increased glycation end products which promote oxidation of physiologically important molecules such as HDL and its apoA-I component [185], resulting in impaired functionality of HDL. A similar study found impaired apoA-I and HDL_2-mediated cholesterol efflux in macrophages treated with albumin from patients with diabetes compared to patients without diabetes [186]. The authors of that study attributed their findings to an impairment in ABCA-1-mediated reverse cholesterol transport due to advanced HDL glycation. The primary cause of dysfunctional HDL in diabetes is believed to be due to oxidative modification of the HDL particle and its main protein component apoA-I [137].

The relationship between the percentage of HbA1c and HDL cholesterol efflux capacity was not significant. This observation didn't support previous findings of impaired cholesterol efflux capacity of HDL in poorly managed diabetic conditions [137] with the potential for increased glycation end products leading to structural and functional HDL modifications. One of the limitations of our comparison was excluding participants with HbA1c levels higher than 12% from the study, therefore narrowing the data set for HbA1c. Recruitment of participants with

higher HbA1c levels in future studies will establish whether there is a significant negative correlation between HbA1c levels and the cholesterol efflux capacity of HDL.

As expected, the rate of post-amputation wound closure was slower in diabetic versus non-diabetic participants. It is well established that the rate of wound closure is significantly impaired in diabetic compared to non-diabetic populations. Diabetes is a significant factor underlying the formation of chronic wounds [187]. As discussed in Chapter 1, many factors, such as prolonged inflammation and impaired angiogenesis, lead to an attenuated rate of wound closure in diabetes [148]. In our study, the average time required for 100% wound closure was approximately 6 weeks longer for the diabetic group than the non-diabetic amputation group. This observation is consistent with our findings in mice in Chapter 3, in which wound closure was also significantly impaired in diabetic mice compared to non-diabetic mice post-wounding.

One element that may explain the delayed wound healing in the diabetes group was the significant elevation in C-reactive protein (CRP) compared to the healthy group. CRP is a highly conserved acute phase plasma protein which is primarily synthesised and released by the liver as a systemic response to inflammation [188]. Interestingly, CRP levels were elevated in the diabetic and not the non-diabetic amputation group (Groups 1 and 2, respectively). This presents a potential explanation for the delayed wound healing in the diabetic group as CRP is likely to be elevated by foot sepsis in this group. CRP plays an integral role in the inflammatory processes of wound healing, exhibiting chemotactic properties that recruit circulating leukocytes (white blood cells) to the wound [189]. Consistent with this, we also observed a significantly higher number of neutrophils and a higher total white cell count in the diabetic group compared to the healthy group. While CRP is essential for the inflammation phase, an excessive amount exacerbates inflammation and results in delayed wound healing.

The levels of total cholesterol were significantly lower in the diabetic and non-diabetic amputation groups compared to healthy controls. Interestingly, we also observed lower levels of LDL in both the diabetic and non-diabetic amputation groups compared to the healthy controls. We also observed significantly lower levels of HDL-cholesterol in the diabetic and non-diabetic groups. The likely explanation for this is that the majority of the diabetic study participants were on statins (lipid-lowering medications) (Table 4.2). Lipids in the diabetic and non-diabetic amputation groups were measured at 1-month and 6-months post-amputation; no differences were observed between the two groups. Previous studies have shown an association between low levels of HDL (HDL_2 subtype) and the risk of developing type 2 diabetes [130]. It is suggested that HDL-cholesterol stimulates insulin secretion from pancreatic β-cells and modulates glucose uptake in skeletal muscle in animal models and in clinical trials [190, 191]. We also observed lower HDL-cholesterol levels in the diabetic group suggesting there was insufficient HDL-cholesterol to stimulate insulin secretion from pancreatic β-cells and a failure in glucose uptake leading to hyperglycaemia. It is important to mention that further prospective studies using Mendelian randomisation and clinical trials did not find an association between reduced HDL-cholesterol and increased risk of type 2 diabetes [192].

We explored the relationship between the levels of HDL-cholesterol and HDL cholesterol efflux capacity. A landmark study investigating the association between HDL cholesterol efflux capacity and risk of coronary artery disease found a significant positive correlation between HDL cholesterol efflux capacity and HDL-cholesterol levels [136]. In contrast, our study did not support this correlation. Boosting patient numbers in future studies would likely increase the power and may reveal a significant association. One of the main functions of HDL is cholesterol efflux, hence it is logical that higher levels of HDL-cholesterol indicate higher levels of HDL and therefore increased cholesterol efflux.

This study also identified that circulating neutrophils were significantly higher in both the diabetic and non-diabetic amputation groups compared to the healthy control group. Neutrophils respond to infection and play an integral role in the inflammation phase of the wound healing process, releasing cytokines such as IL-8, IL-1β and TNF-α [193]. Previous studies have shown that neutrophils from patients with diabetes have an impaired capacity to migrate to sites of inflammation, reduced phagocytotic ability and release proteases and reactive oxygen species [193]. It would appear, however, that the elevation in neutrophils is not from diabetes but is a response to acute infection post-amputation, as patients without diabetes and toe amputations also had higher neutrophil levels. Indeed, a retrospective observational study [194] recommended the neutrophil-lymphocyte ratio (NLR) and platelet-to-lymphocyte ratio (PLR) as a reliable predictive factor for DFU post-amputation outcomes, such as mortality. NLR and PLR are novel biomarkers for systemic inflammation and patients undergoing toe/s amputation experience local infection and systemic inflammation as discussed previously with high CPR levels showing increased inflammation.

In line with the increase in neutrophils, the number of white cells were significantly higher in the diabetic and non-diabetic amputation groups compared to the healthy control group. This suggests an increased systemic and local inflammatory response for patients undergoing amputation surgery. Our study also found significantly lower haemoglobin levels in the diabetic and non-diabetic amputation groups compared to the healthy control group. Indeed, low haemoglobin levels and consequent anaemia are common in patients with diabetes, and low haemoglobin concentration contributes to progression of many diabetic complications such as diabetic nephropathy and retinopathy [195].

In conclusion, this study was the first to examine the relationship between the rate of post-amputation wound closure and HDL-cholesterol concentration, and HDL cholesterol efflux capacity in diabetic and non-diabetic participants who had undergone toe/s amputation, with

the aim of examining whether HDL functionality could be a predictive factor for determining the rate of post-amputation wound closure. Whilst our study did find a correlation between HDL-cholesterol levels and the rate of wound closure in the diabetic group, there was no relationship with the HDL functionality measure of cholesterol efflux capacity and the rate of wound closure. We did, however, identify that diabetic HDL has an impaired HDL cholesterol efflux capacity. In the next Chapter, we explore other main functions of HDL (anti-inflammatory and proangiogenic) in all study groups and investigate the relationship between the rate of wound closure with those HDL functions.

CHAPTER 5 – THE ANTI-INFLAMMATORY AND PRO-ANGIOGENIC PROPERTIES OF HDL IN PARTICIPANTS WITH/WITHOUT DIABETES AND TOE AMPUTATIONS

5.1 Introduction

HDL has well-established anti-inflammatory properties [196]. As discussed in detail in Chapter 1, HDL suppresses inflammation in various cell types, including endothelial cells, and inhibits monocyte/macrophage recruitment to sites of inflammation [110]. HDL suppresses endothelial cell adhesion molecules including *ICAM-1* and *VCAM-1*, and inhibits the expression of chemokines *CCL2*, *CCL5* and *CX_3CL1 in vitro* and *in vivo* [116]. Adhesion molecules and chemokines play integral roles in facilitating the recruitment and trafficking of monocytes [145, 197]. HDL isolated from patients with type 2 diabetes is reported to elicit impaired anti-inflammatory effects when compared to HDL from healthy patients, losing its ability to suppress endothelial VCAM-1 expression [198]. One mechanism for this impairment was found to be the non-enzymatic glycation and oxidation of HDL by advanced glycation end products [199].

Another key function of HDL is its ability to promote angiogenesis in response to hypoxia/ischaemia and in diabetes [159]. Angiogenesis is a physiological process through which new blood vessels develop from a pre-existing vascular network. It is essential for tissue regeneration and repair, making it an integral part of successful wound healing. *In vitro* studies show laboratory-purified rHDL promotes endothelial cell proliferation, migration, and tubule formation in high glucose conditions and in response to hypoxia. Consistent with this, infusions of rHDL augment ischaemia-driven angiogenesis and rescue diabetes-impaired angiogenesis in murine hind-limb ischaemia and wound healing models [155]. *Ex vivo* testing of endogenous HDL functionality has revealed that HDL from patients with diabetes exhibits an impaired capacity to stimulate endothelial cell migration and proliferation. Mechanistically this has been reported to be due to diabetes-induced down-regulation of SR-BI, an important cell surface receptor that interacts with HDL, and an impaired ability to maintain Akt activation [200]. Consistent with this, another clinical study found that the pro-angiogenic ability of HDL isolated from diabetic Australian Indigenous people, was attenuated. This was reflected by an impaired ability of diabetic HDL to promote endothelial tubule formation and increase HIF1-α expression when compared to HDL from non-diabetic control patients [201].

In summary, there is increasing evidence that the functionality of HDL is impaired in diabetes. This includes a reduced ability of HDL to impart anti-inflammatory effects and promote angiogenesis. Furthermore, HDL functionality is increasingly being recognised as a better predictive marker of coronary artery disease, yet its predictive value has never been previously examined on the backdrop of diabetic wound healing. Accordingly, in this Chapter, we investigated the relationship between wound closure and the anti-inflammatory and pro-angiogenic effects of HDL isolated from diabetic and non-diabetic participants undergoing a toe amputation. We also compared differences in these key HDL functionality measures between HDL isolated from diabetic, non-diabetic, and healthy individuals.

5.2 Methods

5.2.1 Plasma HDL preparation

To isolate HDL from plasma, 500–700 μL of plasma was incubated with equal volumes of polyethylene glycol (PEG-6000, 200 mg/mL in MilliQ water) at room temperature for 5 minutes to precipitate the apoB-containing lipoproteins. The samples were then centrifuged at 13,000 rpm for 5 minutes at 4°C using an Eppendorf centrifuge 5145R (Eppendorf, Hamburg, Germany). The supernatant (containing the HDL fraction) was collected and filter-sterilised using a 0.22 μm filter. HDL concentration was determined using the Pierce™ BCA Protein Assay Kit, following the manufacturer's instructions. Isolated participant HDL was used for subsequent cell culture studies to assess anti-inflammatory and angiogenic capacity.

5.2.2 Cell culture and treatments

Anti-inflammatory capacity of HDL

HCAECs (Donor 3003, Passage 4, Cell Applications Inc.) were cultured in MesoEndo media. Cells were seeded at $1.5x10^5$ cells/well and $1.2x10^5$ cells/well to measure the anti-inflammatory and angiogenic capacity of HDL, respectively. The cells were seeded in 6-well plates and incubated at 37˚C for 24 h. To assess the anti-inflammatory effects of HDL, HCAECs were treated with either PBS, rHDL (positive control) or isolated HDL (final protein concentration, 20 μM) for 16 h (triplicate wells per condition). HCAECs were then stimulated with 0.6 ng/mL TNFα for 4.5 h to mimic a pro-inflammatory environment. Cell lysates were isolated to assess gene expression of inflammatory mediators including *Rela*, *Ccl2*, *Ccl5*, *Cxcl3*, *Icam-1* and *Vcam-1* (Figure 5.1A).

Pro-angiogenic capacity of HDL

To assess the angiogenic capacity of HDL, HCAECs were treated with PBS (vehicle control), rHDL (positive control) or HDL from all three participant groups (final protein concentration 20 μM) for 18 h (triplicate wells per condition). HCAEC media was then replaced

with fresh MesoEndo media containing either 5 mM or 25 mM D-glucose for 48 h to mimic both normal and diabetic glucose environments. Treated cells were then assessed for their ability to form vascular networks using the Matrigel tubulogenesis assay (Figure 5.1B).

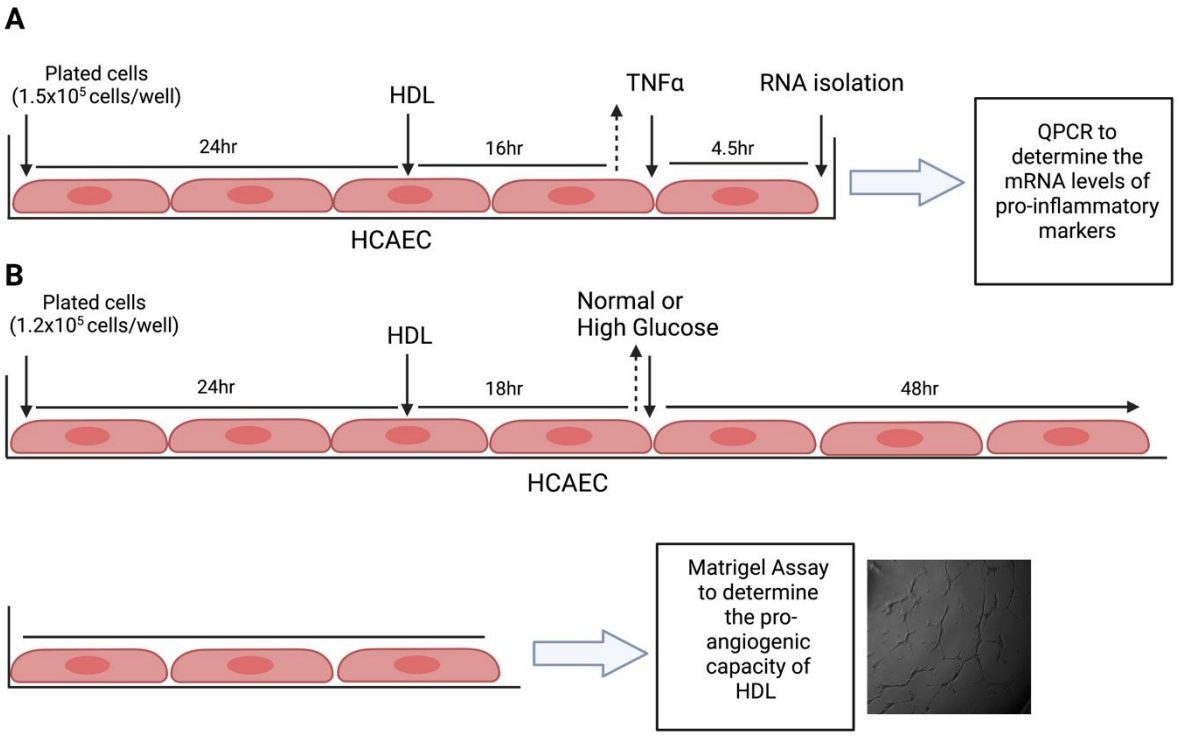

Figure 5.1 Schematic representation of the HDL anti-inflammatory and pro-angiogenic assay protocols. (A) HCAECs were incubated with HDL for 16 h, after which TNFα was added for 4.5 h. RNA was isolated from treated cells and changes in mRNA levels of inflammatory markers were determined. **(B)** HCAECs were incubated with HDL for 18 h, after which the cells were incubated with normal (5 mM) or high glucose (25 mM) for 48 h. Treated HCAECs were then used in a Matrigel assay to measure their capacity to form tubules. HDL: high density lipoprotein; HCAECs: human coronary artery endothelial cells; TNFα, tumour necrosis factor α.

5.2.3 RNA extraction, cDNA synthesis and quantitative real-time PCR

Total RNA was extracted from HCAECs using a TRI reagent phenol-chloroform extraction. RNA concentration was quantified using a Nanodrop 8000 spectrophotometer (Thermo Fisher Scientific). All samples were within the 1.8 – 2.0 absorbance ratio (A260/A280) range and normalised to 100±2 ng/mL; 400 ng total RNA was reverse transcribed to cDNA using an iScript cDNA synthesis kit (BioRad). Quantitative real-time PCR was used to determine the expression of *NF-κB-p65 (RELA)*, *CCL2*, *CCL5*, *CX3CL1*, *VCAM1* and *ICAM1* using SSoAdvanced™ Universal SYBR Green Supermix in a Quant Studio 7 Flex Real-Time PCR System (Applied Biosystems). Relative changes in mRNA levels were normalised using the ΔΔCt method to reference gene β2-microglobulin.

5.2.4 Matrigel Tubulogenesis Assay

Growth factor reduced Matrigel (40 μL) was added to a 96-well plate and swirled to ensure an even coating in each well. The Matrigel was left to polymerise at 37°C for 30 minutes. Treated cells were trypsinised and seeded at 1.5 x 10^4 cells/well (4-5 replicates per condition) on polymerised Matrigel in the respective glucose media. The plate was incubated at 37°C for 8 h and each well was imaged at 2.5X magnification under light microscopy using a Carl Zeiss Microscopy AxioCam E1Zc 5s camera (Zeiss, Oberkochen, Germany) on an Axio Zeiss Vert.A1 microscope (Zeiss, Oberkochen, Germany). To compare changes in angiogenesis capability, the number of tubules, branch points, and tubule length were counted using custom MATLAB software developed by our team [202]. Tubule number, branch point number, and tubule length were identified by the software (Figure 5.3). The algorithm used for developing this software consisted of the steps: (1) reading image; (2) image adjusting; (3) black/white filtering; (4) vessel outline extraction; and (5) finding individual vessels.

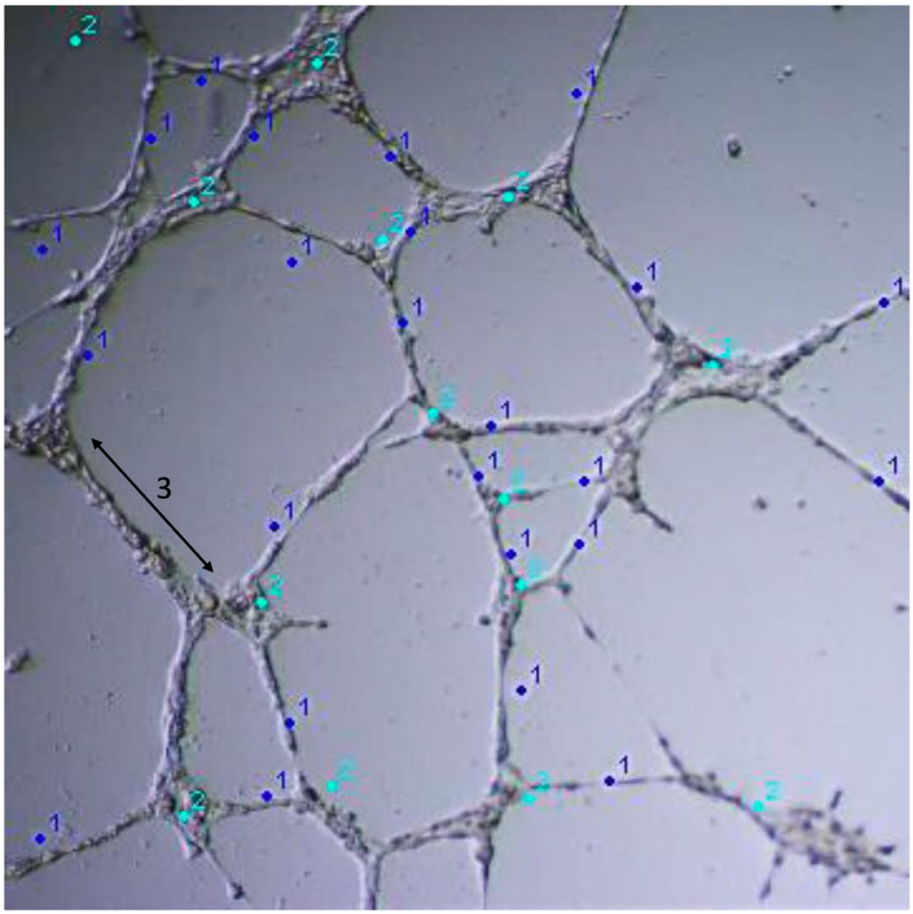

Figure 5.2 Matrigel tubulogenesis assay measures. Light microscopy image at 2.5X magnification. Tubule number represented as 1 (dark blue). Branch points represented as 2 (aqua). Tubule length represented as 3 (black arrowed line).

5.2.5 Statistical analysis

GraphPad Prism (version 9) and SPSS (version 27) were used for graph preparation and data analysis. Inter-group comparisons were performed using either one-way ANOVA with post hoc Tukeys test or paired and unpaired two-group t-tests. The association of HDL anti-inflammatory and proangiogenic capacity with the rate of wound healing was assessed using the linear correlation test in SPSS, with wound size at baseline adjusted. P value of 0.05 indicated statistical significance.

5.3 Results

5.3.1 Impaired anti-inflammatory properties of diabetic HDL

We first sought to determine the inflammatory response of HCAECs to incubation with participant HDL. Figure 5.3 illustrates the results from all timepoints (post-amputation, 1-month and 6-months post amputation) combined. Interestingly, HDL from the non-diabetic amputation group elicited significantly lower *RELA* mRNA levels in HCAECs compared to HDL from the diabetic amputation group (51.4%; $P<0.01$; Figure 5.3A). Incubation of HCAEC with HDL from healthy controls significantly decreased mRNA levels of *CCL5* (26.3%; $P<0.05$; Figure 5.3B) compared to PBS-treated controls. *CCL5* mRNA levels were higher following incubation of HCAECs with HDL from diabetic participants than healthy control HDL (63.7%; $P<0.01$) and non-diabetic HDL (88.2%; $P<0.01$). We also observed that incubation with HDL from healthy controls and non-diabetic participants resulted in significantly lower *CCL5* mRNA levels compared to PBS controls (26.3%; $P<0.05$ and 35.9%; $P<0.05$ respectively; Figure 5.3B).

Compared to PBS controls, incubation of HCAECs with HDL from healthy controls (37.9%; $P<0.0001$), non-diabetic (45.0%; $P<0.0001$) and diabetic participants (35.1%; $P<0.0001$) significantly reduced *CCL2* mRNA levels (Figure 5.3C). Furthermore, non-diabetic HDL elicited significantly lower *CCL2* levels than diabetic HDL (15.3%; $P<0.05$; Figure 5.3C). We also observed significantly lower mRNA levels of *CX_3CL1* following treatment of HCAECs with HDL obtained from healthy controls, diabetic and non-diabetic participants (53.8%, $P<0.0001$; 46.9%; $P<0.0001$ and 48.8%, $P<0.001$, respectively; Figure 5.4D) compared to PBS controls. Similarly, incubation of HCAECs with healthy, diabetic, and non-diabetic HDL led to significant reductions in mRNA levels of *ICAM-1* (46.8%; $P<0.0001$, 35.9%; $P<0.001$ and 57.1%; $P<0.0001$, respectively; Figure 5.3E) and *VCAM-1* (44.6%; $P<0.0001$, 44.9%; $P<0.0001$ and 48.23%, $P<0.0001$, respectively; Figure 5.3F) compared to

PBS controls. Furthermore, non-diabetic HDL caused a greater reduction in *ICAM-1* mRNA than diabetic HDL (33.1%, $P<0.05$; Figure 5.3E).

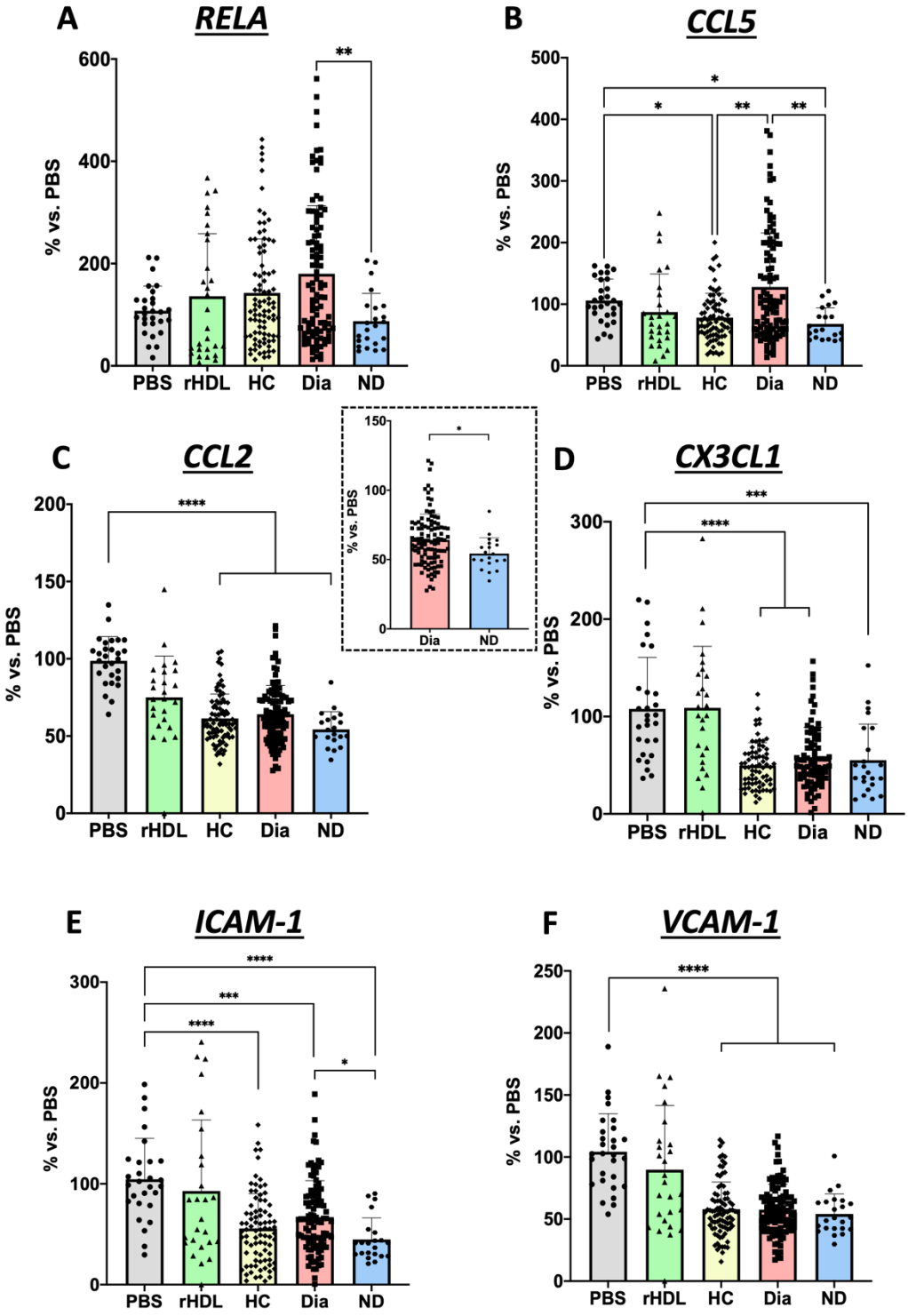

Figure 5.3 HDL inhibits inflammatory mediators in endothelial cells. HCAECs were treated with PBS, rHDL or participant HDL (20 μM) for 16 h. From RNA isolated from treated cells, mRNA levels of **(A)** *RELA*, **(B)** *CCL5*, **(C)** *CCL2*, **(D)** *CX_3CL1*, **(E)** *ICAM-1*, and **(F)** *VCAM-1* were measured using the $^{\Delta\Delta}$Ct method normalised to β2-microglobulin. Data are expressed as mean ± SD. Data points represent triplicates for each participant sample. *P<0.05, **P<0.01, ***P<0.001 and ****P<0.0001 by one-way ANOVA with Tukey's post hoc

comparison test for parametric and Kruskall-Wallis test with post hoc Dunn's comparison for non-parametric data. HC: healthy control, Dia: diabetes and ND: non-diabetes.

5.3.2 Changes in the anti-inflammatory effects of HDL over time post-amputation

Blood samples were collected from the diabetic and non-diabetic groups at three different time points post-toe amputation. Changes in the anti-inflammatory effects of these HDLs on HCAECs were next investigated. This revealed that HCAECs treated with HDL from non-diabetic participants at the time of the surgery had lower levels of *RELA* mRNA than diabetic HDL-treated HCAECs (44.2%; $P<0.05$, Figure 5.4A, inset). When comparing changes in *RELA* mRNA following treatment with diabetic HDL over time, we observed that *RELA* mRNA was lowered most effectively by diabetic HDL obtained 6-months post-amputation and was significantly lower than HCAECs incubated with HDL obtained at 1-month post amputation (52.0%; $P<0.05$, Figure 5.4B), indicating HDL gained anti-inflammatory functionality over time post-amputation.

The mRNA levels of *CCL5* were significantly higher in HCAECs treated with HDL from diabetic participants at 1-month post-surgery compared to healthy control levels (104.5%; $P<0.01$, Figure 5.4C). No changes were noted in the effectiveness of diabetic HDL to suppress *CCL5* over time (Figure 5.4D). At each time point post-amputation, there were no differences in the effect of HDL on *CCL2* mRNA levels between HDL in diabetic and non-diabetic amputation groups. When comparing the different diabetic HDL over time, a reduction in *CCL2* was observed following incubation with HDL from diabetic participants 1-month post-amputation compared to HDL at baseline (16.1%; $P<0.05$, Figure 5.4F).

The levels of *Cx3cl1* mRNA were significantly lower in HCAECs treated with HDL from healthy controls (53.8%; $P<0.0001$), participants with diabetes at baseline (39.7%; $P<0.01$), 1-month post-amputation (55.6%; $P<0.001$), and 6-months post-amputation (53.7%; $P<0.05$), and patients without diabetes 1-month post-amputation (71.7%; $P<0.001$) compared to PBS controls (Figure 5.4G). We also observed that the mRNA levels of *Cx3cl1* were lower following incubation with HDL from patients without diabetes compared to participants with diabetes 1-

month post-amputation (36.2%; *P*=0.09, Figure 5.4G, inset). No significant changes were observed in *Cx3cl1* mRNA levels with HDL from diabetic participants over time (Figure 5.4H).

We observed lower levels of *Icam-1* mRNA elicited from HDL from healthy controls (46.8%; *P*<0.0001), diabetic participants at baseline (33.1%; *P*<0.05) and at 6-months post-amputation (43.0%; *P*<0.05), and non-diabetic participants at 1-month post-amputation (66.7%; *P*<0.01) compared to PBS controls (Figure 5.4I). Interestingly, the HDL from non-diabetic participants 1-month post-amputation significantly lowered the mRNA levels of *ICAM-1* compared to HDL from diabetic participants at the same time point (47.0%; *P*<0.05; Figure 5.4I). No changes were observed in the effectiveness of diabetic HDL to suppress *ICAM-1* over time post-amputation (Figure 5.4J).

As illustrated in Figure 5.4K, the mRNA levels of *VCAM-1* were significantly decreased by HDL obtained from healthy controls (44.6%; *P*<0.0001), diabetic participants at baseline (42.0%; *P*<0.0001), non-diabetic participants at Baseline (46.7%, *P*<0.001), diabetic participants 1-month post-amputation (42.7%; *P*<0.0001), non-diabetic participants 1-month post-amputation (51.2%; *P*<0.01), and diabetic participants 6-months post-amputation (53.5%; *P*<0.05) when compared to PBS controls. We observed no significant change in *VCAM-1* mRNA expression following incubation with HDL from diabetic participants over time post-amputation (Figure5.4L).

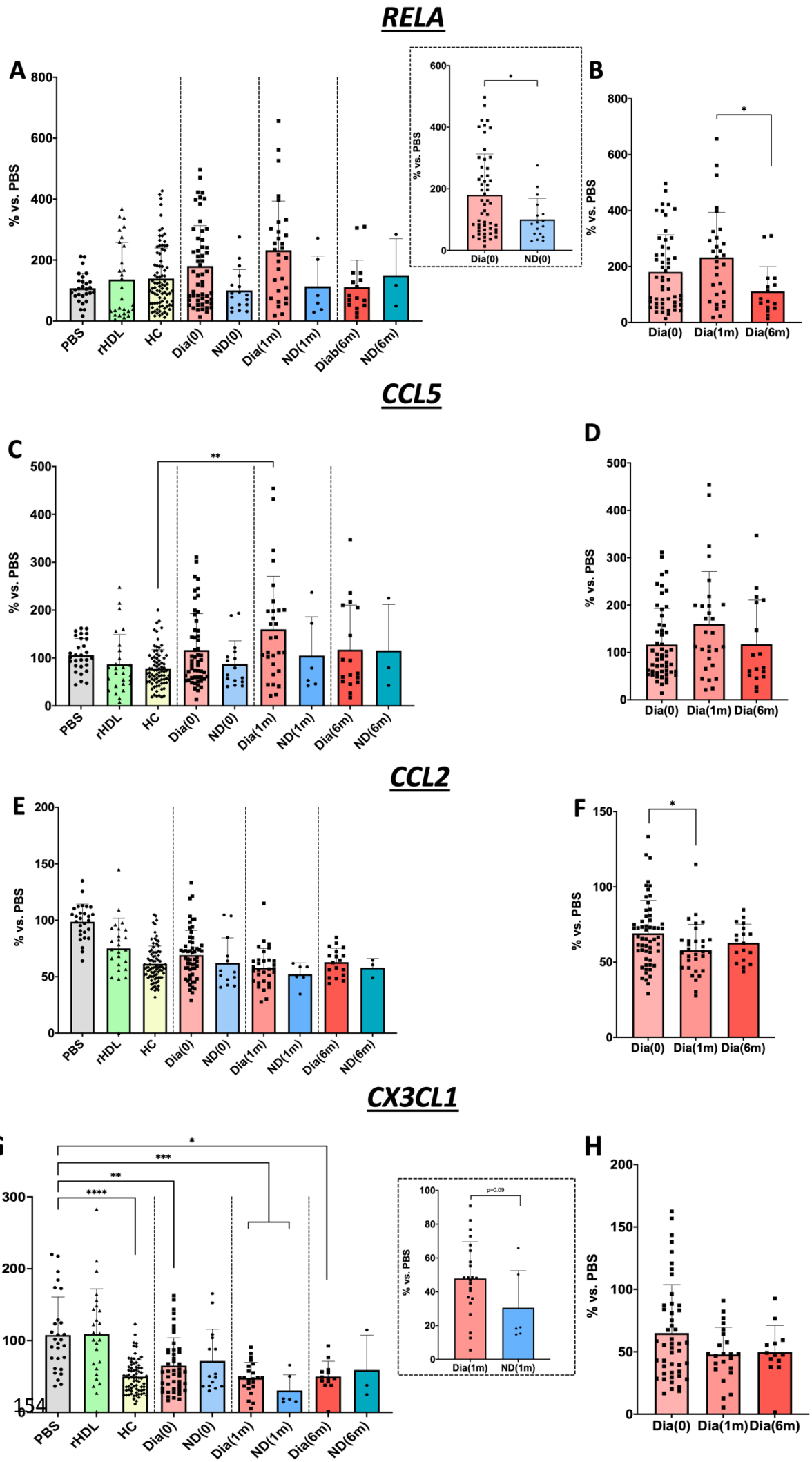
RELA
A
% vs. PBS
PBS
rHDL
HC
Dia(0)
ND(0)
Dia(1m)
ND(1m)
Diab(6m)
ND(6m)
*
B
Dia(0)
Dia(1m)
Dia(6m)
CCL5
C
**
D
CCL2
E
F
CX3CL1
G
*
***
**
****
p=0.09
H

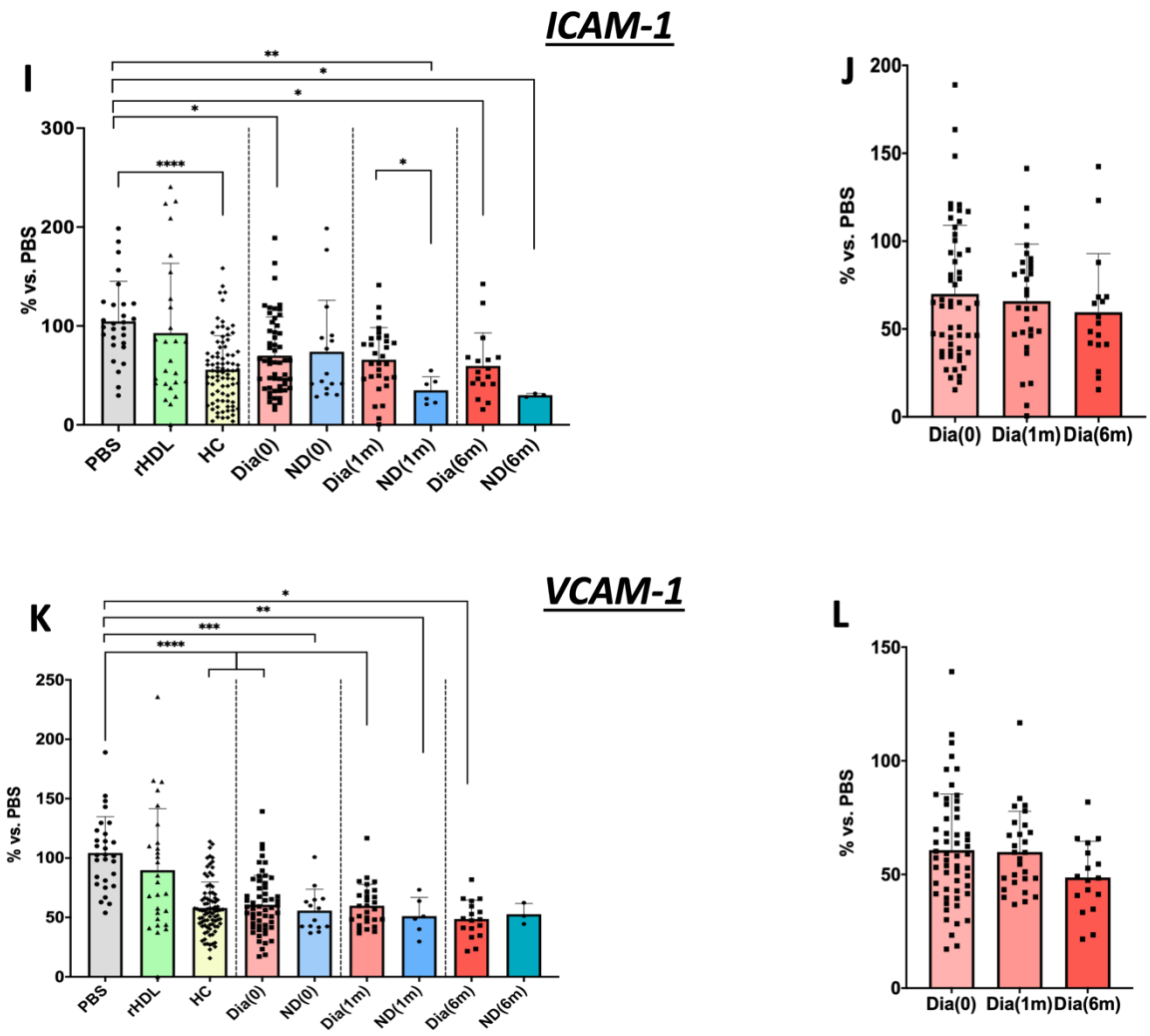

Figure 5.4 Changes in HDL anti-inflammatory capacity in endothelial cells over time post-amputation. HCAECs were treated with PBS, rHDL or participant HDL (20 μM) for 16 h. From RNA isolated from treated cells mRNA levels of **(A)** *RELA*, **(B)** diabetic HDL *RELA* over time, **(C)** *CCL5*, **(D)** diabetic HDL *CCL5* over time, **(E)** *CCL2*, **(F)** diabetic HDL *CCL2* over time, **(G)** *CX3CL1*, **(H)** diabetic HDL *CX3CL1* over time, **(I)** *ICAM-1*, **(J)** diabetic HDL *ICAM-1* over time, **(K)** *VCAM-1*, **(L)** diabetic HDL *VCAM-1* over time were measured using the $^{\Delta\Delta}$Ct method normalised to β2-microglobulin. Data are expressed as mean ± SD. Data points represent triplicate for each individual participant sample. **P*<0.05, ***P*<0.01, ****P*<0.001, and *****P*<0.0001 by one-way ANOVA with Tukey's post hoc comparison test for parametric, and Kruskall-Wallis test with post hoc Dunn's comparison for non-parametric data.

5.3.3 Anti-inflammatory properties of patients HDL with TNFα stimulation

We next sought to determine changes in the ability of HDL to suppress cytokine (TNFα)-stimulated inflammation in HCAEC. Figure 5.5 illustrates the results from all timepoints (post-amputation, 1-month and 6-months post amputation) combined. Unexpectedly, we did not observe an increase in *RELA* following TNFα stimulation in the PBS control, compared to the unstimulated PBS control (Figure 5.5A). Incubation with HDL from the diabetic group following stimulation with TNFα, significantly increased *RELA* mRNA levels (85.0%; $P<0.05$; Figure 5.5A) compared to PBS controls. Incubation with HDL from the non-diabetic group elicited significantly lower levels of TNFα-stimulated *RELA* mRNA (30.4%; $P=0.054$; Figure 5.5A, inset) compared to HDL from the diabetic group.

We observed a significant increase in *CCL5* mRNA expression in cells treated with rHDL following TNFα stimulation (111.6%; $P<0.05$; Figure 5.5B) compared to unstimulated PBS controls. HDL from diabetic participants also induced higher *CCL5* expression in TNFα-stimulated cells (64.0%; $P<0.05$; Figure 5.5B) compared to unstimulated PBS controls. Stimulation by TNFα significantly increased the expression of *CCL2* across all treatments when compared to unstimulated PBS controls (Figure 5.5C). Furthermore, pre-incubation with HDL from non-diabetic participants suppressed *CCL2* mRNA levels to a greater extent than HDL from diabetic participants (27.6%; $P<0.05$, respectively; Figure 5.5C, inset).

Investigating the mRNA levels of *CX3CL1* revealed a significant increase in *CX3CL1* in all treatment groups following TNFα stimulation compared to PBS unstimulated controls (Figure 5.5D). No significant changes were noted for *CX3CL1* mRNA levels in cells treated with HDL from the different groups after TNFα stimulation (Figure 5.5D) compared to PBS stimulated controls. *ICAM-1* and *VCAM-1* mRNA levels were also significantly increased in all treatment groups after stimulation with TNFα when compared to PBS controls (Figure 5.5E-F). We did

not observe changes in mRNA levels of *ICAM-1* and *VCAM-1* between the different groups with TNFα stimulation (Figure5.5E -F).

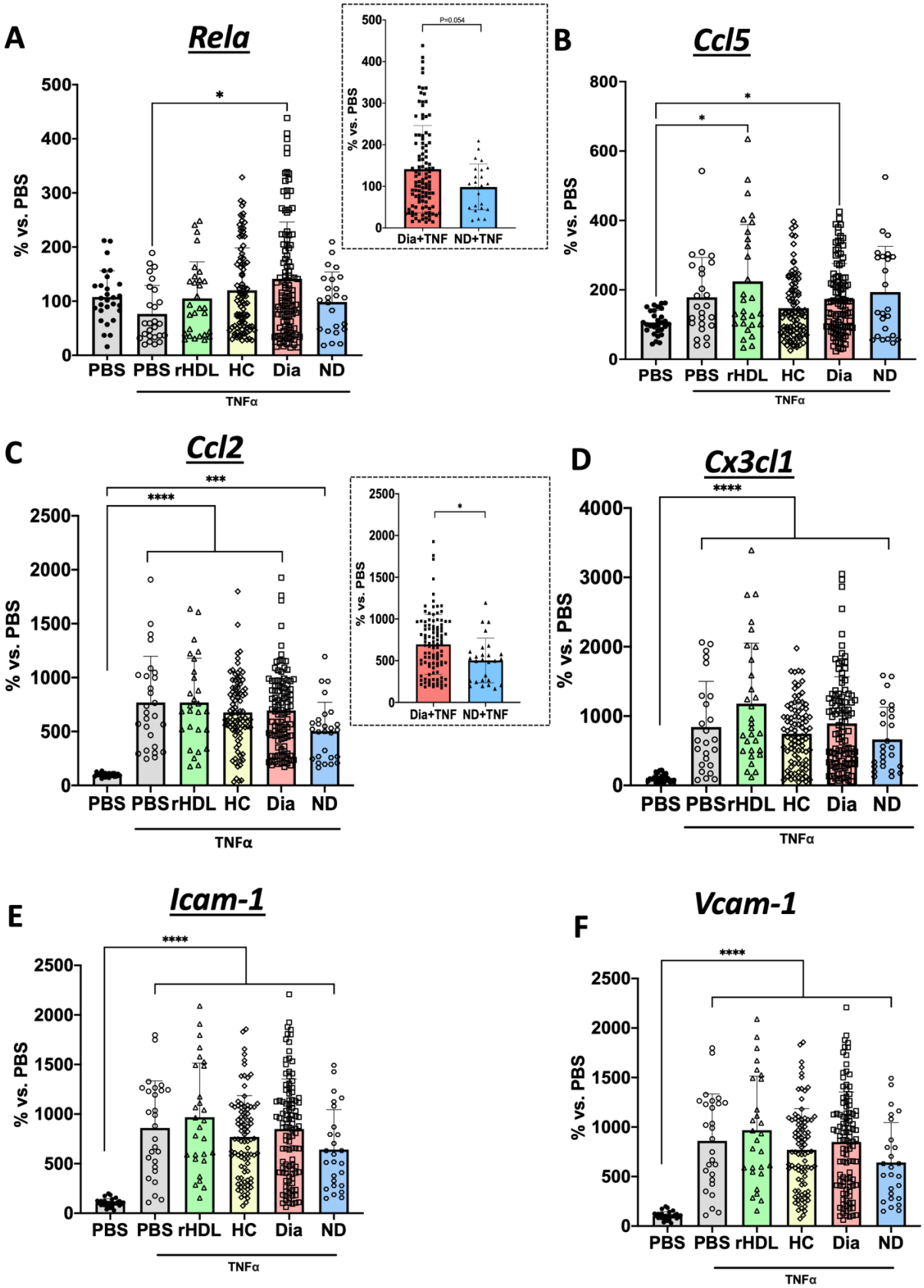

Figure 5.5 The HDL anti-inflammatory response to TNFα stimulation in endothelial cells. HCAECs were treated with PBS, rHDL or participant HDL (20 μM) for 16 h. Cells were then stimulated with TNFα. From RNA isolated from treated cells, mRNA levels of **(A)** *RELA*, **(B)**

CCL5, **(C)** CCL2, **(D)** CX3CL1, **(E)** ICAM-1, and **(F)** VCAM-1 were measured using qPCR by the $^{\Delta\Delta}$Ct method normalised to β2-microglobulin. Data are expressed as mean ± SD. Data points represent triplicate for each individual participant sample. *P<0.05, **P<0.01, ***P<0.001, and ****P<0.0001 by one way ANOVA with Tukey's post hoc comparison test for parametric, and Kruskall-Wallis test with post hoc Dunn's comparison for non-parametric data. HC: healthy control, Dia: diabetes and; ND: non-diabetes.

5.3.4 The relationship between the rate of wound closure and the anti-inflammatory capacity of HDL from participants with toe amputations

We next investigated the relationship between the anti-inflammatory capacity of HDL and the rate of wound closure 1-month post-amputation in participants with and without diabetes. As shown in Figure 5.6, we observed no significant correlation between the rate of wound closure and mRNA levels of *CCL5* (r= -0.54; *P*= 0.07; Figure 5.6A) and no significant correlation for *CX3CL1* (r= -0.49, *P*= 0.10; Figure 5.6B), and *RELA* (r= -0.47; *P*= 0.12; Figure 5.6C) following incubation with patient HDL collected 1-month post-amputation. There were no other correlations of note between the rate of wound closure and other inflammatory markers.

We next assessed the relationship between the anti-inflammatory functionality of HDL in response to TNFα stimulation with the rate of wound closure 1-month post-amputation. As illustrated in Figure 5.7A, we observed a significant negative trend between *CCL2* mRNA levels and the rate of wound closure 1-month post-amputation (r = -0.64; *P*=0.028; Figure 5.7A). A significant negative correlation was also found between the mRNA levels of *ICAM-1* and the rate of wound closure 1-month post-amputation (r = -0.71; *P*=0.012; Figure 5.7B). Finally, there was no significant correlation between *CX_3CL1* mRNA levels with TNFα stimulation and the rate of wound closure (r = -0.49; *P*=0.11; Figure 5.7C). No other correlations of note were identified.

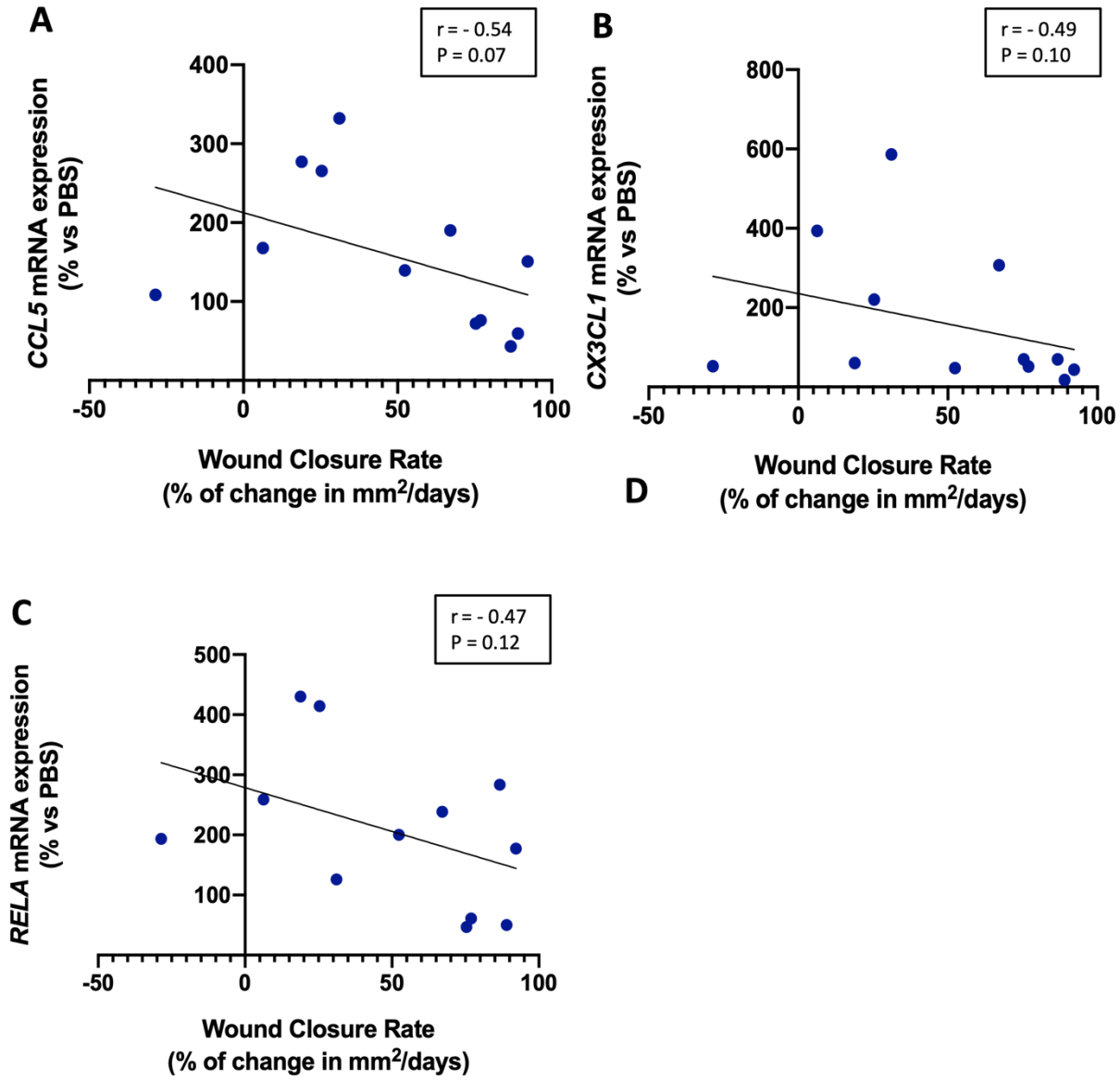

Figure 5.6 Non-significant negative association between the anti-inflammatory effects of patient HDL and the rate of wound closure. Scatter plot showing the correlation between the mRNA levels of **(A)** *CCL5*, **(B)** *CX3CL1*, and **(C)** *RELA* expressed by HCAECs treated with HDL obtained from diabetic and non-diabetic participants with the percentage of change in wound closure (mm^2/days) at 1-month post-amputation. Correlation analyses performed by Spearman's Correlation; r value is the correlation coefficient.

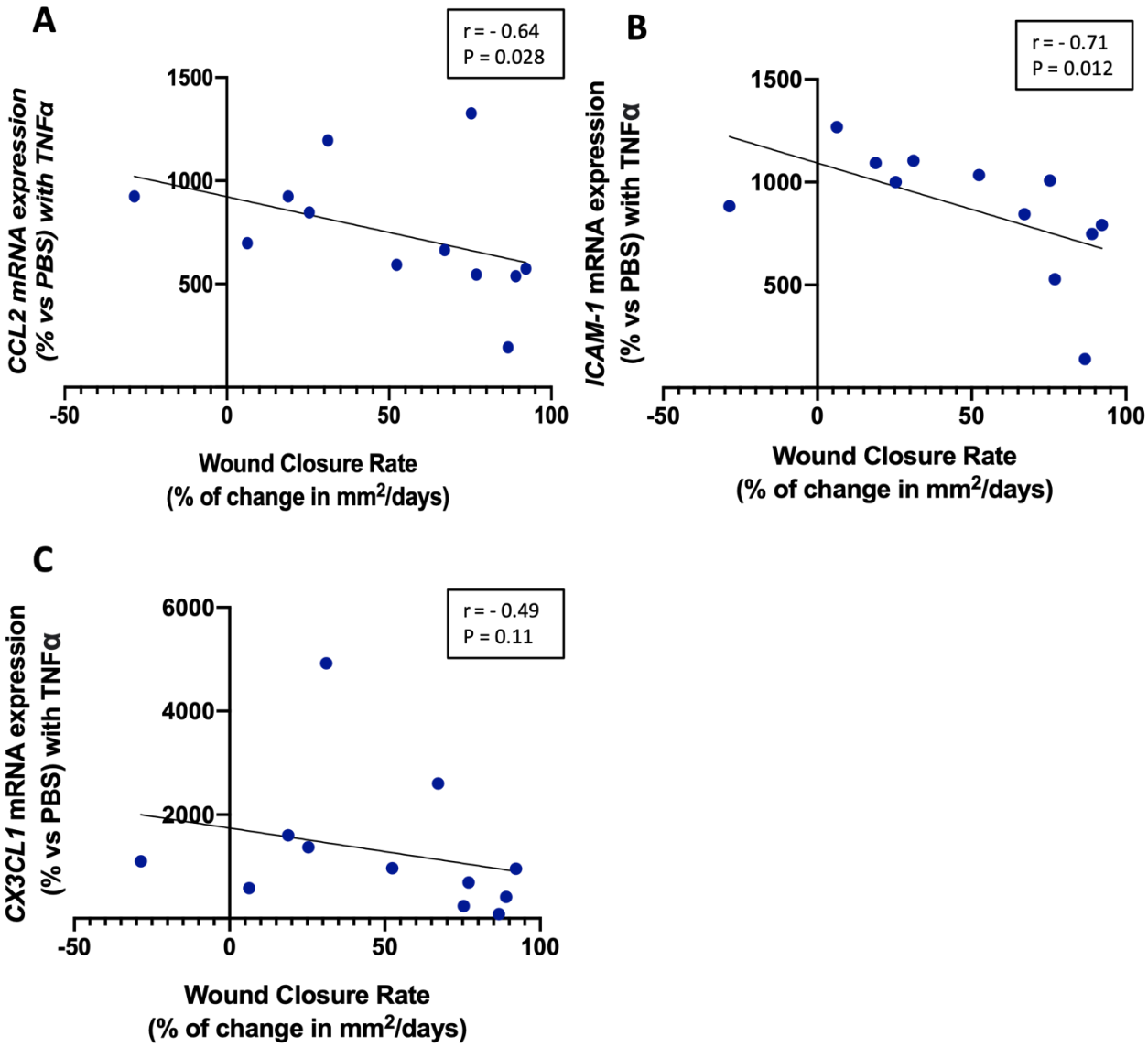

Figure 5.7 Negative correlation between *CCL2* and *ICAM-1* inflammatory mediators post TNFα stimulation and the rate of wound closure 1-month post-amputation. Scatter plot showing the correlation between the mRNA levels of **(A)** *CCL2*, **(B)** *ICAM-1*, and **(C)** *CX_3CL1* expressed by HCAECs pre-incubated with HDL from diabetic and non-diabetic participants and stimulated with TNFα, with the percentage change in wound closure (mm^2/days) at 1-month post-amputation. Correlation analyses performed by Spearman's Correlation. Data were considered statistically significant at $P<0.05$; r value is the correlation coefficient.

5.3.5 HDL from diabetes participants has reduced angiogenic capacity

HDL exhibits pro-angiogenic properties [201]. The pro-angiogenic effects of patient HDL were next tested. In this study, using custom software, we were able to investigate changes in three key parameters of endothelial cell vascular network formation when using the *in vitro* Matrigel tubulogenesis assay. These included: tubule number; branch point number (sprouting); and tubule length.

We first investigated changes in tubule number following incubation of endothelial cells in 5mM or 25mM glucose with HDL obtained from healthy controls and diabetic and non-diabetic amputation participants at different time points post-amputation. Interestingly, in endothelial cells exposed to 25 mM glucose, diabetic HDL induced a significantly higher number of tubules than the non-diabetic group at the time of amputation (113.1%; $P<0.01$; Figure 5.8A). When comparing the effect of diabetic HDL over time, we noted that HDL obtained from patients with diabetes at 6-months post-amputation induced a significantly lower number of tubules in normal glucose conditions compared to diabetic HDL at the time of amputation (37.0%; $P<0.01$; Figure 5.8 B). We observed a similar decline in tubule formation by diabetic HDL at both 1-month and 6-months at 25 mM glucose (37.8%; $P<0.001$ and 44.8%; $P<0.05$, respectively; Figure 5.8 B) compared to at the time of amputation. This suggests that the pro-angiogenic capacity of diabetic HDL becomes increasingly poorer with time post-amputation.

Non-diabetic HDL stimulated a significantly higher number of tubules at 1-month (46.1%; $P=0.054$; Figure 5.8C) and 6-months (103.6%; $P<0.001$; Figure 5.8D) post-amputation compared to diabetic HDL in 5 mM glucose. We also observed a significantly higher tubule number in cells treated with HDL from non-diabetic participants 1-month post-amputation (60.7%; $P<0.05$; Figure 5.8E), compared to diabetic HDL at 25mM glucose.

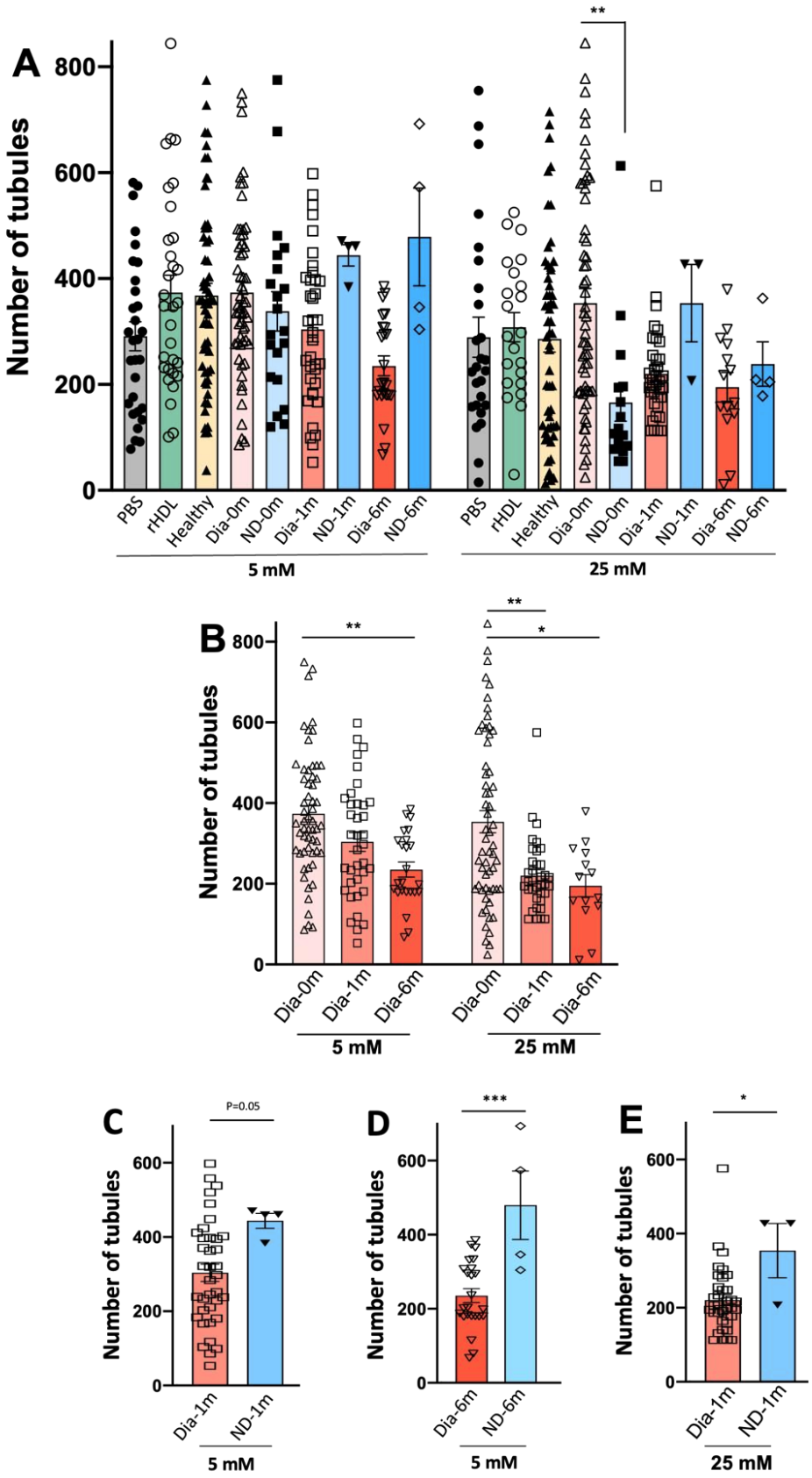

Figure 5.8 Diabetic HDL induces fewer tubules and its pro-angiogenic capacity declines over time post-amputation. HCAECs were treated with PBS, rHDL or participant HDL (20 μM) for 18 h and cultured under 5 mM or 25 mM glucose conditions for 48 h. Angiogenic

capacity was assessed using the Matrigel tubulogenesis assay, quantifying tubule numbers. Data are expressed as mean ± SD. *P<0.05, **P<0.01, and ***P<0.001 by one-way ANOVA (Tukey's post hoc comparison test for parametric and Kruskall-Wallis test with post hoc Dunn's comparison for non-parametric data). Dia: diabetes; ND: non-diabetes obtained at the time of recruitment (0), 1-month post-amputation (1m) and 6-months post-amputation (6m).

Branch point number provides critical information regarding the capacity of HDL to induce angiogenic sprouting. Similar with tubule number, branch point number was found to be higher following incubation with diabetic HDL collected at the time of amputation than non-diabetic HDL at 25 mM glucose (58.7%; $P<0.01$; Figure 5.9A). We also found that diabetic HDL elicited a decline in branch point number over time post-amputation. This reached significance in the 5 mM glucose treatment group when comparing diabetic HDL at the time of amputation to 6-months post-amputation (50.4%; $P<0.01$; Figure 5.9B). HDL from non-diabetic participants 6-months post-amputation induced a significantly higher number of branch points compared to the HDL from diabetic participants (127.7%; $P<0.001$; Figure 5.9C).

Tubule length was next determined. Once again, at 25mM glucose a significantly greater tubule length was noted following treatment with HDL from diabetic participants at baseline compared to cells treated with HDL from non-diabetic participants at the same time point (12.1%; $P<0.01$; Figure 5.10A). No changes were found in tubule length elicited by diabetic HDL over time post-amputation (Figure 5.10B). A trend for an increase in tubule length was, however, noted following treatment with non-diabetic HDL collected 1-month post-amputation compared to the diabetic HDL group at 5 mM glucose (10.8%; $P= 0.054$; Figure 5.10C).

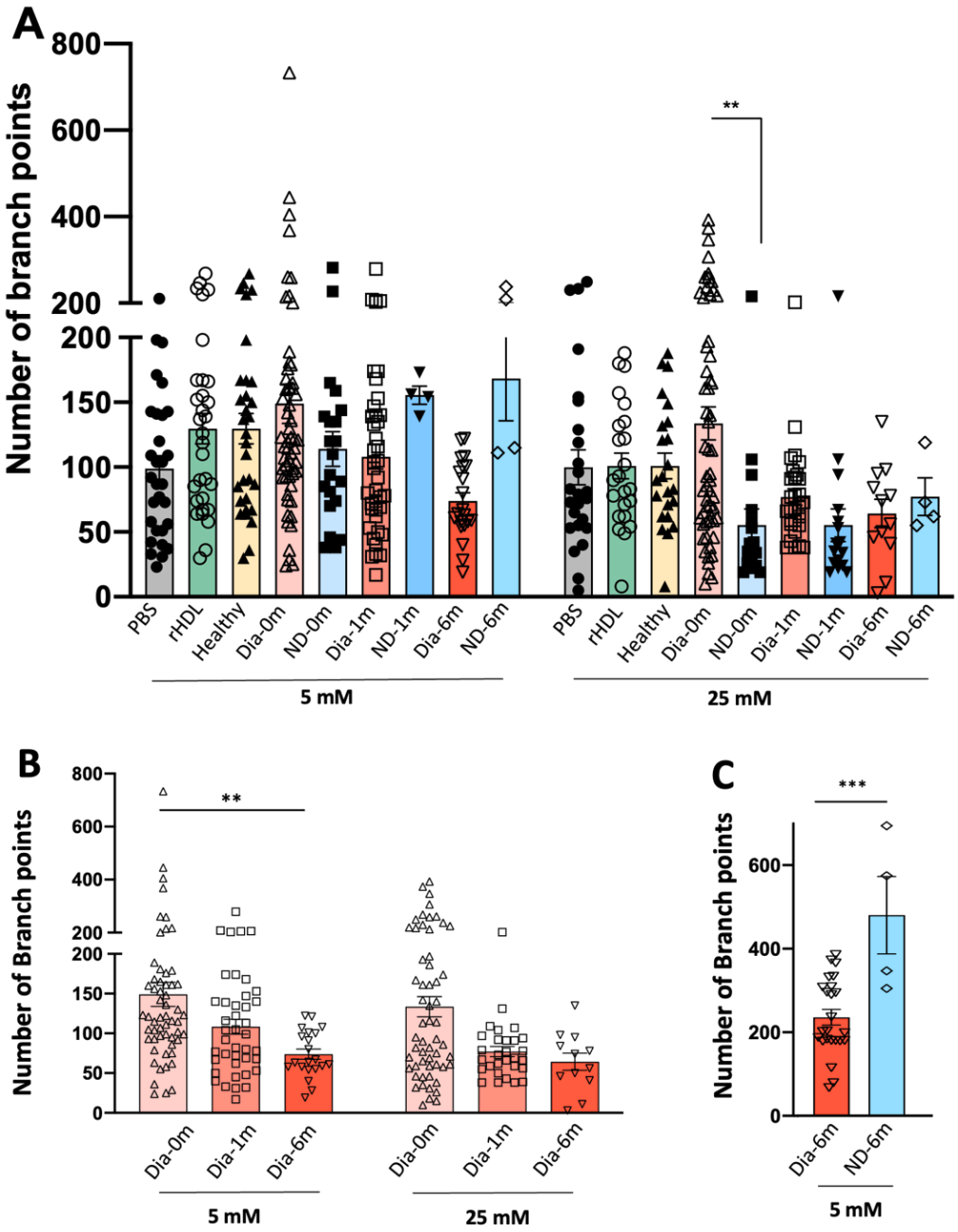

Figure 5.9 Diabetic HDL induces fewer branch points and its pro-angiogenic capacity declines over time post-amputation. HCAECs were treated with PBS, rHDL or participant HDL (20 μM) for 18 h and cultured under 5 mM or 25 mM glucose conditions for 48 h. Angiogenic capacity was assessed using the Matrigel tubulogenesis assay, quantifying tubule numbers. Data are expressed as mean ± SD. *P<0.05, **P<0.01, and ***P<0.001 by one-way ANOVA (Tukey's post hoc comparison test for parametric and Kruskall-Wallis test with post hoc Dunn's comparison for non-parametric data). Dia: diabetes; ND: non-diabetes obtained at the time of recruitment (0), 1-month post-amputation (1m) and 6-months post-amputation (6m).

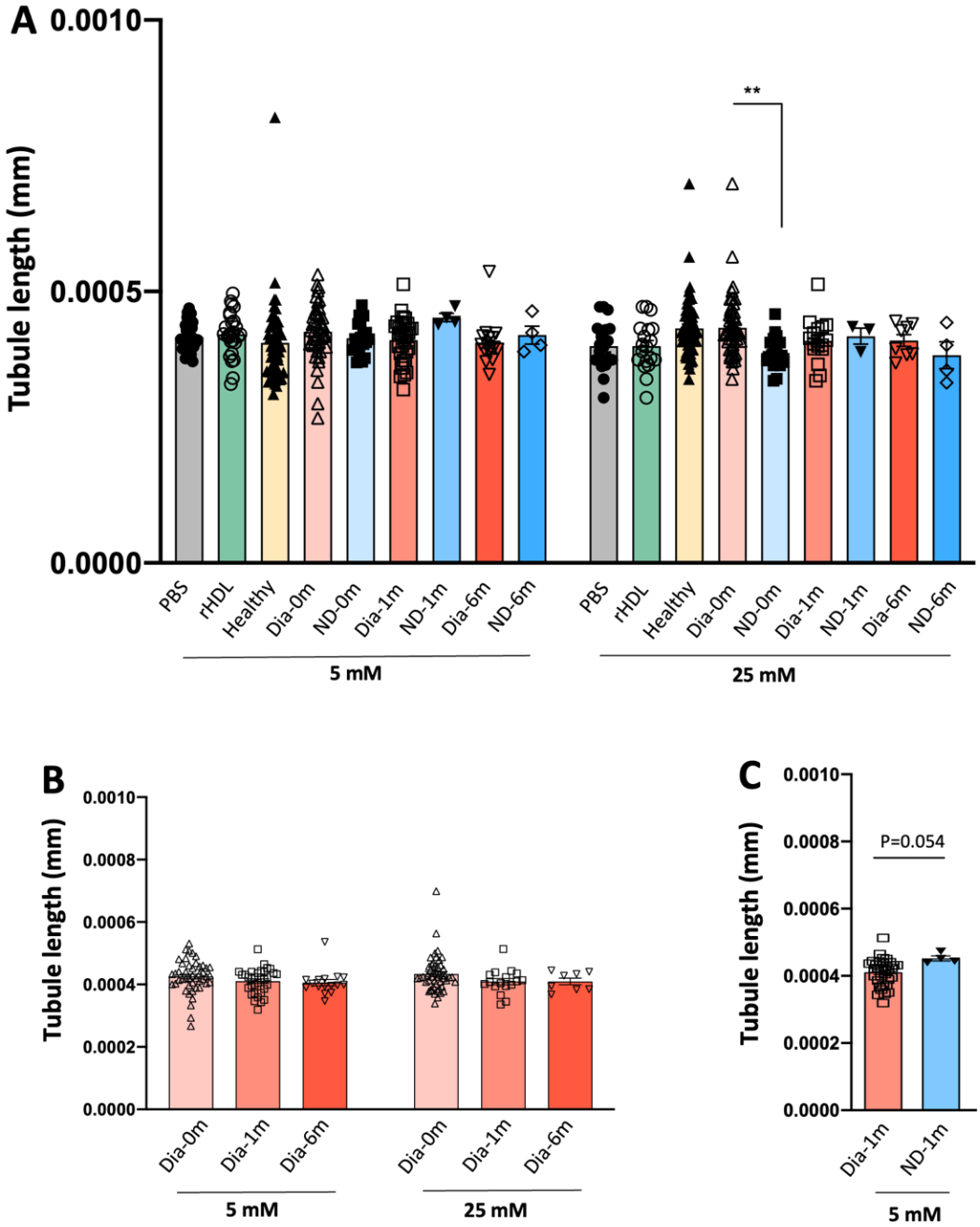

Figure 5.10 No change in tubule length with participant HDL. HCAECs were treated with PBS, rHDL or participant HDL (20 μM) for 18 h and cultured under 5 mM or 25 mM glucose conditions for 48 h. Angiogenic capacity was assessed using the Matrigel tubulogenesis assay, quantifying tubule length. Data are expressed as mean ± SD. *P<0.05, **P<0.01, and ***P<0.001 by one-way ANOVA (Tukey's post hoc comparison test for parametric and Kruskall-Wallis test with post hoc Dunn's comparison for non-parametric data). Dia: diabetes; ND: non-diabetes obtained at the time of recruitment (0), 1month post-amputation (1m) and 6-months post-amputation (6m).

5.3.6 No correlation between the pro-angiogenic capacity of HDL and the rate of wound closure

We next assessed the relationship between the pro-angiogenic capacity of HDL and the rate of wound closure in diabetic participants 1-month post-amputation. We found no correlations between the rate of wound closure and the three angiogenesis measures of tubule number, branch point number, and tubule length (Table 5.1). Unlike inflammation, it appears that the angiogenic capacity of HDL is not an indicator of the rate of wound healing in the diabetic participant group.

Matrigel outcomes	**5mM**		**25mM**	
	r	**P**	**r**	**P**
Tubule number	0.19	0.55	0.05	0.88
Branch point number	0.17	0.59	0.09	0.8
Tubule length	0.4	0.25	0.04	0.91

Table 5.1 No association between the pro-angiogenic properties of patient HDL and the rate of wound closure. The r and P values represent the correlation coefficient and significance for correlation between tubule number, branch point, and tubule length, and the rate of wound closure 1-month post amputation. Correlation analyses performed by Spearman's Correlation. Data were considered statistically significant at $P<0.05$.

5.4 Discussion

Building upon our clinical findings from the previous Chapters, in this chapter we aimed to investigate the anti-inflammatory and pro-angiogenic properties of patient HDL, two additional important HDL functions. This Chapter identified: (1) a significant inverse correlation between the expression of pro-inflammatory markers (*CCL2*, *ICAM-1* and *CX_3CL1*) with TNFα stimulation in endothelial cells treated with HDL from the diabetic and non-diabetic group and the rate of wound closure 1-month post-amputation; (2) HDL from non-diabetic participants more effectively reduced the expression of pro-inflammatory markers (*RELA*, *CCL5*, *CCL2* and *ICAM-1*) than HDL from diabetic participants; and (3) HDL in non-diabetic participants elicited greater pro-angiogenic effects than diabetic HDL collected at 1-month and 6-months post-amputation. Our findings have implications for the anti-inflammatory effects of HDL as a future biomarker that predicts wound healing success.

In both *in-vitro* and *in-vivo* settings, HDL has demonstrated anti-inflammatory effects. For example, *in vitro* studies have shown rHDL suppresses the inflammatory mediators *CCL2*, *CCL5*, *CX_3CL1* [145] and reduces the adhesion molecules *VCAM-1* and *ICAM-1* [116] in endothelial cells. We examined the anti-inflammatory function of participant HDL by measuring these inflammatory mediators and adhesion molecules as well as *RELA ex-vivo* with and without TNFα stimulation. Indications of an impairment in HDL functionality would be reflected in the reduced ability of HDL to suppress inflammatory marker expression. We consistently found that HDL from diabetic participants did not suppress inflammation as effectively as HDL from non-diabetic participants, with higher levels of *RELA*, *CCL5*, *CCL2* and *ICAM-1* elicited following diabetic HDL incubation. This also occurred - although to a lesser extent - when endothelial cells were stimulated with TNFα, possibly due to the greater challenge for HDL to suppress TNFα-exacerbated inflammation. Overall, our observations suggest a more pro-inflammatory HDL (or less anti-inflammatory) is present in diabetic participants. Indeed, HDL has been shown to be modified from a functional/anti-inflammatory

HDL to a dysfunctional/pro-inflammatory HDL when circulating in poor metabolic environments with a heightened inflammatory state such as chronic kidney disease, cardiovascular disease, and coronary atherosclerosis [203].

The pro-inflammatory nature of HDL in acute phase responses such as infection, surgery or chronic inflammation is believed to be due to the accumulation of pro-inflammatory proteins such as serum amyloid A, ApoC-II, and ApoC-III on the HDL particle [184]. These pro-inflammatory proteins can shift HDL from an anti-inflammatory to a pro-inflammatory particle. Consistent with this, it has been shown that HDL from patients with atrial fibrillation had an impaired ability to suppress gene expression of the pro-inflammatory adhesion molecules, *ICAM-1* and *VCAM-1* than participants without arterial fibrillation [204].

Blood samples were collected from participants in this study at three timepoints post-amputation. This enabled us to investigate changes in the anti-inflammatory capacity of HDL over time. To our knowledge no other study has longitudinally tracked the functionality of HDL, and certainly not in diabetics with toe amputations. We noted that for diabetic HDL, the anti-inflammatory effects improved with time post-amputation, indicating that HDL functionality was continually being restored. The explanation is likely to be due to a gradual abatement of the heightened systemic inflammation experienced by the diabetic participants at the time of amputation, confirmed by the approximately 30-fold increase in C-reactive protein levels, an important biomarker for measuring inflammation. Indeed, as mentioned above, the content of HDL is altered in an inflammatory environment [205, 206] that includes an increased content of serum amyloid A and a reduced content of apoA-I and paroxenase-1 that exhibit anti-inflammatory effects. This results in HDL particles with pro-inflammatory properties. However, upon resolution of inflammation over time post-amputation, we hypothesised that recycled HDL starts to regain its anti-inflammatory properties, as observed in our studies.

RELA is the gene that transcribes the p65 subunit of the inflammatory transcription factor NF-κB and plays a critical role in inducing inflammation in endothelial cells [207]. Upon phosphorylation of the NF-κB complex, the p65/p50 subunits are translocated to the nucleus and bind to the NF-κB response elements in the promoter region of inflammatory genes. The suppression of *CCL5*, *CCL2,* and *ICAM-1* was significantly lower in cells treated with HDL from non-diabetic than diabetic participants. A similar pattern also occurred with *RELA*. Interestingly, a significant amount of transcription control of *CCL2*, *CCL5* and *ICAM-1* is governed by NF-κB [145]. This suggests that the mechanism for the impaired anti-inflammatory effects of diabetic HDL is mediated via changes in *RELA*.

Our study identified a significant negative correlation between the expression of inflammatory markers *CCL2*, and *ICAM-1* expressed by cells pre-incubated with HDL and stimulated by TNFα, and the rate of wound closure 1-month post-amputation. This significant correlation indicates that people with a slower rate of wound closure (i.e. poorer wound healing) have HDL with impaired anti-inflammatory properties, particularly for the suppression of *CCL2* and *ICAM-1*. This finding has significant implications for clinical translation including: (1) the use of the *ex vivo* anti-inflammatory effects of HDL as a predictive biomarker for wound healing outcomes; and (2) that wound closure outcomes may be enhanced by suppressing the expression of *CCL2* and *ICAM-1* via functional HDL.

The proangiogenic effects of HDL were also tested. HDL has been shown to promote angiogenesis by increasing endothelial proliferation, migration, and tubule formation [159] and rescue diabetes-impaired angiogenesis [155]. Consistent with our findings on the anti-inflammatory properties of participant HDL, the pro-angiogenic capacity of HDL was significantly lower (tubule numbers and branch point number) in cells treated with diabetic HDL compared to non-diabetic HDL obtained both at 1- and 6-months post-amputation. Similar findings were noted when HCAECs were also incubated with high glucose. Together,

these findings indicate an impaired pro-angiogenic capacity of HDL from diabetic compared to non-diabetic participants. This finding is consistent with a previous study by our group that showed an impaired ability of HDL from Australian Indigenous patients with diabetes with severe vascular complications to induce *in vitro* angiogenesis [201]. Furthermore, HDL from type 2 diabetes mellitus patients had an impaired capacity to stimulate endothelial cell migration, proliferation, and ECM adhesion. The mechanism was reported to be via diabetes-induced down-regulation of SR-BI, resulting in an impaired ability to maintain Akt activity [208] which is essential for the pro-angiogenic properties of HDL.

We did not observe a correlation between the pro-angiogenic effects of patient HDL and the rate of wound closure. This was unexpected; however, the low sample size is likely to have been a significant limiting factor. Furthermore, this correlation is calculated from HDL obtained 1-month post-amputation a time at which the pro-angiogenic capacity of HDL may not be as relevant to successful wound healing. Interestingly we also found that the pro-angiogenic capacity of HDL (i.e. number of tubules and the branch points) in diabetic participants declined over time. One likely explanation for this is the possible effect of medications at the time of surgery such as statins, diabetic medication, and heart medication. For example, a similar study to this one has shown the effect of extended-release Niacin (medication for treatment of dyslipidaemia) on both HDL plasma levels and the endothelial-protective functionality of HDL in patients with diabetes causing a boost in pro-angiogenic capacity of HDL [209]. Another explanation for the decline in pro-angiogenic capacity of HDL over time and in patients with diabetes is that HDL is not required to promote angiogenesis at the wound area 6 months post-amputation as the wound healing task is already completed.

In conclusion, our study found that HDL from diabetic participants with toe amputations was impaired in its anti-inflammatory and pro-angiogenic functionality. We also identified a significant negative correlation between the levels of *CCL2* and *ICAM-1* elicited by diabetic

HDL and the rate of wound closure. We did not show a correlation between the pro-angiogenic capacity of HDL and the rate of wound closure, possibly due to low participant numbers. The correlation between the pro-inflammatory capacity of HDL and the rate of wound closure encourages future research to investigate the use of HDL functionality as a biomarker for predicting and improving wound healing outcomes.

CHAPTER 6 – GENERAL DISCUSSION

6.1 Introduction

Diabetes is the one of the most common metabolic disorders, causing world-wide mortality and morbidity and is associated with a range of complications such as DFU [1]. It is estimated that 25% of patients with diabetes develop DFU in their lifetime and, of these, one-quarter do not heal, placing them at risk of lower limb amputation [1]. There are currently no commonly used therapies that actively promote wound healing and exhibit pleiotropic effects. Treatment options are limited to controlling infection, achieving optimal glycaemic control, and invasive revascularisation procedures [92]. Numerous clinical trials have tested a wide variety of interventions, most commonly growth factors, however, none of these have proven to be universally accepted for diabetic wound healing. The failure of these interventions may be attributed to the ability of these agents to only target a single mechanistic pathway of wound healing. Diabetic wound healing suffers from impairments across a range of biological functions including prolonged inflammation and poor angiogenesis; an effective treatment therefore requires pleiotropic actions. HDL are endogenous lipid particles, also known as "good cholesterol", which have anti-inflammatory and pro-angiogenic functions in clinical and animal settings, suggesting it may be a novel therapy that targets multiple important pathways of wound healing [210].

HDL's fame began in the 1980s when the Framingham study identified a strong positive association between coronary heart disease and low HDL-cholesterol levels [211]. Interestingly, a significant positive correlation was later discovered between the pivotal biological function of HDL (known as reverse cholesterol transport), and cardiovascular events [212], redirecting attention from the *quantity* of HDL-cholesterol to its *quality*. HDL functionality has been shown to be impaired in a range of diseases such as in acute and chronic coronary syndromes, chronic kidney diseases, and diabetes [135, 213, 214].

Previous studies have demonstrated the pro-angiogenic capacity of topically applied rHDL on diabetic wounds [155]. Despite significant research on the anti-inflammatory role of HDL *in-vitro* and *in-vivo*, the anti-inflammatory effects of topically applied rHDL on either non-diabetic or diabetic wounds had not been explored. Validating the anti-inflammatory role of topically applied rHDL will facilitate development of rHDL as an agent with pleiotropic actions. In addition, identifying the functionality of circulating HDL in patients with diabetes and DFU and using it as a predictive factor could help determine the correct dose of topical rHDL delivery for wound healing. As such, the aims of this thesis were to: 1) determine the anti-inflammatory properties of topically applied rHDL in a murine model of wound healing and to track its fate; and 2) determine the relationship between HDL functionality and wound closure in diabetic and non-diabetic study participants with an acute toe amputation(s).

6.2 The anti-inflammatory properties of HDL

In Chapter 3, a murine model of diabetic wound healing was used to determine the effect of topically applied rHDL on inflammation during the early- to mid-stages of wound healing. This model closely mimics human healing through the placement of silicon splints around the wound to prevent the contraction mechanism that occurs in rodents. Changes in the mRNA levels of the important wound inflammatory mediators *Rela*, *Ccl2*, *Tgf β-1* and *Il-6*, and protein levels of CCL2, TGFβ-1, and IL-6 were determined. This is the first study to report that topical application of rHDL significantly reduced mRNA expression of *Rela* and *Ccl2* in diabetic mice 72 h post-wounding. A similar observation was noted in Chapter 5, in which the mRNA expression of *RELA* and *CCL2* in HCAECs were significantly reduced by HDL from non-diabetic study participants. Interestingly, these same reductions were not elicited by HDL from diabetic participants, suggesting an impairment in the anti-inflammatory functionality of diabetic HDL.

These findings provide further evidence to support the inhibitory effects of HDL on *RELA* as well as the chemokine *CCL2* that it induces. *CCL2* facilitates the recruitment of macrophages to sites of inflammation [215]. In a diabetic wound environment, high levels of *CCL2* for a prolonged period can result in excessive macrophage recruitment, non-resolving inflammation, and a failure of healing. Indeed, our murine study in Chapter 3 also showed significantly higher numbers of macrophages in diabetic mice than non-diabetic mice, confirming the exacerbated inflammatory environment in diabetic wounds. However, this macrophage increase didn't link well with *Ccl2* changes post-wounding. One explanation for this is the different time points used to measure the changes in *Ccl2* and macrophages, i.e. 72 hr and 7 days post-wounding respectively. Furthermore, there are other range of other chemokines such as CCL21 and CXCL12 which are responsible for recruiting macrophages to the wound site [216]. As shown in our clinical study (Chapter 4), we also observed that levels of C-reactive protein (measurement of inflammation) were significantly higher in diabetic than non-diabetic participants at the time of surgery; elevated levels of neutrophils and white blood cells were also present in diabetic participants. This signifies the importance of anti-inflammatory HDL in diabetic settings to reduce the expression levels of pro-inflammatory markers such as RELA and CCL2 which cause heightened inflammation.

Whilst topical rHDL reduced *RELA* and *CCL2* in diabetic wounds, the expression of other cytokines such as *Tgf β-1* and *Il-6* remained unchanged. One possible explanation for this could be that the transcriptional regulation of *Tgf β-1* and *Il-6* is different to *CCL2* and not affected by HDL. In Chapter 5, the HDL from non-diabetic participants also significantly reduced *CCL5* and *ICAM-1*, suggesting future murine studies exploring changes in wound inflammation should also investigate *CCL5* and *ICAM-1*. Additionally, future studies exploring the change in *TGFβ-1* and *IL-6* in cells treated with HDL from study participants is highly recommended.

Chapter 3 found that topical rHDL did not change the transition of M1 macrophages to M2 macrophages, as previously shown *in vitro* by Sanson *et al* [150]. This may have been due to several factors. Firstly, our study was done in an animal setting with contributions from multiple complex biological factors, whereas the shift of macrophage phenotype by rHDL in the Sanson *et al* study was done in an *in-vitro* setting. Secondly, we characterised the macrophage population at Day 7 post-wounding. This time point was determined in our own pilot studies aimed at deciphering the best time point post-wounding for capturing both M1 and M2 macrophage populations. It is possible that the 7-day time point was slightly too early or late to capture the macrophage transition effect of HDL reported previously. Future studies at different time points post-wounding will help determine the effect of HDL on macrophage polarisation in diabetic wounds.

In Chapter 3, we labelled rHDL with a fluorescent dye (DiO) so that the fate of topically applied rHDL to wounds could be tracked over time. Using live fluorescent imaging we observed that rHDL is retained in the wound for a prolonged period following application, predominantly for the first hour but it could be visualised by fluorescence microscopy in wound tissue sections after 5.5 h and was even retained at low levels out to 48 h, as detected by IVIS. This suggests that rHDL is retained by the wound cells for a prolonged period rather than immediately being cleared by the circulation. This increases the opportunity for rHDL to elicit biological effects at the wound site.

6.3 The pro-angiogenic capacity of HDL

rHDL has previously been shown to rescue diabetes-impaired angiogenesis [155]. We therefore sought to determine the pro-angiogenic capacity of HDL from the participants in our clinical study. Although not reaching statistical significance, we observed that under normal glucose conditions the cells treated with HDL from diabetic participants (at the time of surgery) formed both a higher number of tubules and branch points compared to cells treated with HDL

from non-diabetic participants. Interestingly, this pro-angiogenic capacity of HDL from diabetic participants was lost over time compared to HDL from non-diabetic participants. One explanation for this observation could be the type and the dose of the statin medications taken by the study participants at the time of amputation. As illustrated in Table 4.2, almost 70% of the diabetic participants were taking statins compared with 33% of the non-diabetic participants at the time of recruitment. It is well established that statins increase HDL-cholesterol levels and increase the production of apoA-I [217], which may also be extended to an increase in functionality. Consistent with this, statins have been reported to improve the key functions of HDL, such as increasing reverse cholesterol transport [218], enhancing the anti-inflammatory [219], anti-oxidative, and pro-angiogenic capacity of HDL [220].

HDL activates the S1P1 receptor on endothelial cells, which leads to activation of endothelial nitric oxide synthase, resulting in increased endothelial cell proliferation, mobilisation, and tubulogenesis, which are all characteristics of increased angiogenesis [221]. Statins such as pitavastatin and atorvastatin have been shown to increase both mRNA and protein levels of S1P1receptors and enhance endothelial nitric oxide production through endothelial nitric oxide synthase [220]. Merging these two facts, we propose that the enhanced pro-angiogenic functionality of HDL from diabetic compared to non-diabetic participants (at the time of surgery) was likely due to the action of statin medications which were being taken predominantly by the diabetic participants at the time of surgery. Interestingly, we also observed that the pro-angiogenic capacity of HDL in non-diabetic participants was higher compared to diabetic participants at 1-month and 6-months post-amputation, suggesting that this enhanced pro-angiogenic ability is lost over time. One explanation for this observation could be the inability of HDL to maintain enhanced functionality in the absence of statins over long periods. It is important to note that all diabetic participants were taking at least one anti-diabetic medication, which could have also influenced the pro-angiogenic functionality of HDL.

6.4 Impaired functionality of HDL in Diabetes

One of the main findings from our study was the impaired functionality of HDL in diabetic compared to non-diabetic participants. In Chapter 4, we demonstrated that the cholesterol efflux capacity of HDL - one key metric for HDL functionality - was higher in the non-diabetic group compared to diabetic group at 1-month and 6-months post-amputation. In Chapter 5, we also demonstrated that the anti-inflammatory effects of HDL were higher in non-diabetic HDL than diabetic HDL. Furthermore, we found that HDL from non-diabetic participants was more pro-angiogenic than HDL from diabetic participants.

Previous studies have found that HDL loses its functionality from alterations to its structure and function in environments with heightened inflammation, such as chronic kidney diseases, acute coronary syndrome, and coronary atherosclerosis [203]. In a study with a similar design to ours but targeting patients with atrial fibrillation (a disease involving atrial inflammation), the HDL from patients without atrial fibrillation elicited significantly lower levels of *ICAM-1* and *VCAM-1* compared to HDL from patients with atrial fibrillation [204].

Diabetes has a profound effect on HDL size (small HDL particles; HDL_3) [222], composition (diminished cholesterol ester content) [223], and function, rendering it a more dysfunctional form of HDL (Figure 6.1). Furthermore, it is suggested that three types of changes may transform HDL from a functional particle to a dysfunctional one: firstly, a reduction in the proteome and lipidome components of HDL which contribute to HDL's athero-protective functionality; secondly, increased amounts of pro-inflammatory and pro-oxidant agents within the HDL particle; and thirdly, chemical alterations of HDL composition that diminish its function [203].

Furthermore, alterations in HDL function and structure have been associated with glycation and oxidation of HDL-associated proteins and activity of HDL-metabolising enzymes [130]. In

diabetic environments, the non-enzymatic glycation of apoA-I occurs as a result of spontaneous interaction with reactive α-oxoaldehydes, impairing the cholesterol efflux capacity of HDL [222]. It has also been shown that hyperglycaemia and glycation disturb the cholesterol efflux of HDL by inhibiting both the interaction between apoA-I and ABCA1 [224] as well as the SR-BI-mediated selective uptake of HDL-cholesterol [224].

Moreover, it has been demonstrated that the presence of advanced glycation end products induces changes in the conformation and surface charge of HDL apolipoproteins such as apoA-I. This results in the loss of its anti-inflammatory properties [225] and decreases the activity of HDL-bound enzymes, such as lecithin-cholesterol acyltransferase and paraoxonase-1 that have anti-oxidant and anti-inflammatory properties [130]. Furthermore, diabetes is associated with the presence of chronic inflammation. This has been reported to transform HDL from a functional anti-inflammatory particle to a dysfunctional pro-inflammatory one [226]. Another theory for HDL dysfunction in diabetes is believed to be due to post-translational modifications induced by myeloperoxidase-driven oxidative stress which occurs through carbonylation or site-specific oxidation [227]. Combined, there are a host of changes that occur to HDL in diabetes that can account for the impairment in its functionality, as observed in our clinical study and illustrated in Figure 6.1.

6.5 The association between HDL functionality and the rate of wound closure

One of the main aims of this study was to investigate the correlation between the functionality of HDL and the rate of wound closure. To our knowledge, no other study has investigated this correlation directly. Only one clinical study in Japan [163] investigated the relationship between endogenous HDL-cholesterol levels and different wound healing outcomes. In that study, Ikura and colleagues recruited 163 patients with an existing DFU and assessed different clinical outcomes, such as minor amputation (below ankle amputation), major amputation (above ankle), and wound-related death. This study showed a significant

inverse relationship between circulating HDL-cholesterol levels and the three dependant variables: (1) minor amputation; (2) major amputation; and (3) wound-related death. As explained in Chapter 4, 14 patients were excluded from our study due to post-surgical complications such as negative vacuum therapy and further amputation (for example, above knee amputation and wound sutured post-amputation). These complications and participant exclusions resulted in a reduced sample size thus lowering the statistical power for our analyses. Despite this reduction, we were nevertheless able to show a statistically significant positive correlation between circulating HDL-cholesterol levels and the rate of wound closure. We also identified a significant inverse correlation between the anti-inflammatory properties of HDL, a functionality marker, and the rate of wound closure 1-month post-amputation.

In Chapter 4, we found that the higher the HDL-cholesterol levels of diabetic participants with toe amputation(s) at 1-month post-amputation, the faster the rate of their wound closure 1-month post-amputation, indicating better wound outcomes in patients with higher levels of HDL-cholesterol levels. This observation is consistent with the Framingham study, which showed a significant correlation between serum HDL levels and the risk of myocardial infarction [127]. The other significant correlation discovered by our study and presented in Chapter 5 was the mRNA expression levels of *CCL2* and *ICAM-1* in HCAECs following treatment with HDL from diabetic participants 1-month post-amputation and stimulated with TNFα with the rate of wound closure.

This is the first study to show this significant, positive correlation, confirming the potential of using not only HDL-cholesterol levels as a predictive biomarker for wound healing but also the functionality of HDL, such as its anti-inflammatory function for predicting wound healing, especially in people with DFU. Despite this positive correlation, we did not see any significant correlation between the rate of wound closure and other functionality parameters of HDL, including its pro-angiogenic capacity and the suppression of other pro-inflammatory markers.

We ascribe this to low sample size. Therefore, increasing the number of participants will increase the power of the study for observing such correlations. Furthermore, the pro-angiogenic functionality of HDL at 1-month post-amputation may not be the time point that correlates with wound healing as angiogenesis is critical for the proliferation phase of wound healing which occurs within the first 48-72 h post-wounding. Therefore, exploring other earlier time points could provide more information.

One advantage of our clinical study was retrieving the blood samples and clinical information periodically and being able to track the functionality of HDL over time. Interestingly, we observed alterations in HDL functionality over time as the HDL from diabetic participants at the time of surgery exhibited greater pro-inflammatory and pro-angiogenic functions. In acute phase responses, for example a systemic response to infection, surgery, myocardial infarction or chronic inflammation, HDL is enriched in pro-inflammatory proteins, such as serum amyloid A, myeloperoxidase, Apo-C-III and ceruloplasmin (Figure 6.1), which render the particle pro-inflammatory and pro-atherogenic by limiting its ability to promote CEC. We were able to confirm this in Chapter 4, as the HDL from diabetic participants also showed significantly lower ability to efflux cholesterol compared to the HDL from non-diabetic participants at 1-month and 6-months post-amputation.

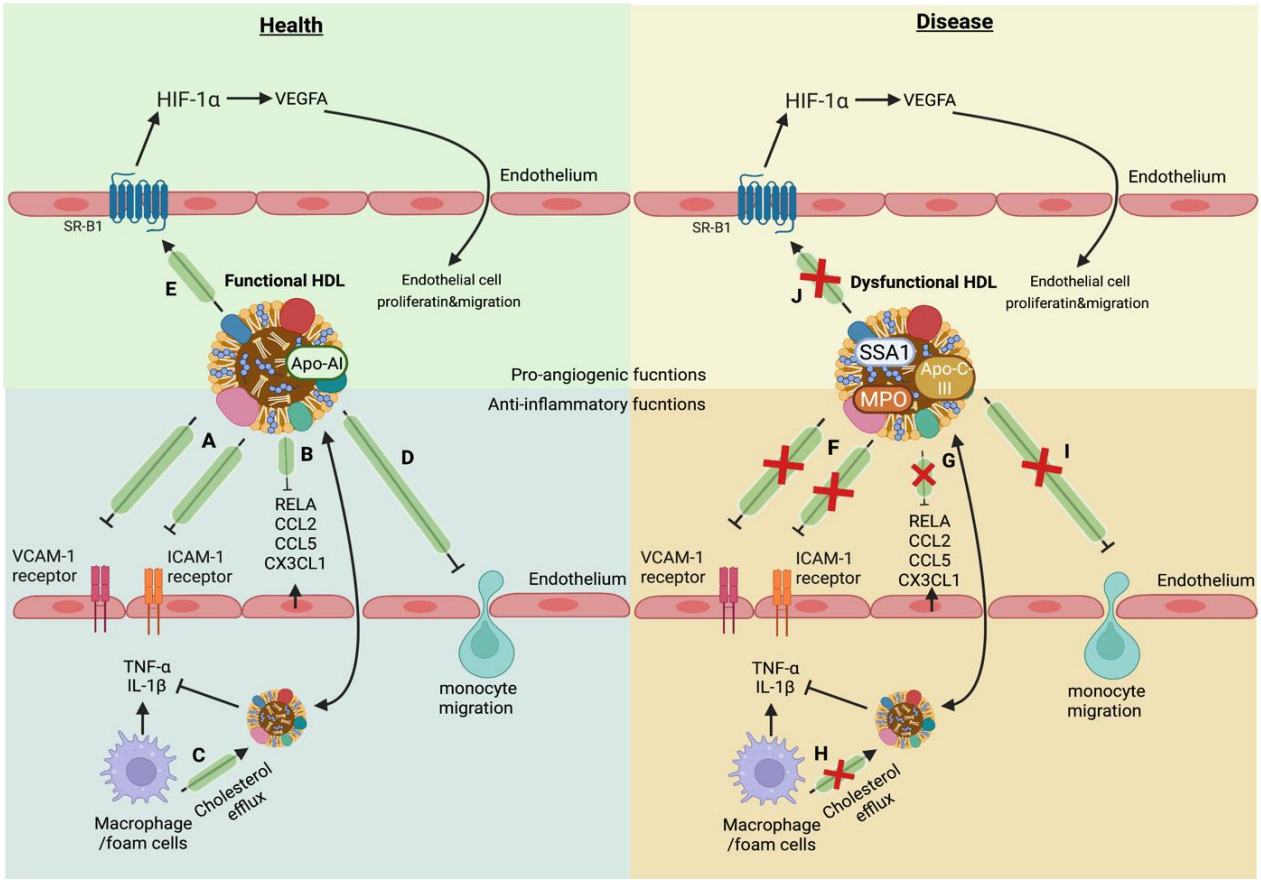

Figure 6.1 Schematic representation of HDLs anti-inflammatory and pro-angiogenic capacity in healthy and disease conditions. In healthy conditions **(left panel)**: **(A)** HDL inhibits the expression of ICAM-1 and VCAM-1 on endothelial cells, preventing the adhesion and influx of monocytes; **(B)** HDL inhibits the expression of pro-inflammatory markers; **(C)** HDL promotes cholesterol efflux from macrophages; **(D)** HDL inhibits monocyte migration; and **(E)** HDL promotes angiogenesis through expressing HIF-1α and VEGF-A. Structural modifications and functional consequences of transformation of functional HDL into dysfunctional HDL. In diseased conditions (right panel): **(F)** HDL's inability to inhibit the expression of ICAM-1 and VCAM-1 on endothelial cells, preventing the adhesion and influx of monocytes; **(G)** HDL's inability to inhibit the expression of pro-inflammatory markers; **(H)** HDL's inability to promote cholesterol efflux from macrophages; **(H)** HDL's inability to inhibit monocyte migration; and **(I)** HDL's inability to promote angiogenesis through expressing HIF-1α and VEGF-A. SAA: serum amyloid A; MPO: myeloperoxidase. Created by Biorender.

6.6 Study Significance

Measurement of HDL functionality (cholesterol efflux, anti-inflammatory, and pro-angiogenic capacity) has the potential for both defining patients at increased risk of non-healing wounds post-amputation and monitoring the effectiveness of therapies capable of modifying these properties. Determining indices of HDL functionality may also identify patients with normal or low HDL levels who are at high risk of developing non-healing DFU. Measuring the functionality of HDL as a biomarker for health outcomes rather than the levels of HDL-cholesterol could be used to explain positive health outcomes in individuals with low levels of HDL-cholesterol.

As we illustrated in Chapter 3, rHDL rescued diabetes-impaired wound healing by exhibiting anti-inflammatory effects. We had previously illustrated the pro-angiogenic capacity for rHDL and can therefore translate our laboratory-based findings to the clinical setting and explore the use of topical rHDL as a promising agent with pleiotropic effects for wound healing, especially for patients with diabetes with dysfunctional systemic HDL.

6.7 Future directions

Promising findings from the correlation between the pro-inflammatory function of HDL (suppression of *ICAM-1* and *CCL2*) and the rate of wound closure strongly suggests that an increased sample size would improve the power for our correlation analyses, thus further validating our findings and confirming the significant differences seen between the diabetic and non-diabetic groups. Further exploration of the anti-inflammatory and pro-angiogenic capacity of HDL in patients without diabetes requiring toe amputations is also worth pursuing as this could provide more predictive information. In particular, the pro-angiogenic function of HDL could be further explored via measuring the mRNA expression of mediators in angiogenesis, such as *HIF-1α* and *VEGF-A*, in cells treated with HDL from different groups under normal and high glucose conditions. A previous study by our group [201] showed the mimicking of

mRNA expression of *HIF-1α* and *VEGF-A* with Matrigel outcomes (i.e. the number of tubules and branch points in cells treated with HDL), indicating the significance of both factors for illustrating the pro-angiogenic capacity of HDL.

Furthermore, conducting an additional functional assay, known as a monocyte migration assay, could be used to determine changes in the secretion of inflammatory mediators from the serum of patients with diabetes that facilitate monocyte migration. This would add to our knowledge regarding the functionality of HDL in patient serum. HDL has an inhibitory effect on a host of inflammatory mediators secreted by endothelial cells and is therefore likely to reduce monocyte recruitment, which has been demonstrated previously [228]. Notably, our study was a pilot study to determine the functionality of serum HDL in patients with diabetes and provide further evidence for HDL as a treatment for wound healing in diabetes. Testing topical rHDL on human DFU and measuring the rate of wound closure, its anti-inflammatory effect, and its pro-angiogenic effect, is the next goal for clinical translation of the work presented in this thesis.

6.8 Conclusion

In summary, the studies conducted in this thesis have shown: 1) the anti-inflammatory role of rHDL in rescuing diabetes-impaired wound healing; 2) impaired HDL functionality in diabetic participants; and 3) a correlation between HDL-cholesterol levels and the anti-inflammatory function of HDL with the rate of wound healing in participants with amputations. The animal study presented in this thesis confirmed that topical application of rHDL rescued diabetes-impaired wound healing by significantly increasing the rate of wound closure and exhibiting anti-inflammatory functions. We were also able to demonstrate higher macrophage populations in diabetic murine wounds compared to non-diabetic murine wounds. However, we did not observe changes in wound M1 (pro-inflammatory) to M2 (anti-inflammatory) phenotype transitions with topical rHDL treatment.

This thesis presents the first clinical study to show a significant positive correlation between the anti-inflammatory function of HDL (i.e. suppressing *CCL2* and *ICAM-1* expression in TNFα-stimulated cells) with the rate of wound closure, 1-month post-amputation. Despite seeing promising trends for other pro-inflammatory and pro-angiogenic markers, we did not see additional significant correlations with the rate of wound closure in participants with toe amputations. Increasing the sample size its likely to improve this. Finally, topical rHDL application may represent a promising and interesting therapeutic target for diabetic wound healing, especially when is the function of systemic HDL is impaired.

REFERENCES

1. Armstrong DG, Boulton AJM, Bus SA. Diabetic Foot Ulcers and Their Recurrence. N Engl J Med. 2017;376(24):2367-75. doi: 10.1056/NEJMra1615439. PubMed PMID: 28614678.
2. Wallace HA, Basehore BM, Zito PM. Wound Healing Phases. StatPearls. Treasure Island (FL)2022.
3. Rodrigues M, Kosaric N, Bonham CA, Gurtner GC. Wound Healing: A Cellular Perspective. Physiol Rev. 2019;99(1):665-706. Epub 2018/11/27. doi: 10.1152/physrev.00067.2017. PubMed PMID: 30475656; PubMed Central PMCID: PMCPMC6442927.
4. Broughton G, 2nd, Janis JE, Attinger CE. The basic science of wound healing. Plast Reconstr Surg. 2006;117(7 Suppl):12S-34S. Epub 2006/06/27. doi: 10.1097/01.prs.0000225430.42531.c2. PubMed PMID: 16799372.
5. Hosgood G. Stages of wound healing and their clinical relevance. Vet Clin North Am Small Anim Pract. 2006;36(4):667-85. Epub 2006/06/22. doi: 10.1016/j.cvsm.2006.02.006. PubMed PMID: 16787782.
6. Golebiewska EM, Poole AW. Platelet secretion: From haemostasis to wound healing and beyond. Blood Rev. 2015;29(3):153-62. Epub 2014/12/04. doi: 10.1016/j.blre.2014.10.003. PubMed PMID: 25468720; PubMed Central PMCID: PMCPMC4452143.
7. Hosgood G. Wound healing. The role of platelet-derived growth factor and transforming growth factor beta. Vet Surg. 1993;22(6):490-5. Epub 1993/11/01. doi: 10.1111/j.1532-950x.1993.tb00426.x. PubMed PMID: 8116205.
8. Pittman K, Kubes P. Damage-associated molecular patterns control neutrophil recruitment. J Innate Immun. 2013;5(4):315-23. Epub 2013/03/15. doi: 10.1159/000347132. PubMed PMID: 23486162; PubMed Central PMCID: PMCPMC6741494.
9. Kolaczkowska E, Kubes P. Neutrophil recruitment and function in health and inflammation. Nat Rev Immunol. 2013;13(3):159-75. Epub 2013/02/26. doi: 10.1038/nri3399. PubMed PMID: 23435331.
10. Krzyszczyk P, Schloss R, Palmer A, Berthiaume F. The Role of Macrophages in Acute and Chronic Wound Healing and Interventions to Promote Pro-wound Healing Phenotypes. Front Physiol. 2018;9:419. Epub 2018/05/17. doi: 10.3389/fphys.2018.00419. PubMed PMID: 29765329; PubMed Central PMCID: PMCPMC5938667.
11. Gonzalez AC, Costa TF, Andrade ZA, Medrado AR. Wound healing - A literature review. An Bras Dermatol. 2016;91(5):614-20. Epub 2016/11/10. doi: 10.1590/abd1806-4841.20164741. PubMed PMID: 27828635; PubMed Central PMCID: PMCPMC5087220.
12. Boniakowski AE, Kimball AS, Jacobs BN, Kunkel SL, Gallagher KA. Macrophage-Mediated Inflammation in Normal and Diabetic Wound Healing. J Immunol. 2017;199(1):17-24. Epub 2017/06/21. doi: 10.4049/jimmunol.1700223. PubMed PMID: 28630109.
13. Murray PJ, Wynn TA. Protective and pathogenic functions of macrophage subsets. Nat Rev Immunol. 2011;11(11):723-37. Epub 2011/10/15. doi: 10.1038/nri3073. PubMed PMID: 21997792; PubMed Central PMCID: PMCPMC3422549.
14. Paladini RD, Takahashi K, Bravo NS, Coulombe PA. Onset of re-epithelialization after skin injury correlates with a reorganization of keratin filaments in wound edge keratinocytes: defining a potential role for keratin 16. J Cell Biol. 1996;132(3):381-97. Epub 1996/02/01. doi: 10.1083/jcb.132.3.381. PubMed PMID: 8636216; PubMed Central PMCID: PMCPMC2120730.
15. Gabbiani G, Chaponnier C, Huttner I. Cytoplasmic filaments and gap junctions in epithelial cells and myofibroblasts during wound healing. J Cell Biol. 1978;76(3):561-8. Epub

1978/03/01. doi: 10.1083/jcb.76.3.561. PubMed PMID: 564911; PubMed Central PMCID: PMCPMC2110008.
16. Goliger JA, Paul DL. Wounding alters epidermal connexin expression and gap junction-mediated intercellular communication. Mol Biol Cell. 1995;6(11):1491-501. Epub 1995/11/01. doi: 10.1091/mbc.6.11.1491. PubMed PMID: 8589451; PubMed Central PMCID: PMCPMC301306.
17. Shirakata Y, Kimura R, Nanba D, Iwamoto R, Tokumaru S, Morimoto C, et al. Heparin-binding EGF-like growth factor accelerates keratinocyte migration and skin wound healing. J Cell Sci. 2005;118(Pt 11):2363-70. Epub 2005/06/01. doi: 10.1242/jcs.02346. PubMed PMID: 15923649.
18. Detmar M, Brown LF, Berse B, Jackman RW, Elicker BM, Dvorak HF, et al. Hypoxia regulates the expression of vascular permeability factor/vascular endothelial growth factor (VPF/VEGF) and its receptors in human skin. J Invest Dermatol. 1997;108(3):263-8. Epub 1997/03/01. doi: 10.1111/1523-1747.ep12286453. PubMed PMID: 9036922.
19. Eilken HM, Adams RH. Dynamics of endothelial cell behavior in sprouting angiogenesis. Curr Opin Cell Biol. 2010;22(5):617-25. Epub 2010/09/08. doi: 10.1016/j.ceb.2010.08.010. PubMed PMID: 20817428.
20. Grant MB, May WS, Caballero S, Brown GA, Guthrie SM, Mames RN, et al. Adult hematopoietic stem cells provide functional hemangioblast activity during retinal neovascularization. Nat Med. 2002;8(6):607-12. Epub 2002/06/04. doi: 10.1038/nm0602-607. PubMed PMID: 12042812.
21. Eyden B. The myofibroblast: a study of normal, reactive and neoplastic tissues, with an emphasis on ultrastructure. J Submicrosc Cytol Pathol. 2007:7-166. Epub 2008/02/19. PubMed PMID: 18277533.
22. Sousa AM, Liu T, Guevara O, Stevens J, Fanburg BL, Gaestel M, et al. Smooth muscle alpha-actin expression and myofibroblast differentiation by TGFbeta are dependent upon MK2. J Cell Biochem. 2007;100(6):1581-92. Epub 2006/12/14. doi: 10.1002/jcb.21154. PubMed PMID: 17163490; PubMed Central PMCID: PMCPMC2586991.
23. Volk SW, Wang Y, Mauldin EA, Liechty KW, Adams SL. Diminished type III collagen promotes myofibroblast differentiation and increases scar deposition in cutaneous wound healing. Cells Tissues Organs. 2011;194(1):25-37. Epub 2011/01/22. doi: 10.1159/000322399. PubMed PMID: 21252470; PubMed Central PMCID: PMCPMC3128157.
24. Kolluru GK, Bir SC, Kevil CG. Endothelial dysfunction and diabetes: effects on angiogenesis, vascular remodeling, and wound healing. Int J Vasc Med. 2012;2012:918267. Epub 2012/05/23. doi: 10.1155/2012/918267. PubMed PMID: 22611498; PubMed Central PMCID: PMCPMC3348526.
25. Dimmeler S, Zeiher AM. Endothelial cell apoptosis in angiogenesis and vessel regression. Circ Res. 2000;87(6):434-9. Epub 2000/09/16. doi: 10.1161/01.res.87.6.434. PubMed PMID: 10988233.
26. Chemokine Regulation of Neutrophil Infiltration of Skin Wounds. Advances in Wound Care. 2015;4(11):631-40. doi: 10.1089/wound.2014.0559.
27. Jorch SK, Kubes P. An emerging role for neutrophil extracellular traps in noninfectious disease. Nat Med. 2017;23(3):279-87. Epub 2017/03/08. doi: 10.1038/nm.4294. PubMed PMID: 28267716.
28. He L, Marneros AG. Macrophages are essential for the early wound healing response and the formation of a fibrovascular scar. Am J Pathol. 2013;182(6):2407-17. Epub 2013/04/23. doi: 10.1016/j.ajpath.2013.02.032. PubMed PMID: 23602833; PubMed Central PMCID: PMCPMC3668032.

29. DiPietro LA, Polverini PJ, Rahbe SM, Kovacs EJ. Modulation of JE/MCP-1 expression in dermal wound repair. Am J Pathol. 1995;146(4):868-75. Epub 1995/04/01. PubMed PMID: 7717454; PubMed Central PMCID: PMCPMC1869244.
30. Willenborg S, Lucas T, van Loo G, Knipper JA, Krieg T, Haase I, et al. CCR2 recruits an inflammatory macrophage subpopulation critical for angiogenesis in tissue repair. Blood. 2012;120(3):613-25. Epub 2012/05/12. doi: 10.1182/blood-2012-01-403386. PubMed PMID: 22577176.
31. Ploeger DT, Hosper NA, Schipper M, Koerts JA, de Rond S, Bank RA. Cell plasticity in wound healing: paracrine factors of M1/ M2 polarized macrophages influence the phenotypical state of dermal fibroblasts. Cell Commun Signal. 2013;11(1):29. Epub 2013/04/23. doi: 10.1186/1478-811x-11-29. PubMed PMID: 23601247; PubMed Central PMCID: PMCPMC3698164.
32. Suga H, Rennert RC, Rodrigues M, Sorkin M, Glotzbach JP, Januszyk M, et al. Tracking the elusive fibrocyte: identification and characterization of collagen-producing hematopoietic lineage cells during murine wound healing. Stem Cells. 2014;32(5):1347-60. Epub 2014/01/22. doi: 10.1002/stem.1648. PubMed PMID: 24446236; PubMed Central PMCID: PMCPMC4096488.
33. Werner S, Krieg T, Smola H. Keratinocyte-fibroblast interactions in wound healing. J Invest Dermatol. 2007;127(5):998-1008. Epub 2007/04/17. doi: 10.1038/sj.jid.5700786. PubMed PMID: 17435785.
34. Piipponen M, Li D, Landen NX. The Immune Functions of Keratinocytes in Skin Wound Healing. Int J Mol Sci. 2020;21(22). Epub 2020/11/26. doi: 10.3390/ijms21228790. PubMed PMID: 33233704; PubMed Central PMCID: PMCPMC7699912.
35. Clayton K, Vallejo AF, Davies J, Sirvent S, Polak ME. Langerhans Cells-Programmed by the Epidermis. Front Immunol. 2017;8:1676. Epub 2017/12/15. doi: 10.3389/fimmu.2017.01676. PubMed PMID: 29238347; PubMed Central PMCID: PMCPMC5712534.
36. Stunova A, Vistejnova L. Dermal fibroblasts-A heterogeneous population with regulatory function in wound healing. Cytokine Growth Factor Rev. 2018;39:137-50. Epub 2018/02/06. doi: 10.1016/j.cytogfr.2018.01.003. PubMed PMID: 29395658.
37. Janson DG, Saintigny G, van Adrichem A, Mahe C, El Ghalbzouri A. Different gene expression patterns in human papillary and reticular fibroblasts. J Invest Dermatol. 2012;132(11):2565-72. Epub 2012/06/15. doi: 10.1038/jid.2012.192. PubMed PMID: 22696053.
38. Frykberg RG, Banks J. Challenges in the Treatment of Chronic Wounds. Adv Wound Care (New Rochelle). 2015;4(9):560-82. Epub 2015/09/05. doi: 10.1089/wound.2015.0635. PubMed PMID: 26339534; PubMed Central PMCID: PMCPMC4528992.
39. Blakytny R, Jude E. The molecular biology of chronic wounds and delayed healing in diabetes. Diabet Med. 2006;23(6):594-608. Epub 2006/06/09. doi: 10.1111/j.1464-5491.2006.01773.x. PubMed PMID: 16759300.
40. McCarty SM, Percival SL. Proteases and Delayed Wound Healing. Adv Wound Care (New Rochelle). 2013;2(8):438-47. Epub 2014/04/02. doi: 10.1089/wound.2012.0370. PubMed PMID: 24688830; PubMed Central PMCID: PMCPMC3842891.
41. Schreml S, Szeimies RM, Prantl L, Karrer S, Landthaler M, Babilas P. Oxygen in acute and chronic wound healing. Br J Dermatol. 2010;163(2):257-68. Epub 2010/04/17. doi: 10.1111/j.1365-2133.2010.09804.x. PubMed PMID: 20394633.
42. Stanley A, Osler T. Senescence and the healing rates of venous ulcers. J Vasc Surg. 2001;33(6):1206-11. Epub 2001/06/05. doi: 10.1067/mva.2001.115379. PubMed PMID: 11389419.

43. Telgenhoff D, Shroot B. Cellular senescence mechanisms in chronic wound healing. Cell Death Differ. 2005;12(7):695-8. Epub 2005/04/30. doi: 10.1038/sj.cdd.4401632. PubMed PMID: 15861190.
44. Ennis WJ, Sui A, Bartholomew A. Stem Cells and Healing: Impact on Inflammation. Adv Wound Care (New Rochelle). 2013;2(7):369-78. Epub 2014/03/04. doi: 10.1089/wound.2013.0449. PubMed PMID: 24587974; PubMed Central PMCID: PMCPMC3842880.
45. Chen WY, Rogers AA. Recent insights into the causes of chronic leg ulceration in venous diseases and implications on other types of chronic wounds. Wound Repair Regen. 2007;15(4):434-49. Epub 2007/07/26. doi: 10.1111/j.1524-475X.2007.00250.x. PubMed PMID: 17650086.
46. Eming SA, Martin P, Tomic-Canic M. Wound repair and regeneration: mechanisms, signaling, and translation. Sci Transl Med. 2014;6(265):265sr6. Epub 2014/12/05. doi: 10.1126/scitranslmed.3009337. PubMed PMID: 25473038; PubMed Central PMCID: PMCPMC4973620.
47. Guariguata L, Whiting DR, Hambleton I, Beagley J, Linnenkamp U, Shaw JE. Global estimates of diabetes prevalence for 2013 and projections for 2035. Diabetes Res Clin Pract. 2014;103(2):137-49. Epub 2014/03/19. doi: 10.1016/j.diabres.2013.11.002. PubMed PMID: 24630390.
48. Pena G, Cowled P, Dawson J, Johnson B, Fitridge R. Diabetic foot and lower limb amputations: underestimated problem with a cost to health system and to the patient. ANZ Journal of Surgery. 2018;88(7-8):666-7. doi: 10.1111/ans.14436.
49. American Diabetes A. Diagnosis and classification of diabetes mellitus. Diabetes Care. 2014;37 Suppl 1:S81-90. Epub 2013/12/21. doi: 10.2337/dc14-S081. PubMed PMID: 24357215.
50. Govers R. Chapter Six - Cellular Regulation of Glucose Uptake by Glucose Transporter GLUT4. In: Makowski GS, editor. Advances in Clinical Chemistry. 66: Elsevier; 2014. p. 173-240.
51. Kerner W, Bruckel J, German Diabetes A. Definition, classification and diagnosis of diabetes mellitus. Exp Clin Endocrinol Diabetes. 2014;122(7):384-6. Epub 2014/07/12. doi: 10.1055/s-0034-1366278. PubMed PMID: 25014088.
52. Rosolova H, Petrlova B, Simon J, Sifalda P, Sipova I, Sefrna F. [Macrovascular and microvascular complications in type 2 diabetes patients]. Vnitr Lek. 2008;54(3):229-37. Epub 2008/06/05. PubMed PMID: 18522290.
53. Soltero-Perez I. Toward a new definition of atherosclerosis including hypertension: a proposal. J Hum Hypertens. 2002;16 Suppl 1:S23-5. Epub 2002/05/03. doi: 10.1038/sj.jhh.1001336. PubMed PMID: 11986888.
54. American Diabetes A. Peripheral arterial disease in people with diabetes. Diabetes Care. 2003;26(12):3333-41. Epub 2003/11/25. doi: 10.2337/diacare.26.12.3333. PubMed PMID: 14633825.
55. Murabito JM, D'Agostino RB, Silbershatz H, Wilson WF. Intermittent claudication. A risk profile from The Framingham Heart Study. Circulation. 1997;96(1):44-9. Epub 1997/07/01. doi: 10.1161/01.cir.96.1.44. PubMed PMID: 9236415.
56. Ridker PM, Cushman M, Stampfer MJ, Tracy RP, Hennekens CH. Plasma concentration of C-reactive protein and risk of developing peripheral vascular disease. Circulation. 1998;97(5):425-8. Epub 1998/03/07. doi: 10.1161/01.cir.97.5.425. PubMed PMID: 9490235.
57. Armstrong DG, Boulton AJM, Bus SA. Diabetic Foot Ulcers and Their Recurrence. New England Journal of Medicine. 2017;376(24):2367-75. doi: 10.1056/NEJMra1615439. PubMed PMID: 28614678.

58. Okonkwo UA, DiPietro LA. Diabetes and Wound Angiogenesis. Int J Mol Sci. 2017;18(7). Epub 2017/07/04. doi: 10.3390/ijms18071419. PubMed PMID: 28671607; PubMed Central PMCID: PMCPMC5535911.
59. Noor S, Zubair M, Ahmad J. Diabetic foot ulcer--A review on pathophysiology, classification and microbial etiology. Diabetes Metab Syndr. 2015;9(3):192-9. Epub 2015/05/20. doi: 10.1016/j.dsx.2015.04.007. PubMed PMID: 25982677.
60. Leese GP, Morris AD. Prediction of diabetic foot ulcer occurrence using commonly available clinical information: response to Boyko et al. Diabetes Care. 2006;29(11):2562-3; author reply 3. Epub 2006/10/27. doi: 10.2337/dc06-1471. PubMed PMID: 17065710.
61. Clayton W, Elasy TA. A Review of the Pathophysiology, Classification, and Treatment of Foot Ulcers in Diabetic Patients. Clinical Diabetes. 2009;27(2):52-8. doi: 10.2337/diaclin.27.2.52.
62. Enoch S, Grey JE, Harding KG. ABC of wound healing. Non-surgical and drug treatments. BMJ. 2006;332(7546):900-3. Epub 2006/04/15. doi: 10.1136/bmj.332.7546.900. PubMed PMID: 16613966; PubMed Central PMCID: PMCPMC1440619.
63. Giurini JM, Lyons TE. Diabetic foot complications: diagnosis and management. Int J Low Extrem Wounds. 2005;4(3):171-82. Epub 2005/08/16. doi: 10.1177/1534734605280136. PubMed PMID: 16100098.
64. Armstrong DG, Cohen K, Courric S, Bharara M, Marston W. Diabetic foot ulcers and vascular insufficiency: our population has changed, but our methods have not. J Diabetes Sci Technol. 2011;5(6):1591-5. Epub 2012/01/10. doi: 10.1177/193229681100500636. PubMed PMID: 22226282; PubMed Central PMCID: PMCPMC3262731.
65. Boulton AJM, Armstrong DG, Kirsner RS, Attinger CE, Lavery LA, Lipsky BA, et al. Diagnosis and Management of Diabetic Foot Complications. Arlington (VA)2018.
66. Gary Sibbald R, Woo KY. The biology of chronic foot ulcers in persons with diabetes. Diabetes Metab Res Rev. 2008;24 Suppl 1:S25-30. Epub 2008/04/30. doi: 10.1002/dmrr.847. PubMed PMID: 18442179.
67. Martinez-Reyes I, Chandel NS. Mitochondrial TCA cycle metabolites control physiology and disease. Nat Commun. 2020;11(1):102. Epub 2020/01/05. doi: 10.1038/s41467-019-13668-3. PubMed PMID: 31900386; PubMed Central PMCID: PMCPMC6941980.
68. Du Y, Miller CM, Kern TS. Hyperglycemia increases mitochondrial superoxide in retina and retinal cells. Free Radic Biol Med. 2003;35(11):1491-9. Epub 2003/12/04. doi: 10.1016/j.freeradbiomed.2003.08.018. PubMed PMID: 14642397.
69. Yamagishi SI, Edelstein D, Du XL, Brownlee M. Hyperglycemia potentiates collagen-induced platelet activation through mitochondrial superoxide overproduction. Diabetes. 2001;50(6):1491-4. Epub 2001/05/26. doi: 10.2337/diabetes.50.6.1491. PubMed PMID: 11375352.
70. Huebschmann AG, Regensteiner JG, Vlassara H, Reusch JE. Diabetes and advanced glycoxidation end products. Diabetes Care. 2006;29(6):1420-32. Epub 2006/05/30. doi: 10.2337/dc05-2096. PubMed PMID: 16732039.
71. Brownlee M. Advanced protein glycosylation in diabetes and aging. Annu Rev Med. 1995;46:223-34. Epub 1995/01/01. doi: 10.1146/annurev.med.46.1.223. PubMed PMID: 7598459.
72. Lee AY, Chung SS. Contributions of polyol pathway to oxidative stress in diabetic cataract. FASEB J. 1999;13(1):23-30. Epub 1999/01/05. doi: 10.1096/fasebj.13.1.23. PubMed PMID: 9872926.
73. Marshall S, Bacote V, Traxinger RR. Discovery of a metabolic pathway mediating glucose-induced desensitization of the glucose transport system. Role of hexosamine

biosynthesis in the induction of insulin resistance. J Biol Chem. 1991;266(8):4706-12. Epub 1991/03/15. PubMed PMID: 2002019.
74. Mirza RE, Fang MM, Ennis WJ, Koh TJ. Blocking Interleukin-1β Induces a Healing-Associated Wound Macrophage Phenotype and Improves Healing in Type 2 Diabetes. Diabetes. 2013;62(7):2579-87. doi: 10.2337/db12-1450.
75. Wong SL, Demers M, Martinod K, Gallant M, Wang Y, Goldfine AB, et al. Diabetes primes neutrophils to undergo NETosis, which impairs wound healing. Nat Med. 2015;21(7):815-9. Epub 2015/06/16. doi: 10.1038/nm.3887. PubMed PMID: 26076037; PubMed Central PMCID: PMCPMC4631120.
76. Karima M, Kantarci A, Ohira T, Hasturk H, Jones VL, Nam BH, et al. Enhanced superoxide release and elevated protein kinase C activity in neutrophils from diabetic patients: association with periodontitis. J Leukoc Biol. 2005;78(4):862-70. Epub 2005/08/06. doi: 10.1189/jlb.1004583. PubMed PMID: 16081595; PubMed Central PMCID: PMCPMC1249507.
77. Delamaire M, Maugendre D, Moreno M, Le Goff M-C, Allannic H, Genetet B. Impaired Leucocyte Functions in Diabetic Patients. Diabetic Medicine. 1997;14(1):29-34. doi: 10.1002/(sici)1096-9136(199701)14:1<29::Aid-dia300>3.0.Co;2-v.
78. Yu CO, Leung KS, Fung KP, Lam FF, Ng ES, Lau KM, et al. The characterization of a full-thickness excision open foot wound model in n5-streptozotocin (STZ)-induced type 2 diabetic rats that mimics diabetic foot ulcer in terms of reduced blood circulation, higher C-reactive protein, elevated inflammation, and reduced cell proliferation. Exp Anim. 2017;66(3):259-69. Epub 2017/04/18. doi: 10.1538/expanim.17-0016. PubMed PMID: 28413186; PubMed Central PMCID: PMCPMC5543247.
79. Ferguson MW, Herrick SE, Spencer MJ, Shaw JE, Boulton AJ, Sloan P. The histology of diabetic foot ulcers. Diabet Med. 1996;13 Suppl 1:S30-3. Epub 1996/01/01. PubMed PMID: 8741826.
80. Das S, Singh G, Majid M, Sherman MB, Mukhopadhyay S, Wright CS, et al. Syndesome Therapeutics for Enhancing Diabetic Wound Healing. Adv Healthc Mater. 2016;5(17):2248-60. Epub 2016/07/08. doi: 10.1002/adhm.201600285. PubMed PMID: 27385307; PubMed Central PMCID: PMCPMC5228475.
81. Muller M, Trocme C, Lardy B, Morel F, Halimi S, Benhamou PY. Matrix metalloproteinases and diabetic foot ulcers: the ratio of MMP-1 to TIMP-1 is a predictor of wound healing. Diabet Med. 2008;25(4):419-26. Epub 2008/04/05. doi: 10.1111/j.1464-5491.2008.02414.x. PubMed PMID: 18387077; PubMed Central PMCID: PMCPMC2326726.
82. Lawrence T. The nuclear factor NF-kappaB pathway in inflammation. Cold Spring Harb Perspect Biol. 2009;1(6):a001651. Epub 2010/05/12. doi: 10.1101/cshperspect.a001651. PubMed PMID: 20457564; PubMed Central PMCID: PMCPMC2882124.
83. Dal-Secco D, Wang J, Zeng Z, Kolaczkowska E, Wong CH, Petri B, et al. A dynamic spectrum of monocytes arising from the in situ reprogramming of CCR2+ monocytes at a site of sterile injury. J Exp Med. 2015;212(4):447-56. Epub 2015/03/25. doi: 10.1084/jem.20141539. PubMed PMID: 25800956; PubMed Central PMCID: PMCPMC4387291.
84. Acosta JB, del Barco DG, Vera DC, Savigne W, Lopez-Saura P, Guillen Nieto G, et al. The pro-inflammatory environment in recalcitrant diabetic foot wounds. Int Wound J. 2008;5(4):530-9. Epub 2008/11/14. doi: 10.1111/j.1742-481X.2008.00457.x. PubMed PMID: 19006574; PubMed Central PMCID: PMCPMC7951400.
85. Mishima Y, Kuyama A, Tada A, Takahashi K, Ishioka T, Kibata M. Relationship between serum tumor necrosis factor-alpha and insulin resistance in obese men with Type 2

diabetes mellitus. Diabetes Res Clin Pract. 2001;52(2):119-23. Epub 2001/04/20. doi: 10.1016/s0168-8227(00)00247-3. PubMed PMID: 11311966.
86. Waltenberger J, Lange J, Kranz A. Vascular endothelial growth factor-A-induced chemotaxis of monocytes is attenuated in patients with diabetes mellitus: A potential predictor for the individual capacity to develop collaterals. Circulation. 2000;102(2):185-90. Epub 2000/07/13. doi: 10.1161/01.cir.102.2.185. PubMed PMID: 10889129.
87. Seitz O, Schurmann C, Hermes N, Muller E, Pfeilschifter J, Frank S, et al. Wound healing in mice with high-fat diet- or ob gene-induced diabetes-obesity syndromes: a comparative study. Exp Diabetes Res. 2010;2010:476969. Epub 2011/02/15. doi: 10.1155/2010/476969. PubMed PMID: 21318183; PubMed Central PMCID: PMCPMC3034929.
88. Qi W, Yang C, Dai Z, Che D, Feng J, Mao Y, et al. High levels of pigment epithelium-derived factor in diabetes impair wound healing through suppression of Wnt signaling. Diabetes. 2015;64(4):1407-19. Epub 2014/11/05. doi: 10.2337/db14-1111. PubMed PMID: 25368097.
89. Eming SA, Koch M, Krieger A, Brachvogel B, Kreft S, Bruckner-Tuderman L, et al. Differential proteomic analysis distinguishes tissue repair biomarker signatures in wound exudates obtained from normal healing and chronic wounds. J Proteome Res. 2010;9(9):4758-66. Epub 2010/07/30. doi: 10.1021/pr100456d. PubMed PMID: 20666496.
90. Eming SA, Lauer G, Cole M, Jurk S, Christ H, Hornig C, et al. Increased levels of the soluble variant of the vascular endothelial growth factor receptor VEGFR-1 are associated with a poor prognosis in wound healing. J Invest Dermatol. 2004;123(4):799-802. Epub 2004/09/18. doi: 10.1111/j.0022-202X.2004.23310.x. PubMed PMID: 15373788.
91. Tan JTM, Ng MKC, Bursill CA. The role of high-density lipoproteins in the regulation of angiogenesis. Cardiovascular Research. 2015;106(2):184-93. doi: 10.1093/cvr/cvv104.
92. Hinchliffe RJ, Forsythe RO, Apelqvist J, Boyko EJ, Fitridge R, Hong JP, et al. Guidelines on diagnosis, prognosis, and management of peripheral artery disease in patients with foot ulcers and diabetes (IWGDF 2019 update). Diabetes Metab Res Rev. 2020;36 Suppl 1:e3276. Epub 2020/01/21. doi: 10.1002/dmrr.3276. PubMed PMID: 31958217.
93. Vas P, Rayman G, Dhatariya K, Driver V, Hartemann A, Londahl M, et al. Effectiveness of interventions to enhance healing of chronic foot ulcers in diabetes: a systematic review. Diabetes Metab Res Rev. 2020;36 Suppl 1:e3284. Epub 2020/03/17. doi: 10.1002/dmrr.3284. PubMed PMID: 32176446.
94. Saap LJ, Falanga V. Debridement performance index and its correlation with complete closure of diabetic foot ulcers. Wound Repair Regen. 2002;10(6):354-9. Epub 2002/11/28. doi: 10.1046/j.1524-475x.2002.10603.x. PubMed PMID: 12453138.
95. Caputo WJ, Beggs DJ, DeFede JL, Simm L, Dharma H. A prospective randomised controlled clinical trial comparing hydrosurgery debridement with conventional surgical debridement in lower extremity ulcers. International Wound Journal. 2008;5(2):288-94. doi: 10.1111/j.1742-481X.2007.00490.x.
96. Jimenez JC, Agnew PS, Mayer P, Clements JR, Caporusso JM, Lange DL, et al. Enzymatic Debridement of Chronic Nonischemic Diabetic Foot Ulcers: Results of a Randomized, Controlled Trial. Wounds. 2017;29(5):133-9. Epub 2017/03/08. PubMed PMID: 28267678.
97. Wilasrusmee C, Marjareonrungrung M, Eamkong S, Attia J, Poprom N, Jirasisrithum S, et al. Maggot therapy for chronic ulcer: a retrospective cohort and a meta-analysis. Asian J Surg. 2014;37(3):138-47. Epub 2014/01/03. doi: 10.1016/j.asjsur.2013.09.005. PubMed PMID: 24382296.
98. Piaggesi A, Goretti C, Mazzurco S, Tascini C, Leonildi A, Rizzo L, et al. A randomized controlled trial to examine the efficacy and safety of a new super-oxidized solution for the

management of wide postsurgical lesions of the diabetic foot. Int J Low Extrem Wounds. 2010;9(1):10-5. Epub 2010/03/09. doi: 10.1177/1534734610361945. PubMed PMID: 20207618.
99. Imran M, Hussain MB, Baig M. A Randomized, Controlled Clinical Trial of Honey-Impregnated Dressing for Treating Diabetic Foot Ulcer. J Coll Physicians Surg Pak. 2015;25(10):721-5. Epub 2015/10/12. doi: 10.2015/JCPSP.721725. PubMed PMID: 26454386.
100. Donaghue VM, Chrzan JS, Rosenblum BI, Giurini JM, Habershaw GM, Veves A. Evaluation of a collagen-alginate wound dressing in the management of diabetic foot ulcers. Adv Wound Care. 1998;11(3):114-9. Epub 1998/09/08. PubMed PMID: 9729942.
101. Edmonds M, Lazaro-Martinez JL, Alfayate-Garcia JM, Martini J, Petit JM, Rayman G, et al. Sucrose octasulfate dressing versus control dressing in patients with neuroischaemic diabetic foot ulcers (Explorer): an international, multicentre, double-blind, randomised, controlled trial. Lancet Diabetes Endocrinol. 2018;6(3):186-96. Epub 2017/12/25. doi: 10.1016/S2213-8587(17)30438-2. PubMed PMID: 29275068.
102. Shaw J, Hughes CM, Lagan KM, Stevenson MR, Irwin CR, Bell PM. The effect of topical phenytoin on healing in diabetic foot ulcers: a randomized controlled trial. Diabet Med. 2011;28(10):1154-7. Epub 2011/04/13. doi: 10.1111/j.1464-5491.2011.03309.x. PubMed PMID: 21480976.
103. Jensen JL, Seeley J, Gillin B. Diabetic foot ulcerations. A controlled, randomized comparison of two moist wound healing protocols: Carrasyn Hydrogel Wound dressing and wet-to-moist saline gauze. Adv Wound Care. 1998;11(7 Suppl):1-4. Epub 1999/05/18. PubMed PMID: 10326334.
104. Krause FG, deVries G, Meakin C, Kalla TP, Younger AS. Outcome of Transmetatarsal Amputations in Diabetics Using Antibiotic Beads. Foot & Ankle International. 2009;30(6):486-93. doi: 10.3113/fai.2009.0486. PubMed PMID: 19486624.
105. Game F, Jeffcoate W, Tarnow L, Jacobsen JL, Whitham DJ, Harrison EF, et al. LeucoPatch system for the management of hard-to-heal diabetic foot ulcers in the UK, Denmark, and Sweden: an observer-masked, randomised controlled trial. Lancet Diabetes Endocrinol. 2018;6(11):870-8. Epub 2018/09/24. doi: 10.1016/S2213-8587(18)30240-7. PubMed PMID: 30243803.
106. Game F, Jeffcoate W, Tarnow L, Day F, Fitzsimmons D, Jacobsen J. The LeucoPatch(R) system in the management of hard-to-heal diabetic foot ulcers: study protocol for a randomised controlled trial. Trials. 2017;18(1):469. Epub 2017/10/12. doi: 10.1186/s13063-017-2216-9. PubMed PMID: 29017535; PubMed Central PMCID: PMCPMC5633898.
107. Armstrong DG, Lavery LA, Diabetic Foot Study C. Negative pressure wound therapy after partial diabetic foot amputation: a multicentre, randomised controlled trial. Lancet. 2005;366(9498):1704-10. Epub 2005/11/18. doi: 10.1016/S0140-6736(05)67695-7. PubMed PMID: 16291063.
108. Uchi H, Igarashi A, Urabe K, Koga T, Nakayama J, Kawamori R, et al. Clinical efficacy of basic fibroblast growth factor (bFGF) for diabetic ulcer. Eur J Dermatol. 2009;19(5):461-8. Epub 2009/07/30. doi: 10.1684/ejd.2009.0750. PubMed PMID: 19638336.
109. Park KH, Han SH, Hong JP, Han SK, Lee DH, Kim BS, et al. Topical epidermal growth factor spray for the treatment of chronic diabetic foot ulcers: A phase III multicenter, double-blind, randomized, placebo-controlled trial. Diabetes Res Clin Pract. 2018;142:335-44. Epub 2018/06/15. doi: 10.1016/j.diabres.2018.06.002. PubMed PMID: 29902542.
110. Ansell BJ, Watson KE, Fogelman AM, Navab M, Fonarow GC. High-density lipoprotein function recent advances. J Am Coll Cardiol. 2005;46(10):1792-8. Epub 2005/11/16. doi: 10.1016/j.jacc.2005.06.080. PubMed PMID: 16286161.

111. Tabet F, Rye KA. High-density lipoproteins, inflammation and oxidative stress. Clin Sci (Lond). 2009;116(2):87-98. Epub 2008/12/17. doi: 10.1042/CS20080106. PubMed PMID: 19076062.
112. Calabresi L, Gomaraschi M, Simonelli S, Bernini F, Franceschini G. HDL and atherosclerosis: Insights from inherited HDL disorders. Biochim Biophys Acta. 2015;1851(1):13-8. Epub 2014/07/30. doi: 10.1016/j.bbalip.2014.07.015. PubMed PMID: 25068410.
113. Blanche PJ, Gong EL, Forte TM, Nichols AV. Characterization of human high-density lipoproteins by gradient gel electrophoresis. Biochim Biophys Acta. 1981;665(3):408-19. Epub 1981/09/24. doi: 10.1016/0005-2760(81)90253-8. PubMed PMID: 7295744.
114. Eisenberg S. High density lipoprotein metabolism. J Lipid Res. 1984;25(10):1017-58. Epub 1984/10/01. PubMed PMID: 6392459.
115. Cheung MC, Albers JJ. Characterization of lipoprotein particles isolated by immunoaffinity chromatography. Particles containing A-I and A-II and particles containing A-I but no A-II. J Biol Chem. 1984;259(19):12201-9. Epub 1984/10/10. PubMed PMID: 6434538.
116. Murphy AJ, Woollard KJ. High-density lipoprotein: a potent inhibitor of inflammation. Clin Exp Pharmacol Physiol. 2010;37(7):710-8. Epub 2009/11/26. doi: 10.1111/j.1440-1681.2009.05338.x. PubMed PMID: 19930423.
117. Mackness MI, Durrington PN. HDL, its enzymes and its potential to influence lipid peroxidation. Atherosclerosis. 1995;115(2):243-53. Epub 1995/06/01. doi: 10.1016/0021-9150(94)05524-m. PubMed PMID: 7661883.
118. Prosser HC, Ng MK, Bursill CA. The role of cholesterol efflux in mechanisms of endothelial protection by HDL. Curr Opin Lipidol. 2012;23(3):182-9. Epub 2012/04/11. doi: 10.1097/MOL.0b013e328352c4dd. PubMed PMID: 22488423.
119. Wang K. Investigation of total HDL and HDL subclass kinetics using stable isotope techniques in healthy subjects 2015.
120. Dixon JL, Ginsberg HN. Hepatic synthesis of lipoproteins and apolipoproteins. Semin Liver Dis. 1992;12(4):364-72. Epub 1992/11/01. doi: 10.1055/s-2008-1040406. PubMed PMID: 1465621.
121. Hamilton RL, Williams MC, Fielding CJ, Havel RJ. Discoidal bilayer structure of nascent high density lipoproteins from perfused rat liver. J Clin Invest. 1976;58(3):667-80. Epub 1976/09/01. doi: 10.1172/JCI108513. PubMed PMID: 182724; PubMed Central PMCID: PMCPMC333225.
122. Zhou L, Li C, Gao L, Wang A. High-density lipoprotein synthesis and metabolism (Review). Mol Med Rep. 2015;12(3):4015-21. Epub 2015/06/18. doi: 10.3892/mmr.2015.3930. PubMed PMID: 26082200.
123. Barter PJ, Nicholls S, Rye KA, Anantharamaiah GM, Navab M, Fogelman AM. Antiinflammatory properties of HDL. Circ Res. 2004;95(8):764-72. Epub 2004/10/16. doi: 10.1161/01.RES.0000146094.59640.13. PubMed PMID: 15486323.
124. Schwartz CC, VandenBroek JM, Cooper PS. Lipoprotein cholesteryl ester production, transfer, and output in vivo in humans. J Lipid Res. 2004;45(9):1594-607. Epub 2004/05/18. doi: 10.1194/jlr.M300511-JLR200. PubMed PMID: 15145983.
125. Lusa S, Jauhiainen M, Metso J, Somerharju P, Ehnholm C. The mechanism of human plasma phospholipid transfer protein-induced enlargement of high-density lipoprotein particles: evidence for particle fusion. Biochem J. 1996;313 (Pt 1):275-82. Epub 1996/01/01. doi: 10.1042/bj3130275. PubMed PMID: 8546695; PubMed Central PMCID: PMCPMC1216894.
126. Arca M, Montali A, Valiante S, Campagna F, Pigna G, Paoletti V, et al. Usefulness of atherogenic dyslipidemia for predicting cardiovascular risk in patients with angiographically

defined coronary artery disease. Am J Cardiol. 2007;100(10):1511-6. Epub 2007/11/13. doi: 10.1016/j.amjcard.2007.06.049. PubMed PMID: 17996510.
127. Gordon T, Castelli WP, Hjortland MC, Kannel WB, Dawber TR. High density lipoprotein as a protective factor against coronary heart disease. The Framingham Study. Am J Med. 1977;62(5):707-14. Epub 1977/05/01. doi: 10.1016/0002-9343(77)90874-9. PubMed PMID: 193398.
128. Assmann G, Schulte H, von Eckardstein A, Huang Y. High-density lipoprotein cholesterol as a predictor of coronary heart disease risk. The PROCAM experience and pathophysiological implications for reverse cholesterol transport. Atherosclerosis. 1996;124:S11-S20. doi: https://doi.org/10.1016/0021-9150(96)05852-2.
129. Sharrett AR, Ballantyne CM, Coady SA, Heiss G, Sorlie PD, Catellier D, et al. Coronary heart disease prediction from lipoprotein cholesterol levels, triglycerides, lipoprotein(a), apolipoproteins A-I and B, and HDL density subfractions: The Atherosclerosis Risk in Communities (ARIC) Study. Circulation. 2001;104(10):1108-13. Epub 2001/09/06. doi: 10.1161/hc3501.095214. PubMed PMID: 11535564.
130. Femlak M, Gluba-Brzozka A, Cialkowska-Rysz A, Rysz J. The role and function of HDL in patients with diabetes mellitus and the related cardiovascular risk. Lipids Health Dis. 2017;16(1):207. Epub 2017/11/01. doi: 10.1186/s12944-017-0594-3. PubMed PMID: 29084567; PubMed Central PMCID: PMCPMC5663054.
131. Chen Y, Zhi Y, Li C, Liu Y, Zhang L, Wang Y, et al. HDL cholesterol and risk of diabetic nephropathy in patient with type 1 diabetes: A meta-analysis of cohort studies. Diabetes Res Clin Pract. 2016;122:84-91. Epub 2016/11/07. doi: 10.1016/j.diabres.2016.10.013. PubMed PMID: 27816683.
132. Andrews J, Janssan A, Nguyen T, Pisaniello AD, Scherer DJ, Kastelein JJ, et al. Effect of serial infusions of reconstituted high-density lipoprotein (CER-001) on coronary atherosclerosis: rationale and design of the CARAT study. Cardiovasc Diagn Ther. 2017;7(1):45-51. Epub 2017/02/07. doi: 10.21037/cdt.2017.01.01. PubMed PMID: 28164012; PubMed Central PMCID: PMCPMC5253449.
133. Tardif J-C, Grégoire J, L'Allier PL, Ibrahim R, Lespérance J, Heinonen TM, et al. Effects of Reconstituted High-Density Lipoprotein Infusions on Coronary AtherosclerosisA Randomized Controlled Trial. JAMA. 2007;297(15):1675-82. doi: 10.1001/jama.297.15.jpc70004.
134. Riwanto M, Rohrer L, Roschitzki B, Besler C, Mocharla P, Mueller M, et al. Altered activation of endothelial anti- and proapoptotic pathways by high-density lipoprotein from patients with coronary artery disease: role of high-density lipoprotein-proteome remodeling. Circulation. 2013;127(8):891-904. Epub 2013/01/26. doi: 10.1161/CIRCULATIONAHA.112.108753. PubMed PMID: 23349247.
135. Besler C, Heinrich K, Rohrer L, Doerries C, Riwanto M, Shih DM, et al. Mechanisms underlying adverse effects of HDL on eNOS-activating pathways in patients with coronary artery disease. J Clin Invest. 2011;121(7):2693-708. Epub 20110623. doi: 10.1172/JCI42946. PubMed PMID: 21701070; PubMed Central PMCID: PMCPMC3223817.
136. Khera AV, Cuchel M, de la Llera-Moya M, Rodrigues A, Burke MF, Jafri K, et al. Cholesterol efflux capacity, high-density lipoprotein function, and atherosclerosis. N Engl J Med. 2011;364(2):127-35. doi: 10.1056/NEJMoa1001689. PubMed PMID: 21226578; PubMed Central PMCID: PMCPMC3030449.
137. Srivastava RAK. Dysfunctional HDL in diabetes mellitus and its role in the pathogenesis of cardiovascular disease. Mol Cell Biochem. 2018;440(1-2):167-87. Epub 20170821. doi: 10.1007/s11010-017-3165-z. PubMed PMID: 28828539.

138. Srivastava RAK. Dysfunctional HDL in diabetes mellitus and its role in the pathogenesis of cardiovascular disease. Molecular and Cellular Biochemistry. 2018;440(1):167-87. doi: 10.1007/s11010-017-3165-z.
139. Kashyap SR, Osme A, Ilchenko S, Golizeh M, Lee K, Wang S, et al. Glycation Reduces the Stability of ApoAI and Increases HDL Dysfunction in Diet-Controlled Type 2 Diabetes. J Clin Endocrinol Metab. 2018;103(2):388-96. Epub 2017/10/28. doi: 10.1210/jc.2017-01551. PubMed PMID: 29077935; PubMed Central PMCID: PMCPMC5800833.
140. Nobecourt E, Tabet F, Lambert G, Puranik R, Bao S, Yan L, et al. Nonenzymatic glycation impairs the antiinflammatory properties of apolipoprotein A-I. Arterioscler Thromb Vasc Biol. 2010;30(4):766-72. Epub 20100128. doi: 10.1161/ATVBAHA.109.201715. PubMed PMID: 20110571; PubMed Central PMCID: PMCPMC3038672.
141. Shao B, Oda MN, Oram JF, Heinecke JW. Myeloperoxidase: an oxidative pathway for generating dysfunctional high-density lipoprotein. Chem Res Toxicol. 2010;23(3):447-54. Epub 2010/01/02. doi: 10.1021/tx9003775. PubMed PMID: 20043647; PubMed Central PMCID: PMCPMC2838938.
142. Zheng L, Nukuna B, Brennan M-L, Sun M, Goormastic M, Settle M, et al. Apolipoprotein A-I is a selective target for myeloperoxidase-catalyzed oxidation and functional impairment in subjects with cardiovascular disease. The Journal of Clinical Investigation. 2004;114(4):529-41. doi: 10.1172/JCI21109.
143. Traldi P, Castilho G, Sartori CH, Machado-Lima A, Nakandakare ER, Correa-Giannella ML, et al. Glycated human serum albumin isolated from poorly controlled diabetic patients impairs cholesterol efflux from macrophages: an investigation by mass spectrometry. Eur J Mass Spectrom (Chichester). 2015;21(3):233-44. Epub 2015/08/27. doi: 10.1255/ejms.1322. PubMed PMID: 26307703.
144. Mineo C, Yuhanna IS, Quon MJ, Shaul PW. High density lipoprotein-induced endothelial nitric-oxide synthase activation is mediated by Akt and MAP kinases. J Biol Chem. 2003;278(11):9142-9. Epub 20030102. doi: 10.1074/jbc.M211394200. PubMed PMID: 12511559.
145. Bursill CA, Castro ML, Beattie DT, Nakhla S, van der Vorst E, Heather AK, et al. High-density lipoproteins suppress chemokines and chemokine receptors in vitro and in vivo. Arterioscler Thromb Vasc Biol. 2010;30(9):1773-8. Epub 2010/08/13. doi: 10.1161/ATVBAHA.110.211342. PubMed PMID: 20702809.
146. Nicholls SJ, Dusting GJ, Cutri B, Bao S, Drummond GR, Rye KA, et al. Reconstituted high-density lipoproteins inhibit the acute pro-oxidant and proinflammatory vascular changes induced by a periarterial collar in normocholesterolemic rabbits. Circulation. 2005;111(12):1543-50. Epub 2005/03/23. doi: 10.1161/01.CIR.0000159351.95399.50. PubMed PMID: 15781735.
147. Van Lenten BJ, Navab M, Shih D, Fogelman AM, Lusis AJ. The role of high-density lipoproteins in oxidation and inflammation. Trends Cardiovasc Med. 2001;11(3-4):155-61. Epub 2001/11/01. doi: 10.1016/s1050-1738(01)00095-0. PubMed PMID: 11686006.
148. Lotfollahi Z, Dawson J, Fitridge R, Bursill C. The Anti-inflammatory and Proangiogenic Properties of High-Density Lipoproteins: An Emerging Role in Diabetic Wound Healing. Adv Wound Care (New Rochelle). 2021;10(7):370-80. Epub 2020/11/13. doi: 10.1089/wound.2020.1308. PubMed PMID: 33176621; PubMed Central PMCID: PMCPMC8165473.
149. Murphy AJ, Woollard KJ, Hoang A, Mukhamedova N, Stirzaker RA, McCormick SP, et al. High-density lipoprotein reduces the human monocyte inflammatory response. Arterioscler Thromb Vasc Biol. 2008;28(11):2071-7. Epub 2008/07/12. doi: 10.1161/ATVBAHA.108.168690. PubMed PMID: 18617650.

150. Sanson M, Distel E, Fisher EA. HDL induces the expression of the M2 macrophage markers arginase 1 and Fizz-1 in a STAT6-dependent process. PLoS One. 2013;8(8):e74676. Epub 2013/08/31. doi: 10.1371/journal.pone.0074676. PubMed PMID: 23991225; PubMed Central PMCID: PMCPMC3749183.
151. Liu T, Dhanasekaran SM, Jin H, Hu B, Tomlins SA, Chinnaiyan AM, et al. FIZZ1 stimulation of myofibroblast differentiation. Am J Pathol. 2004;164(4):1315-26. Epub 2004/03/25. doi: 10.1016/S0002-9440(10)63218-X. PubMed PMID: 15039219; PubMed Central PMCID: PMCPMC1615359.
152. Burger D, Dayer JM. High-density lipoprotein-associated apolipoprotein A-I: the missing link between infection and chronic inflammation? Autoimmun Rev. 2002;1(1-2):111-7. Epub 2003/07/10. doi: 10.1016/s1568-9972(01)00018-0. PubMed PMID: 12849067.
153. De Nardo D, Labzin LI, Kono H, Seki R, Schmidt SV, Beyer M, et al. High-density lipoprotein mediates anti-inflammatory reprogramming of macrophages via the transcriptional regulator ATF3. Nat Immunol. 2014;15(2):152-60. Epub 2013/12/10. doi: 10.1038/ni.2784. PubMed PMID: 24317040; PubMed Central PMCID: PMCPMC4009731.
154. Seetharam D, Mineo C, Gormley AK, Gibson LL, Vongpatanasin W, Chambliss KL, et al. High-density lipoprotein promotes endothelial cell migration and reendothelialization via scavenger receptor-B type I. Circ Res. 2006;98(1):63-72. Epub 2005/12/13. doi: 10.1161/01.RES.0000199272.59432.5b. PubMed PMID: 16339487.
155. Tan JT, Prosser HC, Dunn LL, Vanags LZ, Ridiandries A, Tsatralis T, et al. High-Density Lipoproteins Rescue Diabetes-Impaired Angiogenesis via Scavenger Receptor Class B Type I. Diabetes. 2016;65(10):3091-103. Epub 2016/06/11. doi: 10.2337/db15-1668. PubMed PMID: 27284113.
156. Tan JT, Prosser HC, Vanags LZ, Monger SA, Ng MK, Bursill CA. High-density lipoproteins augment hypoxia-induced angiogenesis via regulation of post-translational modulation of hypoxia-inducible factor 1alpha. FASEB J. 2014;28(1):206-17. Epub 2013/09/12. doi: 10.1096/fj.13-233874. PubMed PMID: 24022405.
157. Primer KR, Psaltis PJ, Tan JTM, Bursill CA. The Role of High-Density Lipoproteins in Endothelial Cell Metabolism and Diabetes-Impaired Angiogenesis. Int J Mol Sci. 2020;21(10). Epub 2020/05/28. doi: 10.3390/ijms21103633. PubMed PMID: 32455604; PubMed Central PMCID: PMCPMC7279383.
158. Cannizzo CM, Adonopulos AA, Solly EL, Ridiandries A, Vanags LZ, Mulangala J, et al. VEGFR2 is activated by high-density lipoproteins and plays a key role in the proangiogenic action of HDL in ischemia. The FASEB Journal. 2018;32(6):2911-22. doi: 10.1096/fj.201700617R. PubMed PMID: 29401597.
159. Jin F, Hagemann N, Sun L, Wu J, Doeppner TR, Dai Y, et al. High-density lipoprotein (HDL) promotes angiogenesis via S1P3-dependent VEGFR2 activation. Angiogenesis. 2018;21(2):381-94. Epub 2018/02/17. doi: 10.1007/s10456-018-9603-z. PubMed PMID: 29450744.
160. Miura S, Fujino M, Matsuo Y, Kawamura A, Tanigawa H, Nishikawa H, et al. High density lipoprotein-induced angiogenesis requires the activation of Ras/MAP kinase in human coronary artery endothelial cells. Arterioscler Thromb Vasc Biol. 2003;23(5):802-8. Epub 2003/03/15. doi: 10.1161/01.ATV.0000066134.79956.58. PubMed PMID: 12637339.
161. Tsatralis T, Ridiandries A, Robertson S, Vanags LZ, Lam YT, Tan JTM, et al. Reconstituted high-density lipoproteins promote wound repair and blood flow recovery in response to ischemia in aged mice. Lipids in Health and Disease. 2016;15(1):150. doi: 10.1186/s12944-016-0322-4.
162. Gordts SC, Muthuramu I, Amin R, Jacobs F, De Geest B. The Impact of Lipoproteins on Wound Healing: Topical HDL Therapy Corrects Delayed Wound Healing in Apolipoprotein E

Deficient Mice. Pharmaceuticals (Basel). 2014;7(4):419-32. Epub 2014/04/08. doi: 10.3390/ph7040419. PubMed PMID: 24705596; PubMed Central PMCID: PMCPMC4014700.
163. Ikura K, Hanai K, Shinjyo T, Uchigata Y. HDL cholesterol as a predictor for the incidence of lower extremity amputation and wound-related death in patients with diabetic foot ulcers. Atherosclerosis. 2015;239(2):465-9. doi: 10.1016/j.atherosclerosis.2015.02.006.
164. Prosser HC, Tan JT, Dunn LL, Patel S, Vanags LZ, Bao S, et al. Multifunctional regulation of angiogenesis by high-density lipoproteins. Cardiovasc Res. 2014;101(1):145-54. Epub 2013/10/17. doi: 10.1093/cvr/cvt234. PubMed PMID: 24130189.
165. Wang K, Yu C, Liu Y, Zhang W, Sun Y, Chen Y. Enhanced Antiatherosclerotic Efficacy of Statin-Loaded Reconstituted High-Density Lipoprotein via Ganglioside GM1 Modification. ACS Biomater Sci Eng. 2018;4(3):952-62. Epub 2018/03/12. doi: 10.1021/acsbiomaterials.7b00871. PubMed PMID: 33418777.
166. Livak KJ, Schmittgen TD. Analysis of relative gene expression data using real-time quantitative PCR and the 2(-Delta Delta C(T)) Method. Methods. 2001;25(4):402-8. Epub 2002/02/16. doi: 10.1006/meth.2001.1262. PubMed PMID: 11846609.
167. Duffy D, Rader DJ. Update on strategies to increase HDL quantity and function. Nat Rev Cardiol. 2009;6(7):455-63. Epub 2009/06/03. doi: 10.1038/nrcardio.2009.94. PubMed PMID: 19488077.
168. Van Craeyveld E, Gordts S, Jacobs F, De Geest B. Gene therapy to improve high-density lipoprotein metabolism and function. Curr Pharm Des. 2010;16(13):1531-44. Epub 2010/03/04. doi: 10.2174/138161210791050997. PubMed PMID: 20196736.
169. Biomechanical and Clinical Factors Related to Stage I Posterior Tibial Tendon Dysfunction. Journal of Orthopaedic & Sports Physical Therapy. 2011;41(10):776-84. doi: 10.2519/jospt.2011.3545.
170. van der Vorst EP, Vanags LZ, Dunn LL, Prosser HC, Rye KA, Bursill CA. High-density lipoproteins suppress chemokine expression and proliferation in human vascular smooth muscle cells. FASEB J. 2013;27(4):1413-25. Epub 20121227. doi: 10.1096/fj.12-212753. PubMed PMID: 23271056.
171. The pre-publication history for this paper can be accessed here:http://www.biomedcentral.com/1472-6882/14/6/prepub.
172. Tsatralis T, Ridiandries A, Robertson S, Vanags LZ, Lam YT, Tan JT, et al. Reconstituted high-density lipoproteins promote wound repair and blood flow recovery in response to ischemia in aged mice. Lipids Health Dis. 2016;15(1):150. Epub 20160906. doi: 10.1186/s12944-016-0322-4. PubMed PMID: 27600523; PubMed Central PMCID: PMCPMC5012086.
173. Dunn L, Prosser HC, Tan JT, Vanags LZ, Ng MK, Bursill CA. Murine model of wound healing. J Vis Exp. 2013;(75):e50265. doi: 10.3791/50265. PubMed PMID: 23748713; PubMed Central PMCID: PMCPMC3724564.
174. Deng X, Xu M, Yuan C, Yin L, Chen X, Zhou X, et al. Transcriptional regulation of increased CCL2 expression in pulmonary fibrosis involves nuclear factor-kappaB and activator protein-1. Int J Biochem Cell Biol. 2013;45(7):1366-76. Epub 20130410. doi: 10.1016/j.biocel.2013.04.003. PubMed PMID: 23583295.
175. Hershko DD, Robb BW, Luo G, Hasselgren PO. Multiple transcription factors regulating the IL-6 gene are activated by cAMP in cultured Caco-2 cells. Am J Physiol Regul Integr Comp Physiol. 2002;283(5):R1140-8. doi: 10.1152/ajpregu.00161.2002. PubMed PMID: 12376407.
176. Colin S, Fanchon M, Belloy L, Bochem AE, Copin C, Derudas B, et al. HDL does not influence the polarization of human monocytes toward an alternative phenotype. International Journal of Cardiology. 2014;172(1):179-84. doi: https://doi.org/10.1016/j.ijcard.2013.12.168.

177. Duivenvoorden R, Tang J, Cormode DP, Mieszawska AJ, Izquierdo-Garcia D, Ozcan C, et al. A statin-loaded reconstituted high-density lipoprotein nanoparticle inhibits atherosclerotic plaque inflammation. Nat Commun. 2014;5:3065. doi: 10.1038/ncomms4065. PubMed PMID: 24445279; PubMed Central PMCID: PMCPMC4001802.
178. Game FL, Apelqvist J, Attinger C, Hartemann A, Hinchliffe RJ, Londahl M, et al. Effectiveness of interventions to enhance healing of chronic ulcers of the foot in diabetes: a systematic review. Diabetes Metab Res Rev. 2016;32 Suppl 1:154-68. doi: 10.1002/dmrr.2707. PubMed PMID: 26344936.
179. Ikura K, Hanai K, Shinjyo T, Uchigata Y. HDL cholesterol as a predictor for the incidence of lower extremity amputation and wound-related death in patients with diabetic foot ulcers. Atherosclerosis. 2015;239(2):465-9. Epub 20150207. doi: 10.1016/j.atherosclerosis.2015.02.006. PubMed PMID: 25697577.
180. Knopfholz J, Disserol CC, Pierin AJ, Schirr FL, Streisky L, Takito LL, et al. Validation of the friedewald formula in patients with metabolic syndrome. Cholesterol. 2014;2014:261878. Epub 20140206. doi: 10.1155/2014/261878. PubMed PMID: 24672715; PubMed Central PMCID: PMCPMC3941209.
181. De Nardo D, Kalvakolanu DV, Latz E. Immortalization of Murine Bone Marrow-Derived Macrophages. In: Rousselet G, editor. Macrophages: Methods and Protocols. New York, NY: Springer New York; 2018. p. 35-49.
182. Pena G, Kuang B, Szpak Z, Cowled P, Dawson J, Fitridge R. Evaluation of a Novel Three-Dimensional Wound Measurement Device for Assessment of Diabetic Foot Ulcers. Adv Wound Care (New Rochelle). 2020;9(11):623-31. Epub 20191023. doi: 10.1089/wound.2019.0965. PubMed PMID: 33095125; PubMed Central PMCID: PMCPMC7580588.
183. Davis FM, Kimball A, Boniakowski A, Gallagher K. Dysfunctional Wound Healing in Diabetic Foot Ulcers: New Crossroads. Curr Diab Rep. 2018;18(1):2. Epub 20180123. doi: 10.1007/s11892-018-0970-z. PubMed PMID: 29362914.
184. Kosmas CE, Martinez I, Sourlas A, Bouza KV, Campos FN, Torres V, et al. High-density lipoprotein (HDL) functionality and its relevance to atherosclerotic cardiovascular disease. Drugs Context. 2018;7:212525. Epub 20180328. doi: 10.7573/dic.212525. PubMed PMID: 29623098; PubMed Central PMCID: PMCPMC5877920.
185. Kashyap SR, Osme A, Ilchenko S, Golizeh M, Lee K, Wang S, et al. Glycation Reduces the Stability of ApoAI and Increases HDL Dysfunction in Diet-Controlled Type 2 Diabetes. The Journal of Clinical Endocrinology & Metabolism. 2017;103(2):388-96. doi: 10.1210/jc.2017-01551.
186. Machado-Lima A, Iborra RT, Pinto RS, Castilho G, Sartori CH, Oliveira ER, et al. In type 2 diabetes mellitus glycated albumin alters macrophage gene expression impairing ABCA1-mediated cholesterol efflux. J Cell Physiol. 2015;230(6):1250-7. doi: 10.1002/jcp.24860. PubMed PMID: 25413254.
187. Falanga V. Wound healing and its impairment in the diabetic foot. Lancet. 2005;366(9498):1736-43. doi: 10.1016/S0140-6736(05)67700-8. PubMed PMID: 16291068.
188. Black S, Kushner I, Samols D. C-reactive Protein *. Journal of Biological Chemistry. 2004;279(47):48487-90. doi: 10.1074/jbc.R400025200.
189. Sproston NR, Ashworth JJ. Role of C-Reactive Protein at Sites of Inflammation and Infection. Frontiers in immunology. 2018;9:754-. doi: 10.3389/fimmu.2018.00754. PubMed PMID: 29706967.
190. Drew BG, Duffy SJ, Formosa MF, Natoli AK, Henstridge DC, Penfold SA, et al. High-density lipoprotein modulates glucose metabolism in patients with type 2 diabetes mellitus.

Circulation. 2009;119(15):2103-11. Epub 20090406. doi: 10.1161/CIRCULATIONAHA.108.843219. PubMed PMID: 19349317.
191. Fryirs MA, Barter PJ, Appavoo M, Tuch BE, Tabet F, Heather AK, et al. Effects of high-density lipoproteins on pancreatic beta-cell insulin secretion. Arterioscler Thromb Vasc Biol. 2010;30(8):1642-8. Epub 20100513. doi: 10.1161/ATVBAHA.110.207373. PubMed PMID: 20466975.
192. Haase CL, Tybjaerg-Hansen A, Nordestgaard BG, Frikke-Schmidt R. HDL Cholesterol and Risk of Type 2 Diabetes: A Mendelian Randomization Study. Diabetes. 2015;64(9):3328-33. Epub 20150513. doi: 10.2337/db14-1603. PubMed PMID: 25972569.
193. Hatanaka E, Monteagudo PT, Marrocos MSM, Campa A. Neutrophils and monocytes as potentially important sources of proinflammatory cytokines in diabetes. Clinical and Experimental Immunology. 2006;146(3):443-7. doi: 10.1111/j.1365-2249.2006.03229.x.
194. Chen W, Chen K, Xu Z, Hu Y, Liu Y, Liu W, et al. Neutrophil-to-Lymphocyte Ratio and Platelet-to-Lymphocyte Ratio Predict Mortality in Patients with Diabetic Foot Ulcers Undergoing Amputations. Diabetes Metab Syndr Obes. 2021;14:821-9. doi: 10.2147/DMSO.S284583. PubMed PMID: 33658817.
195. Kwon E, Ahn C. Low hemoglobin concentration is associated with several diabetic profiles. Korean J Intern Med. 2012;27(3):273-4. Epub 20120901. doi: 10.3904/kjim.2012.27.3.273. PubMed PMID: 23019390; PubMed Central PMCID: PMCPMC3443718.
196. Jia C, Anderson JLC, Gruppen EG, Lei Y, Bakker SJL, Dullaart RPF, et al. High-Density Lipoprotein Anti-Inflammatory Capacity and Incident Cardiovascular Events. Circulation. 2021;143(20):1935-45. Epub 20210412. doi: 10.1161/CIRCULATIONAHA.120.050808. PubMed PMID: 33840204.
197. Sans M, Panes J, Ardite E, Elizalde JI, Arce Y, Elena M, et al. VCAM-1 and ICAM-1 mediate leukocyte-endothelial cell adhesion in rat experimental colitis. Gastroenterology. 1999;116(4):874-83. doi: 10.1016/s0016-5085(99)70070-3. PubMed PMID: 10092309.
198. Santos-Gallego CG, Rosenson RS. Role of HDL in those with diabetes. Curr Cardiol Rep. 2014;16(9):512. PubMed PMID: 25199216.
199. Lemmers RFH, van Hoek M, Lieverse AG, Verhoeven AJM, Sijbrands EJG, Mulder MT. The anti-inflammatory function of high-density lipoprotein in type II diabetes: A systematic review. J Clin Lipidol. 2017;11(3):712-24 e5. Epub 20170331. doi: 10.1016/j.jacl.2017.03.013. PubMed PMID: 28442299.
200. Wong NKP, Nicholls SJ, Tan JTM, Bursill CA. The Role of High-Density Lipoproteins in Diabetes and Its Vascular Complications. Int J Mol Sci. 2018;19(6). Epub 20180605. doi: 10.3390/ijms19061680. PubMed PMID: 29874886; PubMed Central PMCID: PMCPMC6032203.
201. Morrison KR, Solly EL, Shemesh T, Psaltis PJ, Nicholls SJ, Brown A, et al. Elevated HDL-bound miR-181c-5p level is associated with diabetic vascular complications in Australian Aboriginal people. Diabetologia. 2021;64(6):1402-11. doi: 10.1007/s00125-021-05414-6.
202. Fouladzadeh A, Dorraki M, Min KKM, Cockshell MP, Thompson EJ, Verjans JW, et al. The development of tumour vascular networks. Commun Biol. 2021;4(1):1111. Epub 20210922. doi: 10.1038/s42003-021-02632-x. PubMed PMID: 34552183; PubMed Central PMCID: PMCPMC8458341.
203. Ndrepepa G. High-density lipoprotein: a double-edged sword in cardiovascular physiology and pathophysiology. Journal of Laboratory and Precision Medicine. 2021;6.
204. Holzwirth E, Fischer-Schaepmann T, Obradovic D, von Lucadou M, Schwedhelm E, Daum G, et al. Anti-inflammatory HDL effects are impaired in atrial fibrillation. Heart Vessels. 2022;37(1):161-71. Epub 20210830. doi: 10.1007/s00380-021-01908-w. PubMed PMID: 34459957; PubMed Central PMCID: PMCPMC8732851.

205. Van Lenten BJ, Wagner AC, Nayak DP, Hama S, Navab M, Fogelman AM. High-density lipoprotein loses its anti-inflammatory properties during acute influenza a infection. Circulation. 2001;103(18):2283-8. doi: 10.1161/01.cir.103.18.2283. PubMed PMID: 11342478.
206. Han CY, Chiba T, Campbell JS, Fausto N, Chaisson M, Orasanu G, et al. Reciprocal and coordinate regulation of serum amyloid A versus apolipoprotein A-I and paraoxonase-1 by inflammation in murine hepatocytes. Arterioscler Thromb Vasc Biol. 2006;26(8):1806-13. Epub 20060518. doi: 10.1161/01.ATV.0000227472.70734.ad. PubMed PMID: 16709944.
207. Kempe S, Kestler H, Lasar A, Wirth T. NF-kappaB controls the global pro-inflammatory response in endothelial cells: evidence for the regulation of a pro-atherogenic program. Nucleic Acids Res. 2005;33(16):5308-19. Epub 20050921. doi: 10.1093/nar/gki836. PubMed PMID: 16177180; PubMed Central PMCID: PMCPMC1226313.
208. Pan B, Ma Y, Ren H, He Y, Wang Y, Lv X, et al. Diabetic HDL is dysfunctional in stimulating endothelial cell migration and proliferation due to down regulation of SR-BI expression. PLoS One. 2012;7(11):e48530. Epub 20121102. doi: 10.1371/journal.pone.0048530. PubMed PMID: 23133640; PubMed Central PMCID: PMCPMC3487724.
209. Sorrentino SA, Besler C, Rohrer L, Meyer M, Heinrich K, Bahlmann FH, et al. Endothelial-vasoprotective effects of high-density lipoprotein are impaired in patients with type 2 diabetes mellitus but are improved after extended-release niacin therapy. Circulation. 2010;121(1):110-22. Epub 20091221. doi: 10.1161/CIRCULATIONAHA.108.836346. PubMed PMID: 20026785.
210. Nissen SE, Tsunoda T, Tuzcu EM, Schoenhagen P, Cooper CJ, Yasin M, et al. Effect of recombinant ApoA-I Milano on coronary atherosclerosis in patients with acute coronary syndromes: a randomized controlled trial. JAMA. 2003;290(17):2292-300. doi: 10.1001/jama.290.17.2292. PubMed PMID: 14600188.
211. Castelli WP, Anderson K, Wilson PW, Levy D. Lipids and risk of coronary heart disease. The Framingham Study. Ann Epidemiol. 1992;2(1-2):23-8. doi: 10.1016/1047-2797(92)90033-m. PubMed PMID: 1342260.
212. Qiu C, Zhao X, Zhou Q, Zhang Z. High-density lipoprotein cholesterol efflux capacity is inversely associated with cardiovascular risk: a systematic review and meta-analysis. Lipids Health Dis. 2017;16(1):212. Epub 20171110. doi: 10.1186/s12944-017-0604-5. PubMed PMID: 29126414; PubMed Central PMCID: PMCPMC5681808.
213. Zewinger S, Kleber ME, Rohrer L, Lehmann M, Triem S, Jennings RT, et al. Symmetric dimethylarginine, high-density lipoproteins and cardiovascular disease. Eur Heart J. 2017;38(20):1597-607. doi: 10.1093/eurheartj/ehx118. PubMed PMID: 28379378.
214. Vaisar T, Couzens E, Hwang A, Russell M, Barlow CE, DeFina LF, et al. Type 2 diabetes is associated with loss of HDL endothelium protective functions. PLoS One. 2018;13(3):e0192616. Epub 20180315. doi: 10.1371/journal.pone.0192616. PubMed PMID: 29543843; PubMed Central PMCID: PMCPMC5854245.
215. Whelan DS, Caplice NM, Clover AJP. Mesenchymal stromal cell derived CCL2 is required for accelerated wound healing. Scientific Reports. 2020;10(1):2642. doi: 10.1038/s41598-020-59174-1.
216. Ridiandries A, Tan JTM, Bursill CA. The Role of Chemokines in Wound Healing. Int J Mol Sci. 2018;19(10). Epub 20181018. doi: 10.3390/ijms19103217. PubMed PMID: 30340330; PubMed Central PMCID: PMCPMC6214117.
217. Chapman MJ. Are the effects of statins on HDL-cholesterol clinically relevant? European Heart Journal Supplements. 2004;6(suppl_C):C58-C63. doi: 10.1016/j.ehjsup.2004.04.002.

218. Kawano M, Nagasaka S, Yagyu H, Ishibashi S. Pitavastatin decreases plasma prebeta1-HDL concentration and might promote its disappearance rate in hypercholesterolemic patients. J Atheroscler Thromb. 2008;15(1):41-6. Epub 20080209. doi: 10.5551/jat.e532. PubMed PMID: 18270457.
219. Charles-Schoeman C, Khanna D, Furst DE, McMahon M, Reddy ST, Fogelman AM, et al. Effects of high-dose atorvastatin on antiinflammatory properties of high density lipoprotein in patients with rheumatoid arthritis: a pilot study. J Rheumatol. 2007;34(7):1459-64. Epub 20070601. PubMed PMID: 17552046.
220. Igarashi J, Miyoshi M, Hashimoto T, Kubota Y, Kosaka H. Statins induce S1P1 receptors and enhance endothelial nitric oxide production in response to high-density lipoproteins. Br J Pharmacol. 2007;150(4):470-9. Epub 20070115. doi: 10.1038/sj.bjp.0707114. PubMed PMID: 17220911; PubMed Central PMCID: PMCPMC2189725.
221. Tan JT, Ng MK, Bursill CA. The role of high-density lipoproteins in the regulation of angiogenesis. Cardiovasc Res. 2015;106(2):184-93. Epub 20150310. doi: 10.1093/cvr/cvv104. PubMed PMID: 25759067.
222. Cochran BJ, Ong KL, Manandhar B, Rye KA. High Density Lipoproteins and Diabetes. Cells. 2021;10(4). Epub 20210409. doi: 10.3390/cells10040850. PubMed PMID: 33918571; PubMed Central PMCID: PMCPMC8069617.
223. Lamarche B, Rashid S, Lewis GF. HDL metabolism in hypertriglyceridemic states: an overview. Clin Chim Acta. 1999;286(1-2):145-61. doi: 10.1016/s0009-8981(99)00098-4. PubMed PMID: 10511289.
224. Passarelli M, Tang C, McDonald TO, O'Brien KD, Gerrity RG, Heinecke JW, et al. Advanced glycation end product precursors impair ABCA1-dependent cholesterol removal from cells. Diabetes. 2005;54(7):2198-205. doi: 10.2337/diabetes.54.7.2198. PubMed PMID: 15983222.
225. Nobécourt E, Tabet F, Lambert G, Puranik R, Bao S, Yan L, et al. Nonenzymatic glycation impairs the antiinflammatory properties of apolipoprotein A-I. Arterioscler Thromb Vasc Biol. 2010;30(4):766-72. Epub 20100128. doi: 10.1161/atvbaha.109.201715. PubMed PMID: 20110571; PubMed Central PMCID: PMCPMC3038672.
226. Navab M, Reddy ST, Van Lenten BJ, Anantharamaiah GM, Fogelman AM. The role of dysfunctional HDL in atherosclerosis. J Lipid Res. 2009;50 Suppl:S145-9. Epub 20081027. doi: 10.1194/jlr.R800036-JLR200. PubMed PMID: 18955731; PubMed Central PMCID: PMCPMC2674720.
227. Smith JD. Myeloperoxidase, inflammation, and dysfunctional high-density lipoprotein. Journal of clinical lipidology. 2010;4(5):382-8. doi: 10.1016/j.jacl.2010.08.007. PubMed PMID: 21076633.
228. Iqbal AJ, Barrett TJ, Taylor L, McNeill E, Manmadhan A, Recio C, et al. Acute exposure to apolipoprotein A1 inhibits macrophage chemotaxis in vitro and monocyte recruitment in vivo. Elife. 2016;5. Epub 20160830. doi: 10.7554/eLife.15190. PubMed PMID: 27572261; PubMed Central PMCID: PMCPMC5030090.